The Dissertation Committee for Jongsik Gam certifies that this is the approved version of the following dissertation:

Toward High Throughput Directed Evolution of Protease Specificity Using Fluorescence Activated Cell Sorting

Committee:

Christian P. Whitman, Co-Supervisor

Brent L. Iverson, Co-Supervisor

George Georgiou

Hung-wen Liu

Patrick J. Davis

Toward High Throughput Directed Evolution of Protease Specificity Using Fluorescence Activated Cell Sorting

by

Jongsik Gam, B.S., M.S.

Dissertation

Presented to the Faculty of the Graduate School of

The University of Texas at Austin

in Partial Fulfillment

of the Requirements

for the Degree of

Doctor of Philosophy

The University of Texas at Austin

May, 2004

Dedication

To my family

Acknowledgements

It is a great pleasure for me to express my sincere gratitude to many people for their invaluable help and support during my graduate study in UT Austin. First of all, I would like to thank my advisors, Professor Brent L. Iverson and Professor George Georgiou for their encouragement, guidance and support throughout this work. I also would like to thank Professor Christian P. Whitman for his kindness and patience.

I wish to thank the members of the Iverson and Georgiou group; Karl, Andy, Mark, Navin, and Greg. Especially, helpful discussions with Karl and Andy are greatly acknowledged. Thanks are due to Mark in FACS analysis. Thanks go to Edgardo for proofreading. I am grateful to Seung-Joo Lee who helped me when I first came to Austin.

I would like to thank my parents for their love and support, especially to my father who passed away during my graduate study. I also thank my daughters, Seoyoung and Seoyoon, who always make me happy and peaceful. Finally, special thanks to my wife, Jeeyeon Lee, for her love, encouragement, and patience.

Toward High Throughput Directed Evolution of Protease Specificity Using Fluorescence Activated Cell Sorting

Publication No. _____

Jongsik Gam, Ph.D.

The University of Texas at Austin, 2004

Supervisors: Brent L. Iverson and Christian P. Whitman

Directed evolution by high throughput screening is used for improving protein properties and functions. In our laboratory, a FRET peptide probe was used with a Fluorescence Activated Cell Sorting (FACS)-based screening method for OmpT, a native outer membrane protease of *E. coli*. This earlier FRET probe enabled the isolation of an OmpT variant with altered specificity, although wild-type Arg-Arg cleavage activity was still present. Newly devised protease probes that operate via electrostatic capture on the bacterial cell surface allowed a very powerful "two-color" type of FACS sorting, in which new catalytic activities are selected while simultaneously deselecting unwanted activities. Newly designed autoquenching peptide substrates with two identical fluorophores (BODIPY) were used for post screening of new variants on 96 well plates. Using the two-color FACS sorting approach, we were able to isolate OmpT variants 1.2.19 and 1.3.19, displaying a million-fold conversion of specificity (high Ala-Arg cleavage and very low wild-type Arg-Arg cleavage). This study demonstrates that the two-color sorting system

for protein evolution can be used for pinpointing protein functions such as protease specificity and scFv antibody.

To apply Periplasmic Expression with Cytometric Screening (PECS) for high throughput directed evolution of exogenous proteases, a permeabilization study of the *E. coli* outer membrane was carried out using FACS with cells expressing periplasmic scFv antibodies. Probes (>1000 Da) hardly gave practical signals for FACS sorting without a permeabilizer. However, outer membrane permeability toward a peptide probe (~ 2800 Da) was significantly enhanced by adding polymixin B nonapeptide (PMBN) or using a "heptoseless" LPS (lipopolysaccharide) *E. coli* mutant, D21f2. Based on the PECS system, the active form of chymotrypsin, potentially toxic to its hosting cell, was successfully expressed in the periplasm, and its activity was detected using a fluorescent probe and FACS. However, when positive and negative cells were mixed, the FACS signal was not specific to the positive cells. We believe this is due to enzyme leakage to the medium prior to substrate cleavage. Although further FACS screen assays are required to improve signal resolution of positive and negative cells, this work provides the foundation for high throughput directed evolution study of exogenous proteases.

Table of Contents

List of Tables

List of Figures

Chapter 1
Background of directed enzyme evolution

1.1 OVERVIEW OF ENZYMES

1.1.1 Protein

Proteins are critical in biological processes. They serve as structural components, catalysts, chemical messengers, transporters and protecters against disease. Proteins have proven to be increasingly valuable for the chemical and pharmaceutical industries. Hence, the study of structure/function relationships is important in understanding basic biological processes and for engineering proteins for practical applications. However, understanding structure/function relationships can be difficult, especially for mammalian proteins, because they can be unstable and difficult to express in large quantities. The development of molecular cloning techniques has facilitated protein studies by making possible the production of protein in high levels in a heterologous host such as *E. coli* or yeast. These recent advancements have allowed us to employ rational and directed evolution approaches to investigate and engineer proteins.

1.1.2 Enzymes

Enzymes are able to catalyze a variety of chemical reactions such as hydrolysis, polymerization (bond formation), functional group transfer, oxidation-reduction, isomerization and dehydration. Enzymes and chemical catalysts increase the rate of reaction by lowering the activation energy. The rate enhancements of enzyme-catalyzed reactions are typically several orders of magnitude over background, and take place under mild condition. Unlike most chemical catalysts, enzymes are able to catalyze specific and often difficult chemical transformation in aqueous solutions at room temperature and atmospheric

pressure (Tao & Cornish, 2002). Furthermore, enzymes are generally environmentally friendly, economical and clean catalysts. Enzymes currently have commercial applications ranging from food or paper processing to fine chemical synthesis and diagnostic/research reagents. However, enzymes are often poor catalyst for non-natural substrates and they suffer from poor stability. Directed evolution methods have proven to be an effective strategy for improving enzyme properties (Wahler & Reymond, 2001).

1.1.3 Protease

Proteases catalyze peptide bond hydrolysis. They are classified according to their catalytic mechanism and active site residues. Different types of proteases include serine, cysteine, aspartic and metallo proteases (Barrett, 1999). Serine and cysteine proteases use these amino acid side chains as a nucleophile to attack a peptide bond carbonyl, while aspartic and metallo proteases use water molecules as the nucleophile.

Proteases have many commercial uses. One major commercial application is in laundry detergents, which often contain a protease such as subtilisin that has been altered for improved stability and activity. In addition, research on proteolytic enzymes has been driven by the pharmaceutical industry. For example, plasminogen activators (tPA and uPA) are a fibrinolytic serine proteases are important therapeutic agents for thrombolytics (blood clots). Streptokinase is commonly also used as thrombolytic agent in the therapy of ischemic stroke and used in the treatment of complicated parapneumonic effusions and empyemas (Weitz *et al.*, 1999). Collagenase is used for treatment of skin ulcers (Jung & Winter, 1998).

Many proteases are also potential therapeutic targets. For instance, HIV protease is a potential target for the design of specific anti-AIDS drugs. Basic studies have lead to FDA approved HIV-1 protease inhibitors (McQuade *et al*., 1990) such as saquinavir (Invirase), ritonavir and indinavir (Flexner, 1998).

Captopril, enalapril and ramipril are the FDA approved inhibitors of angiotensin-converting enzymes (ACE) for treatment of hypertension and congestive heart failure. There are many other protease drug targets, including caspase, ICE (caspase-1), thrombin, proteasome, hepatitis C virus NS3 protease, trypsin and neutral endopeptidase with ACE. Many of their inhibitors are in clinical trial stages.

1.2 ENZYME EVOLUTION

Organisms evolve to adjust to changing environments, as explained by Darwin's Theory of Evolution. A changing environment challenges and forces them to evolve by modification, mainly through mutation. Darwinian evolution caused by an artificially controlled environmental selective pressure is a very attractive strategy for altering protein activity in the laboratory. This approach, referred to as laboratory directed evolution, is a promising approach to improve enzyme selectivity and evolve function *de novo* (Kurtzman *et al*., 2001, Zhao & Arnold, 1999). General steps of the laboratory directed enzyme evolution strategy consist of mutagenesis/recombination of a parental gene(s), expression of the resulting enzyme variants, and selection/screening for a desired new property as described in Figure 1.1 (Farinas *et al.*, 2001, Tao & Cornish, 2002). These steps can be repeated until the enzyme acquires the desired new activity level. Improved enzymes from directed evolution have been applied to chemical synthesis, biological and medical research, commercial products in the food process and detergent industry, and even as practical pharmaceutical products. Directed evolution provides a powerful tool to understand the mechanisms of enzymatic reactions as well.

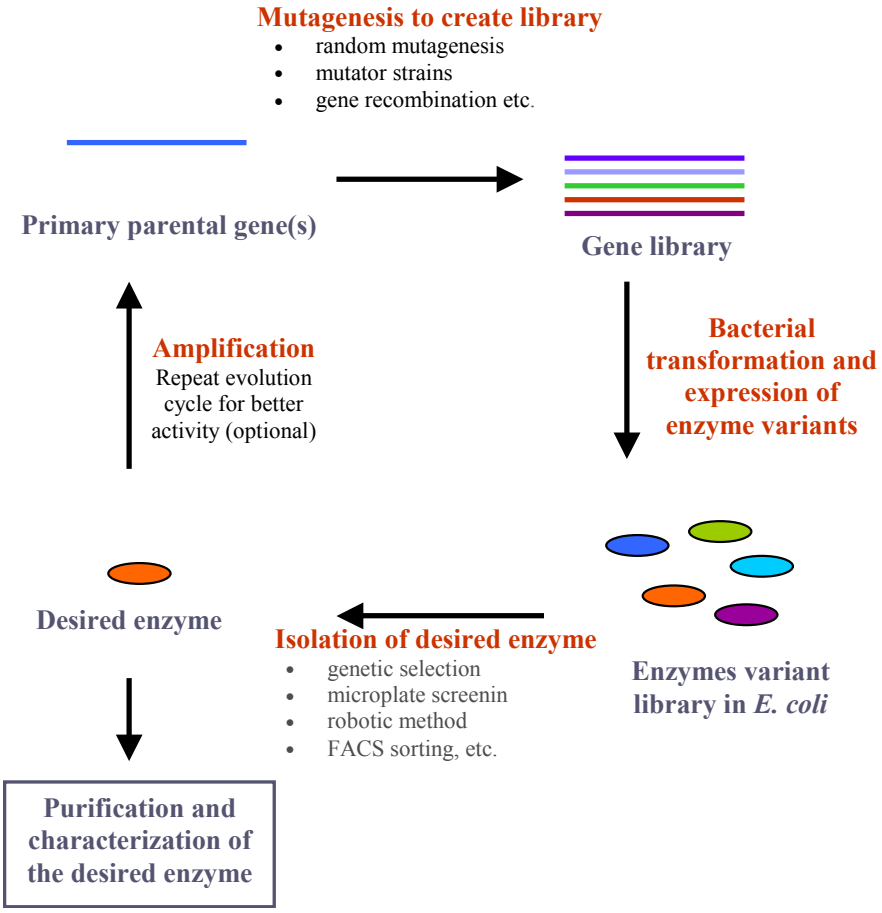

Figure 1.1 Scheme for the directed evolution of an enzyme. A library is generated from the primary parental gene that encodes the enzymes of interest by random mutagenesis or gene recombination from parental homologous genes. A library of mutant enzymes is expressed in a microorganism, such as *E. coli* and yeast. The major step of directed evolution is selection of the desired enzymes from the library. The gene information encoding the desired enzymes of the same cell is sequenced or directly used for optional next rounds of directed enzyme evolution. Finally, the desired enzymes are purified and performed further charaterization.

Many successful examples of enzyme evolution have been reported using well-known mutagenesis methods (Powell *et al.*, 2001). Commercial proteases such as subtilisin (Ness *et al*., 1999) have been studied for 30 years to improve their commercial value. Random mutagenesis and screening resulted in a 470-fold improvement of activity compared to the wild-type in 60% DMF (You & Arnold, 1996). Enzymes have also been evolved for improved activity at elevated and low temperatures (Kano *et al.*, 1997, Taguchi *et al.*, 1999, Zhao *et al.*, 1998, Zhao & Arnold, 1999). Reetz *et al*. improved the enantioselectivity of a *P. aeruginosa* lipase by several rounds of mutagenesis, resulting in an *ee* of more than 90%, compared to 2% *ee* of wild-type lipase (Liebeton *et al.*, 2000). In addition to stereospecificity, improvements in substrate specificity, thermostability, solvent tolerance and enzymatic activity over a broad pH range have been reported. Arnold *et al*. have produced mutants of bacterial cytochrome P450 BM-3 mutant enzyme that have 20-fold higher activity and use a hydrogen peroxidase shunt pathway without requiring a cofactor (NADPH). One newly evolved P450 BM-3 mutant exhibited new substrate selectivity as well as higher turnover rates (Arnold *et al.*, 2003, Glieder *et al.*, 2002). Directed evolution of β-lactamase resulted in 32,000-fold higher enzymatic activity using DNA shuffling method (Stemmer, 1994a). There are many other successful directed evolution examples of enzymes, including atrazine chlorohydrolase, tRNA synthetase, alkyl transferase, amylases, laccases (polyphenol oxidases), cellulases (β-galactosidase or β-xalyanase), phytases, penicillin acylases, nitrile-hydrolyzing enzymes, and hydantoinases for improvements of activity, specificity and stability (Cherry & Fidantsef, 2003, Powell *et al.*, 2001).

1.2.1 Mutagenesis to create gene library

Rational design mutagenesis based on X-ray or NMR structures can be a powerful way to produce proteins with enhanced function. An advantage of the rational design approach is that only a few mutants need to be constructed.

However, in practice, the function of a variant derived by rational design cannot generally be predicted, since enzymes are extremely complex. For example, guided by an X-ray structure, the conversion of trypsin to chymotrypsin was attempted by mutating Asp189 to Ser in the S_1 site. Instead of transforming trypsin to chymotrypsin, this mutation resulted in a poor, nonspecific protease although the anionic residue Asp189 at the bottom of the S_1 binding pocket of trypsin is thought to interact with positive charged residues Lys/Arg of substrate. In another attempt, the switching of 15 amino acid residues of the S_1 pocket and two surface loop regions of chymotrypsin into trypsin gave similar specificity of chymotrypsin, but had considerably sacrificed enzymatic activity (Hedstrom *et al*., 1992, Hedstrom, 1998). Therefore, multiple, unpredictable changes are often needed in order to alter enzyme activity in a useful way.

As an alternative to site directed mutagenesis, scientists have developed ways of mimicking the strategies of genetic variation found in natural biological evolution. In the laboratory, libraries of enzyme mutants can now be achieved by either random mutagenesis or recombination.

Random mutagenesis can result from a few to many changes per gene. Artificial UV/chemical mutagenesis can be used to introduce changes (Lee *et al.*, 2000). This mutation method mimics the natural process of evolution, but the library sizes are relatively small because the number of changes is generally small. Many rounds of mutagenesis and screening may be required to reach a desired new activity.

Another powerful method is error-prone PCR, which introduces random point mutations (Cadwell & Joyce, 1992). **High error rate mutagenesis** can be achieved by high error prone PCR (Rowe *et al*., 2003, Zaccolo & Gherardi, 1999) or by accumulation of low error rate mutagenesis from several cycles of low error prone PCR.

Generally, the more point mutations present in high error rate libraries give a lower fraction of active proteins, but also more interesting protein variants. For

instance, a study on the effect of the mutation rate on the affinity maturation of single chain fragment (scFv) antibodies from our laboratory demonstrated that the fraction of clones that retained binding activity to a hapten decreased exponentially in the low error rate range, 0 - 1% changes at the DNA level. Interestingly, a high error rate library (3% mutation rate, library size was 6×10^6) had significantly more active clones than expected. In addition, the best clone in the high error rate library showed a much greater affinity improvement than those derived from the low error rate library (Daugherty *et al*., 2000a).

One explanation for these results is that a single amino acid in the important region or active site of protein might not be sufficient for a great improvement of activity, because the change may sacrifice protein stability or folding properties. Other mutations may be needed to restore the stability and/or folding of the protein. In the high error rate scFv study, most productive mutations were found to be remote from the binding site. Importantly, these results provide a rationale for why the rational design mutagenesis based on molecular modeling might not be able to achieve a desired high improvement in protein activity.

Gene recombination strategies. DNA shuffling is a method that mimics natural sexual recombination (Stemmer, 1994a, Stemmer, 1994b). It is based on the *in vitro* recombination of two or more homologous genes (Figure 1.2). Briefly a mixture of randomly fragmented homologous genes is reassembled by the polymerase chain reaction (PCR) to yield chimeric full-length genes (Harayama, 1998, Patten *et al.*, 1997, Reid, 2000). DNA shuffling allows one to recombine all beneficial mutations from any previous round (Arnold, 1998, Patten *et al.*, 1997).

The so called ITCHY strategy developed by the Benkovic group is a method to create a hybrid of two truncated genes with a crossover point (Ostermeier *et al*., 1999). Next, SCRATCHY was developed which combines ITCHY method and DNA shuffling in order to give more crossover points than DNA shuffling alone (Lutz *et al*., 2001, Stevenson & Benkovic, 2002). Another gene recombination method, staggered extension process (StEP) (Zhao *et al*., 1998), utilizes partial

DNA polymerase extension reactions of two homologous template genes instead of partial DNA digestion and full PCR reaction as in the DNA shuffling method.

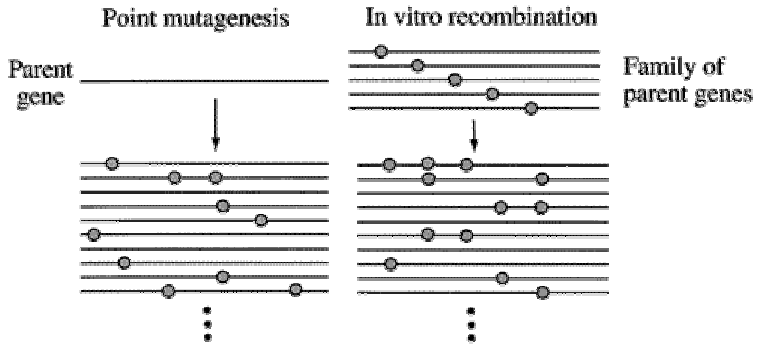

Figure 1.2 Random mutagenesis methods using error-prone PCR to generate a library of genes containing point mutations. Recombination using DNA shuffling generates gene libraries with different combinations of the mutations from more than two homologous parent sequences (Arnold, 1998).

1.2.2 Screening and selection in directed enzyme evolution

The terms screening and selection are often confused because both refer to similar concepts. A screening method is usually based on the individual assay of all library members by linking product formation with a physical property such as a color change. On the other hand, a selection method is based upon controlling life or death of the organism based upon the function of the enzyme (Wahler & Reymond, 2001). The advantage of selections is that larger libraries, on the order of 10^8-10^{10} members can be used. The selection methods are more likely to imitate Darwinian evolution by eliminating inappropriate species (Taylor *et al.*, 2001).

Selection method for a desired enzyme activity

Genetic selection is a powerful method for laboratory directed enzyme evolution offering the advantage of very high-throughput. However, its application is limited because the target activity of the evolved enzyme must be coupled to the survival of the host organism, a requirement that is often impractical. **Antibiotic**

resistance gene evolution using genetic selection is an ideal example. Without active antibiotic resistance, cells cannot grow or grow slowly compared to cells that have active resistance in the presence of antibiotics. For example, genetic selection study of the kanamycin-resistance gene by Hoseki and coworkers demonstrated that thermostability could be enhanced by 20 degree without sacrificing enzyme activity (Hoseki *et al*., 1999). In this case, growth temperature was used to put selective pressure on the kanamycin phosphotransferase enzymes.

In another directed enzyme evolution experiment using the genetic selection method, an evolved mutant of TEM-1 β-lactamase with 2400-fold higher activity against the β-lactam antibiotic cefotaxime compared to the wild-type was isolated. The highly active β-lactamase was isolated from small pools of hypermutated TEM-1 β-lactamases. This result indicates that a powerful selection or screening method coupled with high-error rate mutagensis is critical to successful directed evolution (Zaccolo & Gherardi, 1999).

Genetic selection schemes have not been limited to antibiotic resistance genes. **Selection markers other than antibiotics** have also been reported. For example, genetic selections based on the ability of an enzyme to degrade substrates that provide the sole carbon source for the host organism have been developed. In one example cells were selected based on the utilization of tryptophan to evolve the enzyme, phosphoribosylanthranilate isomerase (Altamirano *et al*., 2000). In another study trypsin was also examined by using genetic selection. Bacteria were grown in arginine free media containing Arg-β-naphthylamide as the sole source of arginine. Active mutants of trypsin expressed into the periplasm of *E. coli* and able to hydrolyze the Arg-β-naphthylamide adduct could survive in the medium (Evnin *et al*., 1990). This method is potentially useful for directed eukaryotic protease evolution as well.

Phage selection has also been applied to directed enzyme evolution. For example, a reaction substrate and product were anchored to the surface of filamentous phage by displaying enzyme-calmodulin chimeric proteins as gene III

fusions. The complexes of enzyme-calmodulin chimeric proteins on phage and the camodulin binding peptide fused with substrate/product are stable enough to be purified and are easily released by addition of a calcium chelator. Using this approach, enrichments of Glutathione-S-transferase and an endopeptidase were demonstrated by multiple rounds of selection with enrichment factors of >50 per round (Demartis *et al*., 1999).

The phage selection system was also used in the directed evolution of DNA polymerases. A mutant library of DNA polymerase displayed on the gene III of phage extend the substrate DNA primer/template duplexes, which are attached to other adjacent gene III coat protein molecules. Phage particles that display RNA polymerase mutants that can accept biotinylated UTP were enriched by streptavidin capture. The activity of ribonucleoside triphosphate (NTP) incorporation in the isolated mutants was comparable to that of deoxyribonucleoside triphosphate (dNTP) incorporation by a DNA polymerase (Figure 1.3) (Xia *et al*., 2002).

Along the same lines, an ***in vitro*** **compartmentalization** has been described involving artificial compartments based on water-in-oil emulsions that mimic the cellular compartments of a cell. For example, a methyltransferase enzyme from the template gene methylated its own gene in a target-specific manner to protect from HaeIII endonuclease digestion. The gene that can express functional methyltransferases was rescued from genes encoding a control enzyme with 10^7-fold enrichment after two cycles of the selections (Tawfik & Griffiths, 1998).

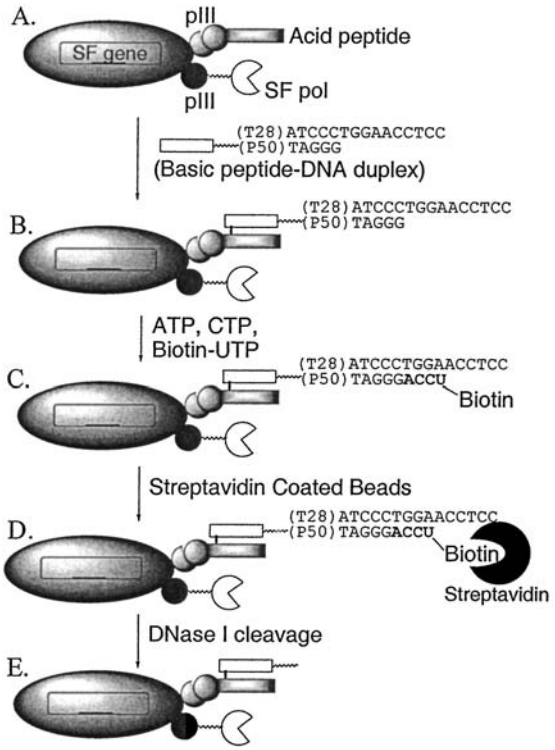

Figure 1.3 The phage selection scheme. (A) Phage particle with displayed polymerase and acidic peptide. (B) Ribonucleotide substrate attachment. (C) Biotinylation of phage particles displaying active polymerases. (D) Immobilization of biotin-tagged phage particles with strepavidin beads. (E) Release of immobilized phage by DNase I cleavage (Xia *et al*., 2002).

Griffiths and coworker extended the application of the compartmentalization approach to the directed evolution of a phosphotriesterase using a microbead to link the gene, the translated enzyme, and the enzyme product as shown in Figure 1.4. The enzyme product on the bead was selected by affinity purification or alternatively using flow cytometry (Griffiths & Tawfik, 2003).

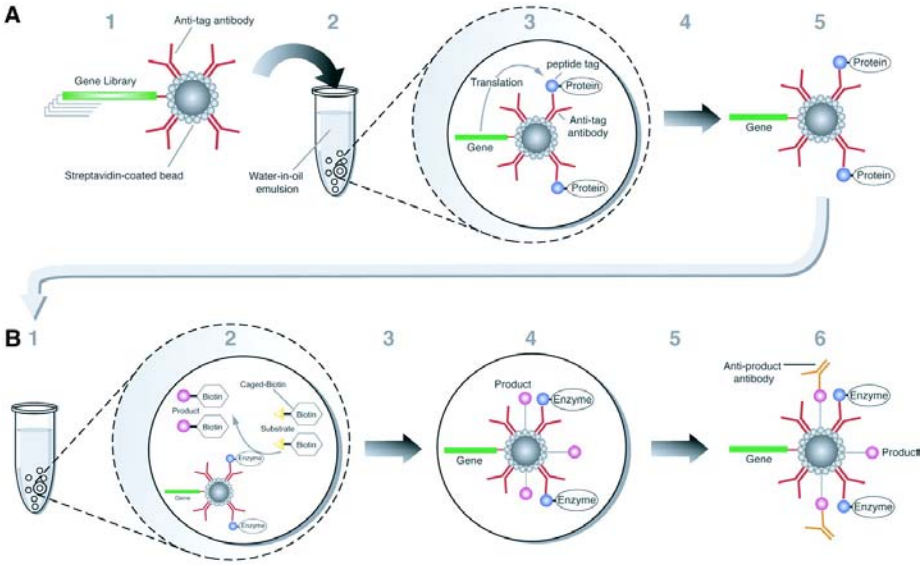

Griffiths & Tawfix, *The EMBO Journal*, Vol. 22, 2003

Figure 1.4 *In vitro* compartmentalization applied to screening method based on linking genotype and phenotype using water-in-oil emulsions. (A) Creation of microbead-display libraries. (B) Enzyme selection by compartmentalization. Product-coated beads can then be enriched (together with the genes attached to them) either by affinity purification or, after reacting with a fluorescent labeled antibody, by flow cytometry (Griffiths & Tawfik, 2003, Tawfik & Griffiths, 1998).

Screening method for a desired enzyme activity

When the genetic selection approach is not available, screening methods are chosen, because screening methods are more applicable, adaptable and simple to set up. In screening methods, the individual microorganisams, usually in the form of colonies of bacteria or yeast on agar plates or in microtiter plates, are examined after physical separation, purification and assays for enzyme activity.

The **microplate screening approach** was used successfully in several enzyme systems such as proteases (Zhao & Arnold, 1999), lipases, and oxygenases (Joo *et al*., 1999). Although, the advantage of screening systems in a 96-well microplate is that product formation is directly detected, the approach is often time-consuming and resource intensive, limiting library size about 10^3-10^4.

In recent years, however, high-throughput technologies have been developed for the screening of large libraries by means of more sophisticated instruments (Turner, 2003). The development of automation and miniaturization is facilitating such screening methods. **A robotics system** has also been introduced that alleviates the iterating steps for assaying huge numbers of individuals libraries (10^6-10^7) so as to save time and cost. A new approach using high-throughput **digital imaging** has been used for the discovery and directed evolution of oxygenases coupled with horseradish peroxidase (HRP) (Joo *et al*., 1999, Joo *et al*., 1999b). Recently, **flow cytometry** has been applied to directed enzyme evolution (Olsen *et al.*, 2000, Olsen *et al.*, 2003b).

In summary, the major factors of selection and screening methods in directed enzyme evolution include; 1) compartmentalization or linkage of genetic information and enzyme activity, 2) isolation of the enzyme product/down stream consequence such as survival or faster growth, and 3) rescue of the genetic information of the desired enzyme from selected compartments.

1.3 FACS FOR HIGH THROUGHPUT SCREENING

Flow cytometry can measure certain physical and chemical characteristics of cells or particles when they pass one by one through a sensor. In a sense a flow cytometer can be considered as a fast and specialized fluorescence microscope with computer analysis. Physical characteristics such as cell size and shape can be examined by light scattering. Cell components or functions are detected using fluorescent compound. FACS has recently been applied to the identification and isolation of more fit variants from large libraries in the directed evolution studies of proteins such as scFv antibodies and enzymes in *E. coli* (Daugherty *et al.*, 1998, Daugherty *et al.*, 2000b, Olsen *et al.*, 2000)

1.3.1 Fluorescence

Many researchers have exploited fluorescent probes to study complex biomolecular assemblies because they are very sensitive for the detection of tiny amount of particular components inside living cells. Fluorescence can be explained by a three-stage process (sequential Stage 1, 2, and 3) in Figure 1.5 (Haugland, 1996). The fluorophore is excited (Stage1), relaxed to a singlet excited state (Stage 2), and then detected by emission (Stage 3), repeatedly. The emission energy in Stage 3 is always lower than the excitation energy, and therefore the wavelength of emission is longer than that of excitation (e.g. Ex = 495 nm and Em = 519 nm for green fluorescein dye).

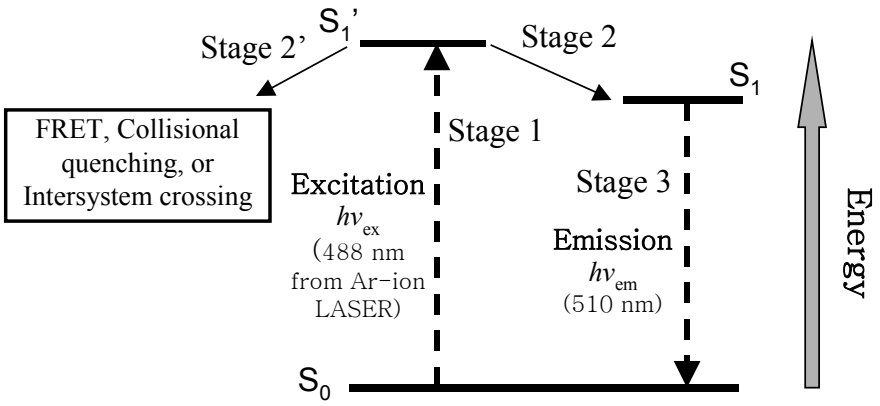

Figure 1.5 Jablonski diagram illustrating the processes involved in the creation of an excited electronic singlet state by optical absorption and subsequent emission of fluorescence (Haugland, 1996). At the Stage 1, the fluorescent dye is excited by a photon of energy hv_{ex} to electronic singlet state (S_1'). The excited state (S_1) exists for a finite time (typically 1–10 nanoseconds). At this S_1' state, the fluorophore undergoes conformational changes and is also subject to a multitude of possible interactions with its molecular environment such as collisional quenching, FRET, and intersystem crossing (Stage 2'), which may also reduce the Stage 2 process. In Stage 2, most of the energy of S_1' is partially dissipated to a relaxed singlet excited state (S_1) unless Stage 2' processes govern the environmental condition. At Stage 3, a photon of energy hv_{em} is emitted and the molecules of the relaxed singlet excited state (S_1) return to the ground state (S_0).

The difference in wavelength is called the Stokes shift, and fluorescence techniques use the Stoke's shift for detection. High fluorescence detection sensitivity is achieved by selection wavelength filter to contrast the original signal of background. The detected light is at a different wavelength than the excitation by a selective wavelength filter. Hence, there is very little background excitation light (Haugland, 1996). In contrast, absorption spectrophotometry, such as UV or IR, usually detects transmitted light at the same wavelength, which causes relatively high incident light levels as background. Extinction coefficient (ε) and fluorescence quantum yield (QY) are key factors for the efficiency of fluorescence. The fluorescence quantum yield (theoretical maximum QY = 1) is expressed by the ratio of fluorescence emission energy to absorption of excitation energy.

The major elements of fluorescence detection instruments are an excitation source, a fluorophore, wavelength filters to isolate emission photons from excitation photons and a detector that records emission photons. On the basis of the four elements, the well-known fluorescence instruments in general use are spectrofluorometers and microplate readers, fluorescence microscopes, and flow cytometers. The wavelength of typical excitation sources in flow cytometers or fluorescence microscopes is the 488 nm spectral line of an argon-ion laser. Fluorescein or BODIPY fluorescent dyes can be excited by this laser, and they emit around 510 nm.

1.3.2 Fluorescence Resonance Energy Transfer

Fluorescence Resonance Energy Transfer (FRET) phenomena and collisional quenching effects provide useful fluorescence probes for detecting spatial changes in the studies of molecular proximity in biochemistry and biology (Cristobal *et al*., 1995). FRET depends on the inverse sixth power of the intermolecular separation between two dye molecules (Stryer & Haugland, 1967). The excited energy of a donor molecule is transferred to an acceptor molecule without emission of a photon. The Förster Radius (R_0) is the distance at which energy transfer is 50% efficient;

expressed by the equation; $R_0 = \{8.8 \times 10^{23} \cdot \kappa^2 \cdot n^4 \cdot QY_D \cdot J(\lambda)\}^{1/6}$ Å, where κ^2 = dipole orientation factor (range 0 to 4; κ^2 = 2/3 for random orientation), n = refractive index, QY_D = The fluorescence quantum yield of the donor, $J(\lambda)$ = spectral overlap integral as shown in Figure 1.6. The Ro value of typical donors and acceptors are 33 to 60 Å in Table 1.1 (Haugland, 1996).

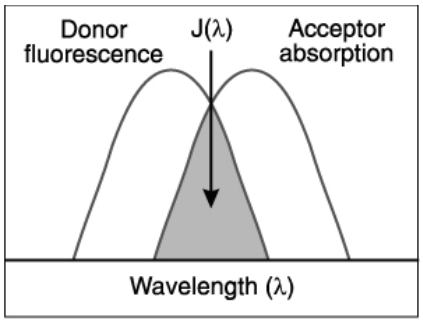

Figure 1.6 Schematic representation of the FRET spectral overlap integral (Haugland, 1996).

Donor	Acceptor	R_0 (Å)
fluorescein	tetramethylrhodamine	55
EDANS	DABCYL	33
BODIPY FL	BODIPY FL	57

Table 1.1 Förster Radius (R_0) values of typical fluorescent dyes (Haugland, 1996).

1.3.3 Fluorescence activated cell sorter (FACS)

A flow cytometer (also called a Fluorescence Activated Cell Sorter (FACS)) can identify and quantify individual cells in a flowing stream from thousands of non-fluorescent or different sized cells. FACS can be used for a directed protein evolution study when the desired cells are fluorescent while unwanted negative cells are not. The cells may express fluorescent molecules such as the green fluorescent

protein (GFP) or they might have specific molecules that are bound by fluorescent probes.

To sort out the desired protein in *E. coli*, the cells harboring active protein must be labeled by a fluorescent probe as described in Figure 1.7. Using fluorescence as a signature of activity, a FACS can identify and isolate fluorescent cells, which are the only ones containing the active protein. For example, if cells expressing active antibodies are labeled specifically by a hapten-fluorophore probe, then these cells can be isolated away from all others. The sorted cells are usually allowed to grow on an agar plate or in a liquid culture and then verified as being active through a secondary activity screen. In addition to sorting out scFv with higher affinity, FACS can be applied to the screening of large libraries of protein mutants expressed in microorganisms quantitatively for desired functions, including ligand binding, catalysis, expression levels and stability (Daugherty *et al.*, 2000b).

FACS can also be used to screen DNA content or the expression level of green fluorescent protein (GFP). Additional applications include screening for expression levels of GFP itself as an indirect reporter. For example, a sophisticated expression system for GFP was developed to study the bacterial twin-arginine translocation pathway (DeLisa *et al*., 2002). The expanded application of FCAS is potentially practical for any field when cells are specifically labeled directly as in scFv screening or indirectly as a consequence of biological processes as in the directed evolution of proteases (Olsen *et al*., 2000)

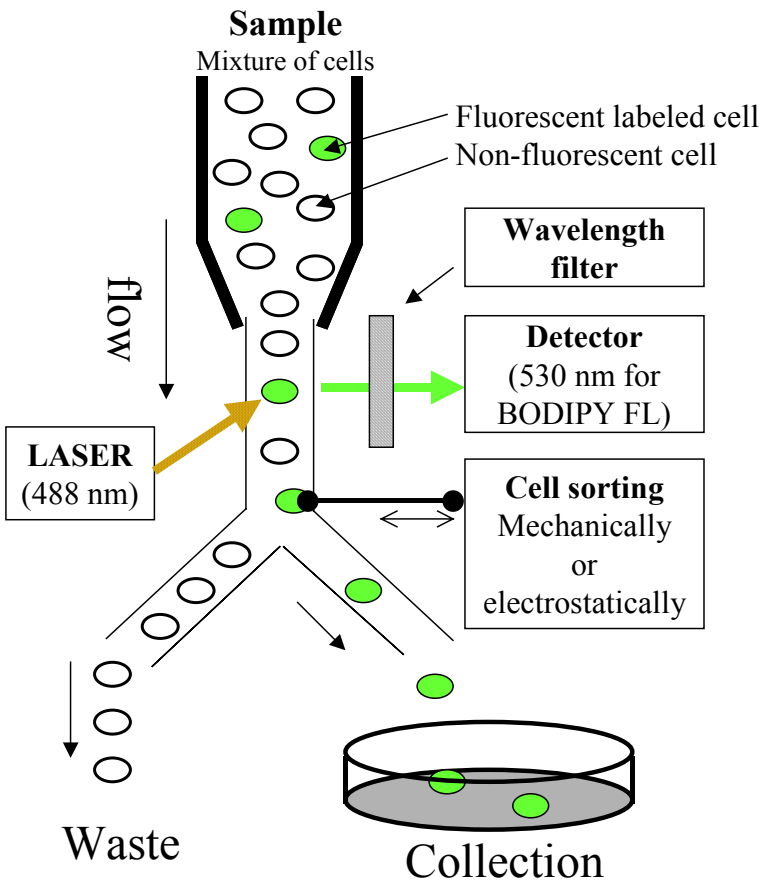

Figure 1.7 Description of the principles of a fluorescence activated cell sorter (FACS). The single cells from a sample of interest, typically labeled with a fluorescent probe, are passing and forming a central core within a fluid sheath of a fast flowing stream. The flowing individual cells are introgated by a laser and then the scatter and fluorescence signals of the cells are detected. Only the fluorescent-labelled cells (green particle in the figure) are sorted out mechanically (Becton-Dickinson FACSCalibur®) or electrostatically (MoFlow®) while the unlabeled, unwanted cells or particles are discarded to a waste tank. Generally, regions and gates of the FACS program define the wanted sub-populations from the major population of cells.

Larger libraries may result in protein variants with significant improvements. This was recently demonstrated in the isolation of an antibody with higher affinity from a library created with a high error rate (Daugherty *et al*., 2000a, Sheets *et al*., 1998). Hence, the key for successful directed evolution is the selection or screening method. Mechanic capture FACS system such as in Becton-Dickinson FACSCaribur® processes up to 10,000/sec, but sorts less than 300/second. Electrostatical sorting FACS systemsn such as Cytomation MoFlow® can process and sort up to 100,000 cells/second. Screening rates of FACS are obviously fast, compared to traditional microplate assays! Flow cytometry can screen 10^6-10^7 sized library routinely in about 30-90 minutes (Wittrup, 2000).

FACS has been used to screen large libraries of the protease OmpT (Olsen *et al*., 2000). In spite of the potential power of FACS screening for directed evolution applications, its use has been rather limited. This is true in part because the application of flow cytometry to directed enzyme evolution raises several technical issues; 1) localization or compartmentalization of an enzyme product, 2) detection of the enzyme product by FACS; 3) compartmentalization of a target enzyme while still allowing access to the enzyme substrate; and 4) how toxicity can be avoided when an enzyme is overexpressed in *E. col*.

Compartmentalization is an important factor for directed evolution. It consist of three essential elements; the gene, the functional protein encoding the gene, and the capture of fluorescent ligands or enzyme products. In short, a physical link must be made between the phenotype and genotype. Assaying activity in the expressing host would be ideal. This can be achieved by using FACS as the functional assay and compartmentalization inside *E. coli.* In case of scFv antibody, the compartmentalization of protein function (antibody affinity) is simple because the antigen stays attached to the active protein (scFv antibody) that is displayed on the cells. However, compartmentalization of enzyme activity (protease product from peptide substrate) is more problematic since products can diffuse from the cells upon release by the enzyme. Recently, a clever substrate design by Olsen *et*

al. (Olsen *et al*., 2000) solved the compartmentalization issue for enzymes. The enzyme is displayed on the *E. coli* surface and the positively charged product electrostatically binds to the cellular surface, which has a strong overall negative charge. The FRET system of the substrate designed by Olsen *et al* (Olsen *et al*., 2000) enable a FACS machine to distinguish an active enzyme from inactive variants in the library, since intact substrate is not fluorescent and substrate cleavage separates quencher and fluorophore leading to a fluorescent signal.

The substrate access issue is resolved by expressing the protein on the outer surface of the outer membrane of *E. coli.* A native bacterial outer membrane protease (OmpT) was chosen for directed 'enzyme' evolution (Olsen *et al*., 2000). It was thought the native protease would give less damage to the cells compared with expressing large amounts of a foreign protease on the outer surface.

To overcome toxicity issues with non-native enzymes, they can be expressed in the periplasm or on the surface of *E. coli*. Substrate accessibility to the enzyme is an additional problem for enzymes expressed in periplasmic space of *E. coli*, so that substrate outer membrane permeability should be considered.

1.4 EXPRESSION OF PROTEINS IN *E. COLI* FOR COMPARTMENTALIZATION

1.4.1 Protein display on bacteriophage

Peptide or protein libraries are now routinely presented on the surface of filamentous phage. For instance, single-chain variable fragments (scFv) are generally fused and displayed on the *N*-terminus of g3p (pIII) protein at the filamentous phage (M13) tip. Panning has been used as a powerful selecting method for ligand binding protein on phage. After phage libraries displaying scFv are incubated with an immobilized antigen, unbound phages are discarded by washing and the remaining phages that have specific scFv with high affinity are recovered by disrupting the scFv-antigen interaction. Using the phage display technology, high affinity scFv antibodies displayed on phage are successfully

selected from large mutant libraries after several rounds of panning (Azzazy & Highsmith, 2002, Kretzschmar & von Ruden, 2002). This panning procedure is not amenable to enzyme assays, however.

1.4.2 Protein display on the surface of bacteria

Protein display on the surface of *E. coli* or yeast is an alternative to bacteriophage display. Functional scFv antibodies that are expressed on the surfaces of *E. coli* or yeast (Boder *et al*., 2000b) have been successfully screened and isolated by flow cytometry. In our laboratory, the technology for the successful FACS screening of an scFv(anti-digoxin) antibody expressed on the external surface of the outer membrane of *E. coli* has been performed. In this case, the scFv antibody was fused to an Lpp-OmpA'(46-159) sequence to target the scFv antibody to the outer surface of the outer membrane. A fluorescently labeled hapten, a digoxin-BODIPY conjugate, was allowed to bind specifically to the functional scFv(anti-dig) antibody on the surface. Cells expressing high affinity scFv antibodies on their surface are highly fluorescent and can be distinguished from excess of control cells that do not have the high affinity scFv antibody (Francisco *et al*., 1993).

Although protein display technologies have proven to be one of the most useful tools for protein engineering, especially the selection of peptides and proteins including antibodies, there are some limitations. Anchoring the protein of interest on the surface of biological particles may reduce the assortment of target proteins that can be displayed, since in some cases the soluble form is required for function. In addition, dimeric or multimeric proteins that are composed of more than one polypeptide may not form functional, correct complexes because the anchor can hamper assembly. Expression as the *C*- or *N*-terminal fusion required for protein display may also have an undesirable effect on protein folding, stability and function. For example, the surface displayed scFv(a-dig) fused on the Lpp-OmpA mentioned above cannot bind a fluoresently labeled hapten with high molecular

weight. The binding site of the scFv antibody is thought to face down and be encircled inside of the forest of LPS on the outer membrane (detail discussion in chapter 4). In addition, the export and presentation of target proteins that are fused with an anchor can cause a dramatic loss of cell viability.

1.4.3 Expression of protein in the cytoplasm of bacteria

Other locations of target protein expression can be considered to overcome weakness of display technologies. For example, the target protein can be expressed in the cytoplasm of *E. coli*. The advantage of cytoplasmic expression is that a high molecular protein of interest can be expressed presumably with the help of the many chaperones in the cytoplasm. However, due to the reducing environment in the cytoplasm disulfide bonds do not form and therefore the protein that contain essential disulfide cannot be expressed as active form in the cytoplasm. Recently, Levy and coworker in our laboratory showed that an scFv antibody requiring disulfide formation is expressed in active form in the cytoplasm of a *trxB gor* mutant strain of *E. coli* with an engineered 'oxidizing' cytoplasm (Levy *et al*., 2001).

1.4.4 Expression of protein in the periplasm of bacteria

Cytoplasmic expression, however, has other disadvantages. First, a cell is likely to be sensitive to a toxic protein expressed in the cytoplasm at a high level. The toxic protein, especially non-specific protease or exogenous protein, probably disturbs essential, biological processes in the cytoplasm. Furthermore, the two barriers, the outer membrane and the inner membrane limit accessibility of any fluorescent-labeled probe or substrate.

Another choice for protein targeting is the periplasmic space of *E. coli*. Periplasmic expression of target proteins is somewhat more flexible. The two *E. coli* membranes serve as an *in vivo* compartment which allows the target proteins to be soluble, and/or multimeric complex without attached anchors. Not only the Sec

pathway for an unfolded polypeptide but also the twin-arginine translocation (Tat) pathway is available for secretion into the periplasm. The Sec pathway is suitable for a protein like an scFv antibody that needs disulfide formation. In contrast, a protein that should be folded in the cytoplasm or contain a cofactor can be transported to the periplasm through the Tat pathway.

A major advantage of periplasmic expression is to diminish toxicity. An example of expressing a toxic protein in *E. coli* is trypsin. A free, matured trypsin was expressed in the periplasm of *E. coli* using a leader sequence (Higaki *et al*., 1989, Vasquez *et al*., 1989). Consequently, the leader peptide is cleaved to result in an active enzyme (Huber & Bode, 1978). Furthermore, the periplasm provides an oxidizing environment that allows disulfide bonds to form correctly.

Periplasmic expression has the potential advantage of placing limitations on probe accessibility. Proteins displayed on the surface are in general less sensitive to the size of the probes that can detect the activity of the protein. However, only a small molecule (> 650 kDa) can diffuse in and out of the periplasmic space though the outer membrane of *E. coli* (Decad & Nikaido, 1976). Thus, the outer membrane is not only working as a biological envelope to hold periplasmic target proteins but also as tough barrier to the external probes penetration.

1.5 PERMEABILITY OF OUTER MEMBRANE OF *E. COLI*

1.5.1 Structure of outer membrane of *E. coli*

Gram-negative bacteria are enclosed by two bilayer membranes, the outer membrane and the inner membrane with peptidoglycan layer sandwiched in between, while gram-positive bacteria have a thicker peptidoglycan layer but no outer membrane. The outer membrane consists of phospholipids, **lipopolysaccharide (LPS)** and outer membrane proteins such as porins and OmpA depicted in Figure 1.8. LPS is a unique component of the gram-negative bacterial outer membrane and an immunogenic glycolipid ("superantigen") that contributes to

endotoxic shock (lethal endotoxemia) as a result of binding of LPS receptor CD14 and the serum protein, lipopolysaccharide binding protein (LBP) (Wright *et al*., 1990). The structure of the outer membrane bilayer is highly asymmetric. The LPS molecules constitute the outer leaflet of the outer membrane and the inner leaflet is occupied by the phospholipids whose composition is similar to that of the inner membrane. Only a few phospholipid molecules are thought to exist in the outer leaflet of outer membrane. There are ~ 3 x 10^6 LPS molecules which cover 4.9 um^2 of 6.7 μm^2 outer surface and ~ 9 x 10^6 phospholipids which cover 4.1 μm^2 of 6.4 μm^2 inner surface of *E. coli* (Nikaido, 1996, Raetz, 1986, Smit *et al.*, 1975).

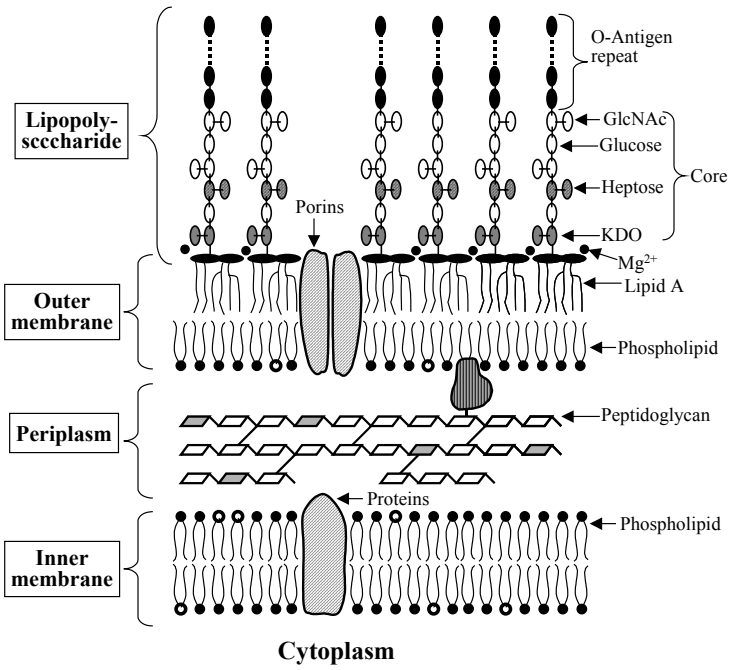

Figure 1.8 Molecular structure of the envelop of *E. coli*. Small ovals are sugar residues. KDO is a 3-deoxy-D-manno-octulosonic acid (Raetz, 1996).

The LPS molecule is composed of three covalently linked domains (Figure 1.7). (i) Lipid A domain is a polar lipid of unusual structure, in which a backbone

of a β-1'-6-linked disaccharide glucosamine is acetylated with six or seven saturated fatty acid residues, phosphorylated, and further glycosylated. The hydrophilic part of LPS is functioning as the membrane anchors in the outer membrane. The lipid A is responsible for pathophysiology in some gram-negative bacerial infections (Khan *et al*., 1998, Masihi *et al*., 1988, Raetz, 1993). The minimal LPS (Re chemotype) for growth of *E. coli* contains lipid A glycosylated with two 3-deoxy-D-manno-octulosonic acid (KDO) residues (Schnaitman & Klena, 1993). (ii) Core domain containing the two KDOs and an additional 6 to 10 core sugars in *E. coli* K-12 strain is a phosphorylated, branched, and non-repeating oligosaccharide. The proximal part of the core oligosaccharide and the disaccharide backbone of the lipid A are highly negatively charged (Boman & Monner, 1975, Schnaitman & Klena, 1993). Strains lacking the phosphate-containing substituents on heptose or lacking the heptose region of deep rough phenotype (*waa* (formerly *rfa*) genes locus) are able to grow but they are hypersensitive to antibiotics and detergents (Brabetz *et al.*, 1997, Kadrmas *et al.*, 1998, Yethon *et al.*, 1998). The core domain and outer membrane protein are involved in outer membrane permeability. (iii) The O-antigen polymer is a repeating immunogenic oligosaccharide that may increase virulence of gram-negative bacteria by preventing phagocytosis. Laboratory strains of *E. coli* K-12 and B do not have the O-antigen because of mutation of *rfb* gene (Ra chemotypes).

1.5.2 Outer membrane as permeation barrier

Many gram-negative bacteria are resistant to hydrophobic antibiotics (macroildes, novobiocins, rifamycins, actinomycins, and fucidic acid) because the outer membrane of gram-negative bacteria is known as a permeability barrier to hydrophobic compounds, such as antibiotics, detergents, dyes, and large molecules (Nakae & Nikaido, 1975). Small hydrophilic molecules are allowed to cross the membrane by simple diffusion and/or through the non-specific channels formed by outer membrane porins. However, the outer membrane tends to exclude large

compounds. Hydrophobic solutes that diffuse rapidly across the typical biological membranes by dissolving into the lipid interior are thought to penetrate through the outer membrane only very slowly because of the unique LPS.

The molecular basis of the integrity of the outer membrane lies in its LPS. The LPS of the outer leaflet of the outer membrane is involved in reducing the permeability to lipophilic solutes (Decad & Nikaido, 1976, Nikaido, 1976). The lipophilic solute first squeezes into the hydrocarbon interior of the bilayer. The formation of transitory crevice in the bilayer may be caused by the movement of glycolipid molecules or by intramolecular movement between the hydrocarbon chains in one lipid molecule (Labischinski *et al*., 1985). The saturated hydrocarbon chains of LPS form a quasicrystalline structure and have very low fluidity. Six or seven hydrocarbon chains in each LPS provide for a very high energy interaction to another neighboring LPS molecules (Takeuchi & Nikaido, 1981), compared to prevalent glycerophospholipid molecule that has only two fatty acid chains (Guo *et al*., 1998). Divalent cations such as Mg^{2+} and Ca^{2+} neutralize the electrostatic inter-LPS repulsion caused by the many negatively charged groups in the inner core and diglucosaminic backbone of lipid A of each LPS. The polyanionic LPS molecules, which have highly ordered quasicrystalline arrangements, are electrostatically linked to each other by divalent cations (Mg^{2+} or Ca^{2+}) to form a stable structure of the outer membrane as in Figure 1.9A. Hence, the outer membrane is a remarkable barrier and the cation-binding sites of LPS are essential for the integrity of the outer membrane.

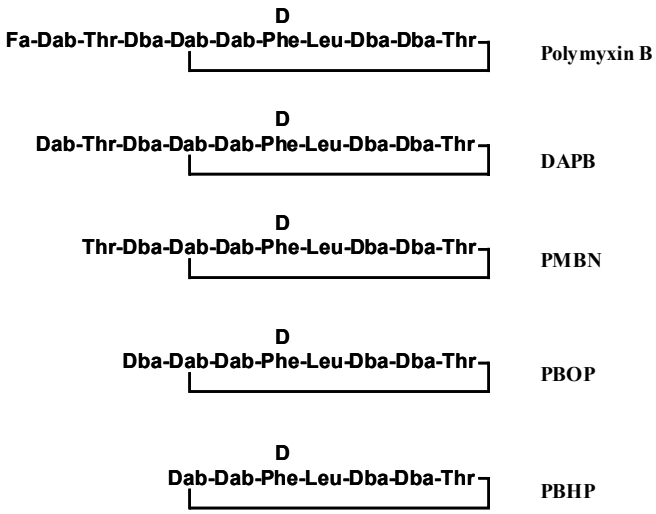

Figure 1.9 Structure of polymyxin B (PM B) and its derivatives; deacylpolymyxin B (DAPB), polymyxin B nonapeptide (PMBN), polymyxin B octapeptide (PBOP), polymyxin B heptapeptide (PBHP). Fa; fatty acid. Dab: α,γ-diaminobutyric acid. D on Phe; configuration of D-Phe amino acid. (Viljanen *et al*., 1991)

1.5.3 Permeabilizers of outer membrane

EDTA chelates Mg^{2+} and Ca^{2+} and it is able to disorganize the outer membrane and increase permeability. Lactic acid, an additive in food, is a potent outer membrane-disintegration agent because it causes LPS release and sensitizes bacteria to detergents or lysozyme (Alakomi *et al*., 2000). Derivatives of the polymyxin, natural polycationic antibiotics, form a complex with LPS and disorganize the outer membrane without lethal action, allowing increased permeability of hydrophobic molecules including some antibiotics. In addition, various antibacterial cationic peptides from vertebrate and invertebrate host tissues have been discovered as well as other permeabilizing agents (Nikaido, 1996).

EDTA has profound effect on the outer membrane permeability barrier of gram-negative bacteria. The removal of stabilizing divalent cations by chelation from their binding sites in the lipid A domain of LPS results in weakened LPS-LPS interactions and the release of a significant proportion of LPS from the cells.

Under certain conditions, the outer membrane becomes ruptured and permeable to macromolecules although prolonged treatment with EDTA is lethal. The EDTA-treated outer membrane allows the penetration of hydrophobic molecules due to the loss of LPS because the loss of LPS lets phospholipids appearing in the outer leaflet of the outer membrane. The phospholipid patches on the outer leaflet act as diffusing channels so that small hydrophobic compounds can penetrate through them. A short treatment of EDTA sensitizes *E. coli* to many antibiotics (erythromyxin, rufampin, novobiocin, actinomycin and cloxacillin) by a factor of 70 to 2300. Excessive Ca^{2+} also increases permeability of the outer membrane by freezing the LPS, which can 'cracks' the outer membrane due to an increase of its melting temperature (Brass, 1986, Bukau *et al*., 1985).

Polymyxin, a pentacationic amphipathic lipopeptide antibiotics, consists of a heptapeptide ring and a fatty acid tail. Bactericidal effects of polymyxin against gram-negative bacteria are the result of a dual action mechanism. The peptide ring part of polymyxin (Morris *et al*., 1995) helps permeabilize the outer membrane (non-lethal action) and the fatty acid tail of polymyxin causes leakage of cytoplasmic components (lethal action) (Vaara & Vaara, 1983b). Polymyxin derivatives lacking the fatty acid tail conserve a remarkable outer membrane permeabilizing action but lose their bactericidal effect (Kimura *et al.*, 1992, Morris *et al.*, 1995, Vaara & Vaara, 1983a, Viljanen *et al.*, 1991). The structure and permeabilizing effect of polymyxins are shown in Figure 1.9 and Table 1.2 and 1.3 (Vaara, 1992, Viljanen *et al.*, 1991). The polymyxin B nonapeptide (PMBN), one of the derivatives of polymyxin B, is not toxic to *E. coli* and *S. typhimurium* at over 300 μg/ml, but very low concentrations (0.3 to 1 μg/ml) are sufficient to permeabilize the outer membrane. The PMBN treatment for permeabilization does not release periplasmic proteins although PMBN binds to LPS of the outer membrane (Vaara & Vaara, 1983c).

Polycationic peptide (permeabilizer)	MIC (μg/ml)[a]	OM-permibilizing conc. (μg/ml)[b]
Polymyxin B	1	0.3-1
DAPA	10-30	0.3-1
PMBN	>300	0.3-1
PBOP	>300	1-3
PBHP	>300	1-3
Linearized PMBN	>300	>300
$Polylysine_{20}$	30-100	0.3-3

Table 1.2 Growth inhibiting and OM permeability-increasing properties of polymyxin derivatives and lysine polymer in *E. coli*. [a] Minimal concentration of the polycations to inhibit bacterial growth. The lower number means more toxic to cells. [b] Minimal concentration of the polycations required to decrease MICs of hydrophobic antibiotics. The lower number of OM-permibilizing concentration of the peptides has more sensitizing effect to the bacteria that implies more OM-permeabilizing effect. (Viljanen *et al*., 1991)

Antibiotics	MIC[a] of antibiotic only	MIC[a] of antibiotic with PMBN[b]
Rifampicin	10	0.1
Erythromycin	100	10
Novabiocin	30	3
Fusidic acid	300	10
Clindamycin	300	3

Table 1.3 MICs of various hydrophobic antibiotics against *E. coli* with or without PMBN as a permeabilizer. [a] μg/ml as in the table 1.2, [b] 3 μg/ml of PMBN was added and PMBN is presumably not toxic to *E. coli* at the concentration which is much lower than its own MIC (>300 μg/ml). (Viljanen *et al*., 1991)

Other small polycationic peptides such as bactenecin, seminalplasmin, defencin and melittin from eukaryotic cells increase the permeability of the outer membrane but all the peptides except bactenecin are toxic to wide varieties of cells including gram-negative and gram-positive bacteria (Vaara, 1992).

1.5.4 Perturbation of the outer membrane in deep rough mutations

Deep rough mutants (Re or Rd strains) (Nikaido & Vaara, 1985) loose a part of the negatively charged inner core oligosaccharides and exhibit increased permeability of the outer membrane. Mutants which lack the entire O-antigen polysaccharide or the outer core (distal portion of the core) do not exhibit altered outer membrane permeability. The deep rough mutants are sensitive to hydrophobic antibiotics, dyes or detergents. D21f2 *E. coli* strain (Boman & Monner, 1975), a heptoseless mutant of Re chemotype, has phospholipids in the outer leaflet which might disturb LPS-LPS interactions. The weakened LPS interaction by the phospholipids in the outer leaflet causes higher permeability in the heptoseless mutant. Hydrophobic molecules go through the phospholipid region. Mechanisms for the permeabilizing effect of EDTA, PMBN and deep rough mutants have been proposed as in Figure 1.10 (Nikaido, 1996, Vaara, 1992). The key to permeability of the outer membrane is highly involved in altering of structure or arrangement of LPS to give perturbation of the outer membrane.

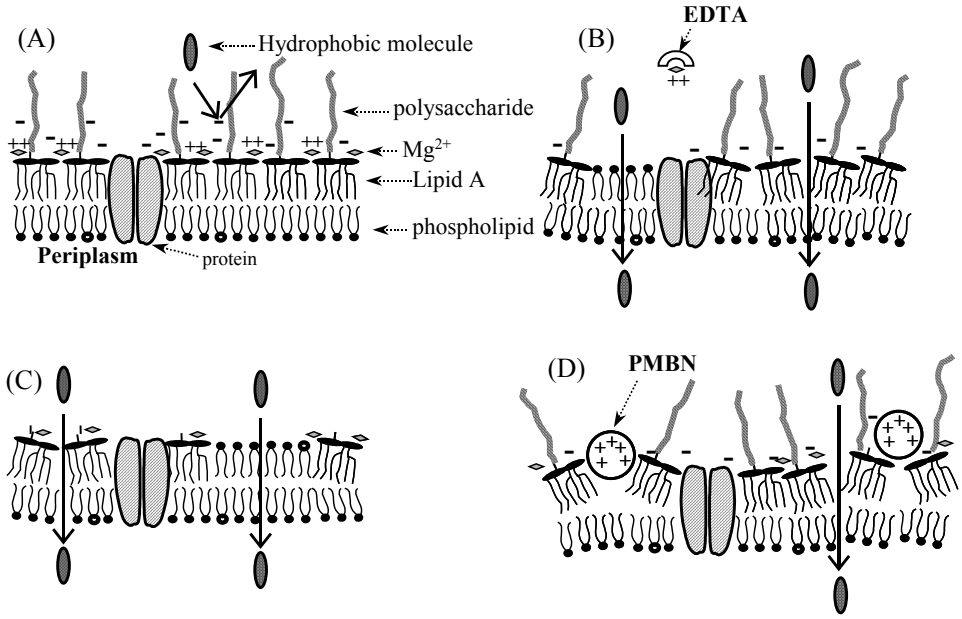

Figure 1.10 Hypothetical outer membrane structures and routes of diffusion of hydrophobic solutes through the outer membrane. (A) The intact outer membrane of untreated wild type cells consists of mostly LPS and proteins. The anionic LPS molecules are linked by divalent cations (Mg^{2+} or Ca^{2+}). Hydrophobic molecules larger than ~650 Da hardly diffuse through the bilayer because of the strong lateral interaction between the LPS molecules. (B) The EDTA treated outer membrane. Part of the LPS is missing because of removal of divalent cations by the chelation of EDTA to weaken the lateral interaction. Phospholipids presumably fill the void space and/or the superamolecular structure of remaining LPS could be distorted. Both effects could increase the outer membrane permeability. (C) Deep rough mutants (Re chemotype) (Nikaido & Vaara, 1985) lack the negatively charged core oligosaccharide. This heptoseless mutant has phospholipids in the outer leaflet which might disturb LPS-LPS interactions. The weakened LPS interaction by the phospholipid in the outer leaflet causes higher permeability in the heptoseless mutant. Hydrophobic molecules go through the phospholipid region. (D) PMBN-treated outer membranes are disturbed. Hydrophobic molecules are assumed to penetrate through the replaced phospholipids or the disturbed LPS domains, which could become more permeable as a result of alterations in the supramolecular structure. (Nikaido, 1996, Vaara, 1992)

Chapter 2

Design and synthesis of new fluorogenic autoquenching protease substrates based on an autoquenching effect

2.1 CHAPTER SUMMARY

2.1.1 Goals

Design and synthesis of new fluorogenic protease substrates employed for post-screening and enzyme kinetics following enzyme directed evolution library sorting experiments.

2.1.2 Approach

A new type of fluorogenic chymotrypsin substrate was designed and synthesized based on the autoquenching phenomenon, i.e. self-quenching of two identical fluorescent dyes in close proximity. A peptide containing a chymotrypsin cleavage site was doubly labeled with BODIPY FL dyes on both the *N*-terminus and *C*-terminus. BODIPY FL dye is a good self-quencher, i.e. it has a longer *R*o value. The new substrate was evaluated for protease activity and compared to additional substrates containing donor and acceptor dyes that operate via traditional fluorescence resonance energy transfer (FRET).

2.1.3 Results

Synthesis of the new protease substrate containing two identical fluorescent dyes (BODIPY FL) was performed in one step following peptide synthesis. Multi-step syntheses of substrates using FRET were also carried out for comparison. Hydrolysis of the autoquenching substrate **2.1** (BODIPY-EAAPY•SLRGK(BODIPY)R-NH_2) by β-chymotrypsin was more sensitive than the

other substrate tested in a microplate assay. This substrate was also found to be capable of determining enzyme catalysis parameter with a simple fluorescent assay.

2.2 INTRODUCTION

Protease activity has previously been detected by various techniques including product analysis and spectrophotometric assays. Fragments of protein substrate digested by a protease can be analyzed by protein SDS gel electrophoresis. High performance liquid chromatography (HPLC) has also been used for analysis of cleaved peptide fragments derived from synthetic peptide substrates. These methods are too time consuming to be practical for the fast screening and analysis of enzyme variants with a variety of different substrates. In addition, they are based on discontinuous measurements and imprecise so they are cumbersome to use when measuring to enzyme reaction kinetics.

Spectrophotometric methods are more commonly used for enzymatic studies. Peptide-*p*-nitroanilides (*p*NA) are often used for protease activity screening and enzyme kinetics. Succinyl-Ala-Ala-Pro-Phe-*p*NA and succinyl-Ala-Ala-Pro-Ala-*p*NA are hydrolyzed specifically by the proteases, chymotrypsin or elastase, resulting in release of a peptide and free *p*-nitroaniline (*p*NA) product, the latter of which is visible as a yellow color, detectable at 410 nm by UV-vis spectroscopy. The coupled *p*-nitroanilides (*p*NA) on the *C*-terminus of the peptide are colorless in solution with a UV absorption maximum at 315 nm. The enzymatic hydrolysis of peptide-*p*NA substrate can be detected using UV-vis spectrophotometer at 410 nm (DelMar *et al*., 1979, Kasafirek *et al*., 1976).

Using the same strategy as the chromogenic substrates, a fluorogenic substrate approach is also in common use because of the higher sensitivity that is possible with fluorescence. In its simplest from, the *p*NA is replaced by common derivatives. For example, 7-amino-3-trifluoromethylcoumarin (AFC) has been used as a leaving group on the *C*-terminus of peptide substrates enabling localization of protease activities *in situ* (Lojda, 1996). A fluorogenic substrate, *N*-

anthraniloyl-Ala-Ala-Phe-*p*NA, was also designed as a highly sensitive substrate for subtilisins based on FRET and the *p*NA leaving group (Stambolieva *et al*., 1992).

Two key residues on protease substrates are the so-called P and P' residues, which are on either side of the scissile bond. Matching sites in the protease active site are called the S and S' subsites. The specificity of the S subsites (bind the P residues) has been well-studied using chromogenic and fluorogenic substrates, having *p*-nitroaniline or coumarin groups on the *C*-termini (Backes *et al.*, 2000, Harris *et al.*, 2000, Lojda, 1996). However, not that inherent in their design, these substrates have only P residues corresponding to S subsites of protease. The P' residue is the chromophore or fluorophore, so specificity in the S' subsite cannot be analyzed. To overcome the limitation, *N*-terminus capped fluorogenic substrates that have P_1 and P_1' residues (e.g. Cbz-Arg•Arg-AMC as an OmpT substrate) were used by coupling aminopeptidase M. Enzymatically cleaved *N*-terminal substrate products were further digested by aminopeptidase M to release highly fluorescent dyes (e.g. free AMC) (Olsen *et al.*, 2000). A new substrate for the HIV-1 protease was developed based on intramolecular fluorescence resonance energy transfer (FRET). The quenched fluorogenic substrate, 4-(4-dimethylaminophenylazo)-benzoic acid (DABCYL)-Ser-Gln-Asn-Tyr•Pro-Ile-Val-Gln-5-[(2-aminoethyl)-amino]naphthalene-1-sulfonic acid (EDANS), has a natural processing site for HIV-1 protease (Figure 2.1A). The specific cleavage of substrate by the protease increases the fluorescent intensity proportionally (Matayoshi *et al*., 1990). Short internally quenched fluorescent substrates, (Abz)-Phe-Arg-X-(EDDnp) (for X = Phe, Leu, Ile, Ala, Pro, Gln, Ser, Lys, and Arg; Abz = *ortho*-aminobenzoic acid; EDDnp = *N*-(ethylenediamine)-2,4-dinitrophenyl amide) have also been reported as sensitive, specific substrates for various proteases (Melo *et al*., 2001). The FRET approach has ever been extended to protein fluorophore. Based on the FRET known effect of green fluorescent protein and a blue fluorescent protein analog, a fusion protein of the two fluorescent proteins linked by cleavage site for proteinases was used as a fluorogenic protein substrate (Tsien *et al*., 1997).

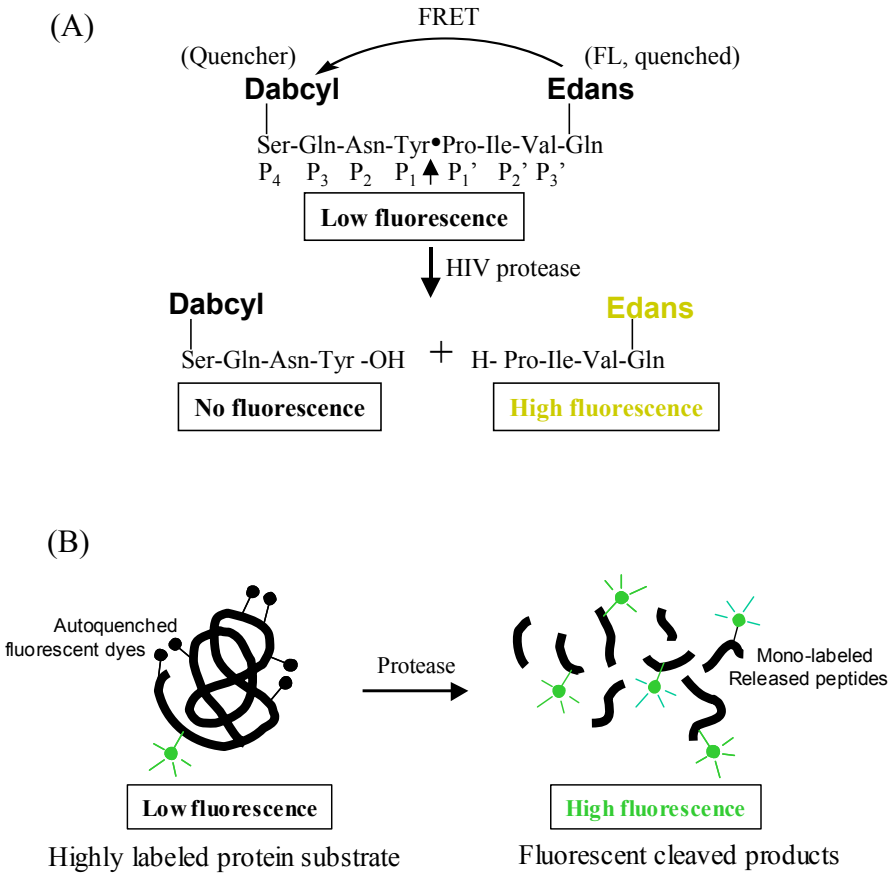

Figure 2.1 (A) Fluorogenic substrate for HIV-1 protease based on the FRET of DABCYL and EDANS. (B) Principle of enzyme detection via the disruption of intramolecular self-quenching of a protein substrate.

Some fluorescent dyes have been reported to have autoquenching (self-quenching) effect when they are in close proximity. They quench the fluorescence of each other by collisional interactions or stacking. Xanthene dyes, such as fluorescein, tetramethyrhodamine, rhodamin B, and Texas Red, are known to form dimers. A doubly labeled peptide substrate at the both *N*- and *C*- termini with tetramethylrhodamine (TAMRA) show low fluorescence because of intrmolecular dimerization (self-quenching) of the fluorophores. Enzyamatic cleavage of the substrate results in an increase in fluorescence intensity by disruption of the dimer (Blackman *et al.*, 2002, Packard *et al.*, 1996). Highly labeled casein and bovine serum protein with BODIPY or fluorescein dyes are also nonfluorescent until the monomeric BODIPY-peptide fragments are released by proteases in Figure 2.1B (Jones *et al*., 1997) and this is commonly used as a general protease assay.

Based on the autoquenching effect of BODIPY, design and facile synthesis of a new fluorogenic specific peptide substrate for chymotrypsin is demonstrated in this chapter to avoid the multistep synthesis of FRET substrate and nonspecificity of the quenched BODIPY-labeled casein substrates.

2.3 MATERIALS AND METHODS

Rink Amide resin (0.72 mmol/g) was purchased from Novabiochem (San Diego, CA). 4,4-difluoro-5,7-dimethyl-4-bora-3a,4a-diaza-*s*-indacene-3-propionic acid, succinimidyl ester (BODIPY FL-SE), 5-carboxytetramethylrhodamine, succinimidyl ester (5-TAMRA-SE), and xanthylium, 9-[2-[[4-[[(2,5-dioxo-1-pyrrolidinyl)oxy]carbonyl]-1-piperidinyl]sulfonyl]phenyl]-3,6-bis(methylphenylamino) chloride (QSY7-SE) was purchased from Molecular Probes (Eugene, OR). 4-dimethylaminopyridine (DMAP), anhydrous *N,N*-dimetylacetamide (DMA), HPLC grade acetonitrile and trifluoroacetic acid (TFA) are purchased from Aldrich (St. Louis, MO). 2,4,6-Trinitrobenzenesulfonic acid solution (TNBS, 5% in water) and bovine β-chymotrypsin were obtained from

Sigma (St. Louis, MO). The lyophilized chymotrypsin was dissolved in 20 mM Tris-HCl (pH7.5), 1mM EDTA and 10% glycerol buffer.

2.3.1 Characterization of peptides using HPLC, FPLC and MS

Analytical HPLC was carried out on System Gold® (Beckman Coulter™) HPLC system equipped using 0.5 μm ODS C18(2) Luna(R) column purchased from Supelco (Bellefonte, PA) with a gradient elution with 0.1% TFA in acetonitrile and 0.1% TFA in water from 10% to 80%. Spectroscopic data were monitored with absorbance at 214nm, 502nm, 342nm, 552nm, and 570nm for peptide, BODIPY FL, TNB, TMR and/or QSY7 derivatives, respectively.

Preparative purification was carried out on FPLC from Amersham Pharmacia Biotech AB (Piscataway, NJ) using a gradient of acetonitrile/water 0.1% TFA from 10 to 50% over ODS packing material (SOURCE 15PC® of Amersham Pharmacia Biotech AB) in 10 x 100 mm column with UV absorbance at 254nm and 365nm for detection. All reactions were monitored by analytical reverse-phase HPLC just before FPLC purification. The fractions containing a single peak on HPLC (more than 97% purity) were collected in 50 ml conical centrifuge tubes, frozen in liquid nitrogen and lyophilized. The product was dissolved in water (~0.5 ml). Concentration of product was determined by UV-vis 8452A Diode Array Spectrophotometer (Hewlett Packard).

All the peptides and conjugates were analyzed by Electrospray ionization (ESI) mass spectroscopy that was obtained on a Finigan LCQ (San Jose, CA). The unmodified peptide cleaved off from resin was also verified by Matrix-assisted laser desorption/ionization (MALDI) time-of-flight mass spectrometry that was performed on a PerSeptive Biosystems Voyager mass spectrometer without delayed extraction.

2.3.2 Automated synthesis of peptide

A standard Fmoc protocol was applied for amino acid assembly. A Fmoc protected peptide was prepared on a Rink Amide MBHA resin as solid support in 0.25 mmole scale using an automated ABI430A peptide synthesizer (Applid Biosystem) at the Peptide Synthesis Facility of the University of Texas at Austin. Double coupling steps were performed to increase purity and yields when necessary. A portion of the Fmoc protected peptide on the resin (~ 20 μmol) was swelled up with DMA in a solid phase syringe reactor of Torviq (Granger, IN). It was treated with 20% piperidine in DMA for 20 minutes twice to remove Fmoc group on the *N*-terminus and then washed thoroughly with 3ml of DMA, methanol, and methylene chloride sequentially. Completion of reaction was checked by Kaiser test (Kaiser *et al.*, 1970). The peptide was cleaved from the resin and deprotected with 95% TFA/2.5% water/2.5%TIS mixture for 2 hours, and the precipitate was collected using a centrifuge for 10 minutes at 3000 rpm and rinsed twice with 30 ml of cold diethyl ether to give a white powder. The peptide in water was passed through Sep-Pak C18 cartridge, and then eluted with 20% acetonitrile in water. The spots of each fraction on silica gel TLC plate were stained by ninhydrin in ethanol (7 mg/ml). The fractions of the peptide solution were freeze-dried and dissolved in water to a final stock concentration of 40 mM.

2.3.3 General method of doubly coupling of BODIPY-FL SE to a peptide

Prior to the preparation scale reaction (1 ~ 4 μmole), each reaction was carried out in small scale (0.02 μmole) monitored by HPLC to verify completion of the reaction.

To a mixture of the 40 mM peptide (2 μmole) in water and 25 μl of 1 M DMAP was added 40 mM 4,4-difluoro-5,7-dimethyl-4-bora-3a,4a-diaza-*s*-indacene-3-propionic acid, succinimidyl ester (BODIPY-FL SE, 2.2 equivalent, activated *N*-hydroxy succinimide ester of BODIPY FL). The reaction mixture was shaken

intermittently at room temperature for 1 hour and diluted with 5 ml of 0.1 % TFA in water. All reactions were performed in 1.5 ml Eppendorf-tubes in the dark. The product was purified by FPLC using a gradient of acetonitrile/water 0.1% TFA from 10% to 50%. The collected pure fractions of product were freeze-dried and the lyophilized product was dissolved in water (0.5 ml). The yield after FPLC purification was estimated with absorbance at 504 nm for BODIPY (ε = 82000 $cm^{-1}M^{-1}$) or at 552 nm for TMR (ε = 90000 $cm^{-1}M^{-1}$) by UV-vis spectroscopy. HPLC and ESI-MS were taken to verify purity and molecular weight of the modified peptide.

Preparation of BODIPY-EAAPYSLRGK(BODIPY)R-NH_2 (2.1)

BODIPY FL SE (2.2 eq.) in DMF, the peptide (H-EAAPYSLRGKR-NH_2) (4 μmole) in water and 35 μl of 1 M DMAP were used as in the general method. The yield after FPLC purifications was 2.3 mg (38%) of dark brown powder. ESI MS (m/z) of BODIPY-EAAPYSLRGK(BODIPY)R-NH_2 conjugate; calculated 1793.91 for M, found 1794.8 for MH^+, and 898.1 for $(MH^2)^{+2}$.

Preparation of BODIPY-EAAPASLRGK(BODIPY)R-NH_2 (2.2)

BODIPY FL SE in DMF, the peptide (H-EAAPASLRGKR-NH_2) (4 μmole) in water and 1 M DMAP (excess) were used as in the general method. The yield after FPLC purifications was 1.7 mg (25%) of dark brown powder. ESI MS (m/z) of BODIPY-EAAPASLRGK(BODIPY)R-NH_2 conjugate; calculated 1701.89 for M, found 1702.8 for MH^+, 852.1 for $(MH^2)^{+2}$.

Preparation of BODIPY-EAAPFSLRGRK(BODIPY)PR-NH_2 (2.3)

BODIPY FL SE (4 μmol) in DMF, the peptide (H-EAAPFSLRGRKR-NH_2) (2 μmole) in water and 1 M DMAP were used as in the general method. The yield after FPLC purifications was 3.9 mg (84% based on BODIPY FL SE) of dark brown powder. ESI MS (m/z) of BODIPY-EAAPFSLRGRK(BODIPY)PR-NH_2

conjugate; calculated 2001.06 for M, found 1001.7 for $(MH^2)^{+2}$, and 1012.9 for $(MH+Na)^{+2}$.

Preparation of BODIPY-AAFRARK(BODIPY)R-NH_2 (2.4)

BODIPY FL SE (3.2 μmole) in DMF, the peptide (H-AAFARKR-NH_2) (1.6 μmole, 0.5 eq. of BODIPY FL SE) in water and 1 M DMAP were used as in the general method. The yield after FPLC purifications was 1.3 mg (43% based on BODIPY FL SE) of dark brown powder. ESI MS (m/z) of BODIPY-AAFARK(BODIPY)R-NH_2 conjugate; calculated 1361.75 for M, found 1362.9 for MH^+, 682.4 for $(MH^2)^{+2}$.

Preparation of H-RAAPYSLRGK(BODIPY)R-NH_2 (2.5)

A Fmoc protected peptide on Rink Amide resin (100 mg/373 mg of 0.25 mmole scale) was cleaved off by 95% TFA and precipitated to give 25 mg of the starting peptide (Fmoc-RAAPYSLRGKR-NH_2). ESI MS (m/z) of Fmoc-RAAPYSLRGKR-NH_2 peptide; calculated 1494.82 for M, found 1495.8 for MH^+, 1609.2 for MH^++TFA, and 748.8 for $(MH^2)^{+2}$.

BODIPY FL SE (4.8 μmole) in DMA was added to a mixture of the peptide (Fmoc-RAAPYSLRGKR-NH_2) (6 μmole, 1.25 eq. for BODIPY FL SE) dissolved in water and 70 μl of 0.5 M DMAP in DMA to make the mono-labeled peptide (Fmoc-RAAPYSLRGK(BODIPY)R-NH_2). The reaction mixture was shaken intermittently at room temperature for 1 hour. When the coupling reaction was completed, 70 μl of piperidine was added to deprotected the Fmoc group and the reaction was monitored by RP-HPLC and terminated by excess TFA. The mixture was applied to FPLC purification followed by freeze-drying to give 3.16 mg (33% based on BODIPY FL SE) of orange powder. ESI MS (m/z) of H-RAAPYSLRGK(BODIPY)R-NH_2 conjugate; calculated 1546.86 for M, found 1547.8 for MH^+, 1661.3 for MH^++TFA, and 774.7 for $(MH^2)^{+2}$.

Preparation of TNB-RAAPYSLRGK(BODIPY)R-NH_2 (2.6)

To a mixture of the mono-labeled peptide **2.5** (H-RAAPYSLRGK(BODIPY)R-NH_2) dissolved in water and 0.5 M DMAP in DMA was added 5% TNBS. The reaction mixture was shaken intermittently at room temperature for 1 hour and diluted with 5 ml of 0.1 % TFA in water. FPLC purification (using a gradient of acetonitrile/water 0.1% TFA from 10% to 50%) of the product yields 100 μl of 1.39 mM solution. ESI MS (m/z) of TNB-RAAPYSLRGK(BODIPY)R-NH_2 peptide; calculated 1757.85 for M, found 1758.5 for MH^+, 880.3 for $(MH^2)^{+2}$.

Preparation of TMR-RAAPYSLRGK(BODIPY)R-NH_2 (2.7)

A product (TMRA-RAAPYSLRGK(BODIPY)R-NH_2) was prepared using TMRA SE instead of TNBS by the same method as above. FPLC purification gives 150 μl of 1.91 mM solution estimated from the absorbance at 552 nm for TMR (ε = 90000 $cm^{-1}M^{-1}$) by UV-vis spectroscopy. ESI MS (m/z) of TMR-RAAPYSLRGK(BODIPY)R-NH_2 peptide; calculated 1959.00 for M, found 980.6 for $(MH^2)^{+2}$.

Preparation of QSY7-RAAPYSLRGK(BODIPY)R-NH_2 (2.8)

A product (QSY7-RAAPYSLRGK(BODIPY)R-NH_2) was prepared using QSY7 SE instead of TNBS by the same method as above. FPLC purification gives 100 μl of 1.05 mM solution estimated from the absorbance at 560 nm for QSY7 (ε = 90000 $cm^{-1}M^{-1}$) by UV-vis spectroscopy. ESI MS (m/z) of QSY7-RAAPYSLRGK(BODIPY)R-NH_2 peptide; calculated 2187.09 for M, found 1094.5 for $(MH^2)^{+2}$.

2.3.4 Enzyme assay time dependence of the *bis*-BODIPY substrate by chymotrypsin

The autoquenching *bis*-BODIPY substrates (**2.1**, **2.2**, **2.3** and **2.4**) and the FRET substrates (**2.6**, **2.7** and **2.8**) stock solutions were diluted to 100 μM in water

and stored at –20°C. Stock solutions of lyophilized β-chymotrypsin and porcine pancreatic elastase suspension were prepared to have 0.1 to 0.6 mg/ml concentration in 0.1 M Tris-HCl (pH 7.5), 1 mM EDTA, and 10% glycerol. The enzymes were serially diluted into the same buffer without glycerol. The assays were performed in a Corning 96-well microplate. Generally, each well contained 2 μl of 100 μM autoquenching substrates or FRET substrates, 78 μl of water and 10 μl of 200 mM Tris-HCl (pH 8.0). After endpoint scanning to measure background fluorescence of the substrate, the reaction was initiated by the addition of 10 μl of 0.34 μg/ml β-chymotrypsin stock solution and stirred for 3 seconds just before fluorescence measurement. The fluorescence was monitored in a Gemini XS Microplate Spectrofluorometer (Molecular Device Corporation, Sunnyvale, CA) using an excitation wavelength of 490 nm and emission wavelength of 515 nm with 9 nm bandwidth. The fluorescence intensity was monitored every 20 seconds for 1 hour.

2.3.5 Quenching effect of the autoquenching substrate

A series of concentrations of the autoquenching substrate **2.1** (BODIPY-EAAPYSLRGK(BODIPY)R-NH_2) were prepared in water. The background fluorescence intensity of the prepared samples at 0.5, 1, 2, 3, 5, 10, 15, and 20 μM was measured in a microplate before the enzyme addition. Excess β-chymotrypsin (200 μg/ml) was added and the fluorescence intensity was monitored until the reaction was completed. One-hour incubation at room temperature was enough to measure final fluorescence intensities for 100% cleaved substrates.

For comparison of the autoquenching substrate and the FRET substrates, hydrolysis of those substrates by β–chymotrypsin was carried out with 5 μM of substrate in 20 mM Tris-HCl reaction buffer.

2.3.6 Kinetic measurement

Enzyme kinetic assays were performed in microplate wells that contained a series of concentrations of the autoquenching substrate in 20 mM Tris-HCl buffer

and 1.32 nM of β-chymotrypsin. The final concentration of the substrate ranged from 0.69 to 27.4 μM. Measurement of fluorescence intensities every 10 seconds was continued for 10 min. To determine the steady-state parameters k_{cat} and K_M for hydrolysis of substrate **2.1** (BODIPY-EAAPYSLRGK(BODIPY)R-NH_2) initial velocities were measured. The slope of the fluorescence intensity increase was determined by linear regression. The data were fitted to the Michaelis-Menten equation ($Vo = V_{max} \times [S]/(K_M + [S])$, where Vo is initial velocity, V_{max} is the maximum velocity at saturation, and [S] is the concentration of substrate, by nonlinear regression using GraphPad Prizm 4 (GraphPad Software, San Diego, CA).

2.4 RESULTS AND DISCUSSION

2.4.1 Design of autoquenching substrate

When fluorophores such as fluorescein, BODIPY FL, and BIODIPY TR-X are conjugated to casein at a high stoichiometric ratio, the self-quenching effect occurs (Jones *et al*., 1997) (Figure 2.1B). The highly labeled casein is a useful substrate for protease assays, but it is suitable for relatively non-specific proteases, such as trypsin, chymotrypsin and protease K because cleavage sites of the casein are not optimized for specific proteases. Casein or BSA might be useful for determining relative activities, but they are not suitable for enzyme kinetics because the protein substrates have many different kinds of cleavage sites.

For fast post-screening of the many enzymes isolated from large enzyme libraries, different sequences of substrates are needed to test the variant proteases with new specificities. Hence, the substrates containing only P residues with chromogenic *p*NA and fluorogenic coumarin molecules on the carboxylic end of the substrates are not appropriate. Combining the concept of the autoquenching protein substrate in Figure 2.1A and FRET substrate that has a specific cleavage site as shown in Figure 2.1B (Grahn *et al.*, 1998, Matayoshi *et al.*, 1990, Wang *et al.*, 1990), a new autoquenching peptide substrate was designed for high throughput

post-screening and easy synthesis as shown in Figure 2.2. When numerous substrates together with an automated microplate enzyme assay are used for post-screening, facile synthesis with high yield is important. The synthesis of the autoquenching substrate has one coupling and purification step and it is straightforward with a very high yield.

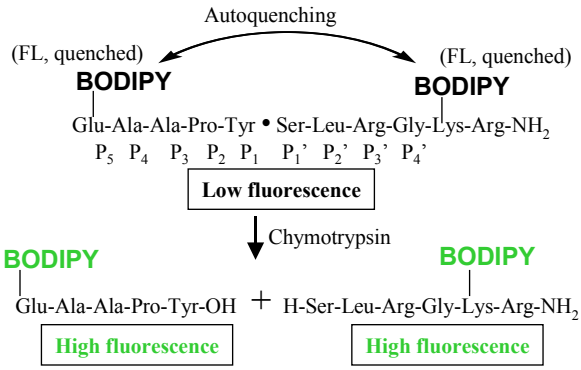

Figure 2.2 Design of proposed new *bis*-BODIPY fluorogenic substrates based on autoquenching between two BODIPY fluorophores.

There are several additional advantages of the autoquenching substrate using BODIPY over FRET substrates using EDANS/DABCYL pair. First, Fluorescence intensity is proportional to extinction coefficient (ε) and quantum yield. The BODIPY has a relatively high fluorescence quantum yield (QY= ~0.9). Moreover, the molar extinction coefficient (ε) is only 5,400 $cm^{-1}M^{-1}$ for EDANS while it is 82,000 $cm^{-1}M^{-1}$ for BODIPY FL (Haugland, 1996). Second, the Förster distance (R_o) for 50% energy transfer between two self-quenching BODIPY FL is much longer (56 Å) than that of EDANS/DABCYL pair (33 Å) (Karolin *et al.*, 1994). The longer R_o implies that more amino acids between the fluorophores can be accommodated with the same quenching effect. Third, the BODIPY emission is not sensitive to pH so a variety of reaction conditions can be used.

To develop and evaluate the new autoquenching substrate that has P and P' residues, chymotrypsin was chosen as a target protease because of its high activity and S' selectivity. The substrate sequence of P residues (P_1 to P_4) that match S

subsites of chymotrypsin is well known as Ala-Ala-Pro-Tyr (or Phe) (DelMar *et al*., 1979).

Even though the S' subsites of chymotrypsin are important in its hydrolytic activity as well as S subsites, little information for the specificity of S' subsites is available from direct chymotrypsin hydrolysis. Acyl-transfer reactions of peptide esters to assorted pentapeptide nucleophiles (amino group of the peptides) by chymotrypsin was studied as an indirect method for the S' subsite specificity (Schellenberger *et al*., 1994). A Ser-Leu-Arg peptide sequence for P' (P_1' to P_3') residues was inferred from the acyl-transfer reaction study for design of the autoquenching substrate as the hydrolysis process and the acyl transfer process are considered to show similar specificity (Fersht *et al*., 1973).

2.4.2 *Bis*-BODIPY substrate design and synthesis

At the *N*- and *C*-termini of our substrate (Ala-Ala-Pro-Tyr•Ser-Leu-Arg), additional Glu and Gly-Lys-Arg sequences were added, respectively (Figure 2.1C and 2.2A). The Glu on the *N*-terminus and Gly on the *C*-terminus were adopted as a spacer to separate the cleavage site and BODIPY FL fluorescent dyes, Lys was added to provide amino group for BODIPY FL SE conjugation, and the Arg at the very *C*-termial end of the substrate was added to increase solubility when the substrate was labeled with two hydrophobic BODIPY FL molecules. In the final structure of the substrate, the BODIPY FL molecules are located on the α-amino group of Glu on the *N*-terminus and the amino group of Lys residue around the *C*-terminus with distance of 10 amino acids.

The synthesis of the substrate was straightforward (Figure 2.3). The peptide was mixed with BODIPY FL SE and DMAP in DMA. The coupling reaction using excess of BODIPY FL SE show a trace amount of hydrophobic by-product (> 10%) which was thought to be a triply BODIPY labeled peptide based on ESI mass spectroscopy. The third BODIPY molecule is thought to be located on hydroxyl group of of either Tyr or Ser.

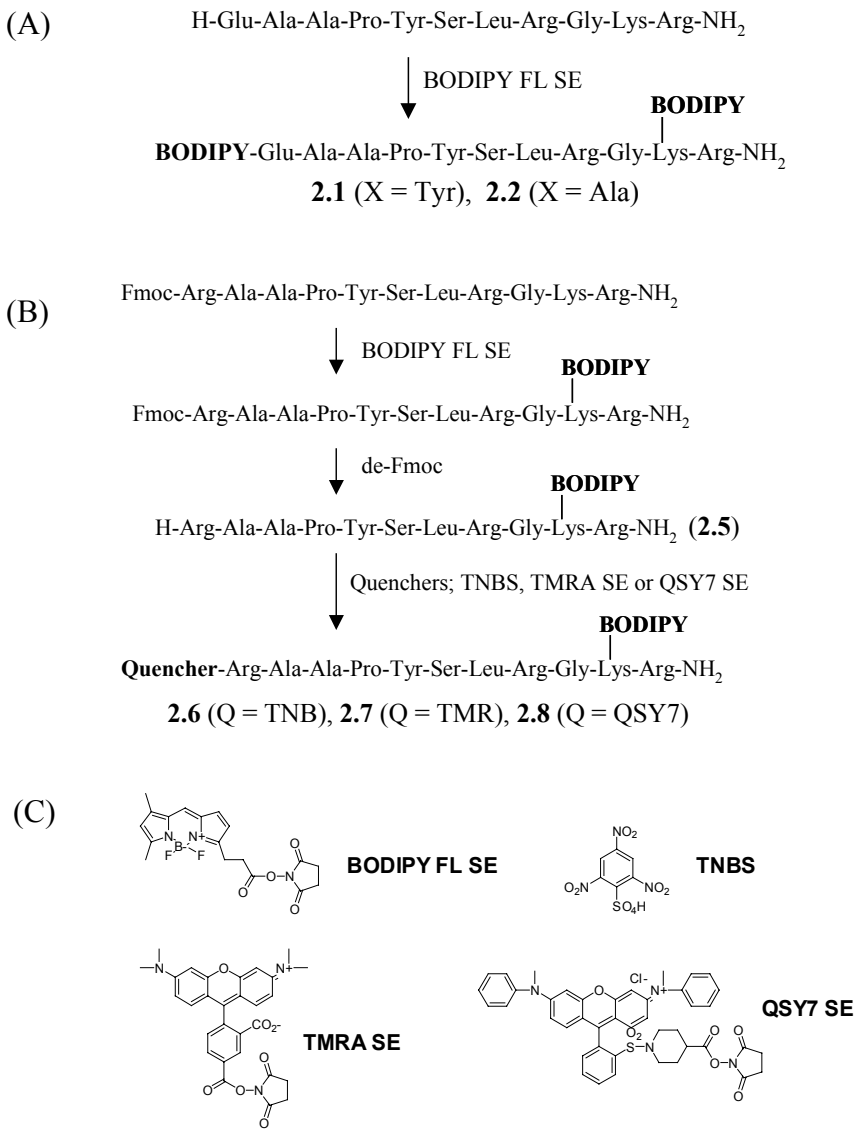

Figure 2.3 (A) Synthesis of *bis*-BODIPY autoquenching substrates. (B) Synthesis of FRET substrates. (C) Structures of coupling reagents used in synthesis of fluorogenic substrates.

To assess new FRET substrates which have different quenchers for BODIPY FL, potential molecules (TNB, TMR, and QSY7) as quenchers were placed on the

amino group of the *N*-terminus of peptide instead of BODIPY while keeping the BODIPY FL on the Lys residue.

At first, solid-phase coupling of the quenchers was attempted. Each quencher was added on the *N*-terminus of the peptide giving moderate yields of quencher coupled peptides (quencher-AAPYSLRGKR-NH_2) that were characterized with RP-HPLC and ESI mass spectrometer. Unfortunately, the next step for BODIPY coupling on the Lys residue was problematic. The reaction mixture gave complicated peaks on RP-HPLC. The major products were isolated and characterized. Unfortunately, they were found to the doubly labeled BODIPY FL peptides. The excess of BODIPY FL SE may cause the additional coupling, which also occurred as in the formation of the by-product, triply BODIPY labeled peptide, during the synthesis of the autoquenching substrate.

The solid-phase coupling of the quencher required excess of the expensive reagents (the activated quenchers) in addition to the by-product formation, so solution-phase synthesis was carried out (Figure 2.3B). The Fmoc-protected peptide on resin was cleaved off first without de-Fmoc to give an Fmoc protected peptide (Fmoc-RAAPYSLRGKR-NH_2), which has only one free amino group on the Lys residue. One BODIPY FL was labeled and Fmoc group was deprotected with piperidine for a short time to avoid the possible decomposition of the products. After FPLC purification on the mono-labeled peptide the quencher molecules were coupled on the *N*-terminus to give the final products (**2.6** for TNB, **2.7** for TMR and **2.9** for QSY7 in Quencher-RAAPYSLRGK(BODIPY)R-NH_2).

2.4.3 Assay for chymotrypsin activity with autoquenching substrate

First, HPLC assay was performed for the cleavage of the *bis*-BODIPY autoquenching substrate with detection at 504 nm wavelength in Figure 2.4. The substrate without proteolytic hydrolysis was eluted at 7.47 min as a single peak (**a**, BODIPY-EAAPYSLRGK(BODIPY)R-NH_2) in Figure 2.4A. β-Chymotrypsin digestion resulted in two product peaks by specifically cleaving a peptide bond

between Tyr and Ser of the substrate. The first peak **b** at 4.86 min in Figure 2.4B is the *N*-terminal cleavage product H-SLRGK(BODIPY)R-NH_2 and the second peak **c** at 6.53 min is the *C*-terminal cleavage product BODIPY-EAAPY-OH. The peak **b** is expected to elute earlier than peak **c** because of the three positively-charged groups of the peptide product in **b**. This was further verified by the HPLC assay with the FRET substrates that release the same *C*-terminal BODIPY labeled peptides at 4.86 min.

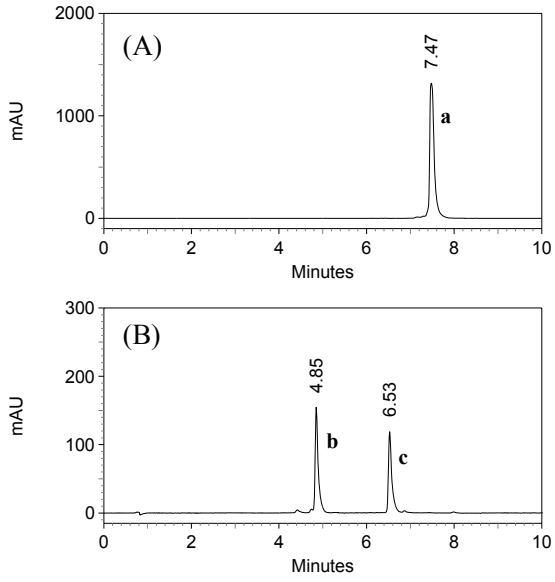

Figure 2.4 HPLC analysis of (A) the autoquenching substrate **2.1** at 504 nm for BODIPY FL before addition of β-chymotrypsin. (B) Products of the substrate (5 μM) after full proteolytic hydrolysis by β-chymotrypsin (0.32 μg/ml) at 23°C for 5 min in Tris-HCl buffer (pH 8.0). Linear gradient of 20% to 70% actoniltrile in water with 0.1% TFA in 9 min was used. (peak **a,** uncleaved substrate **2.1;** peaks **b** and **c**, mono-labeled products).

A fluorescence microplate assay was performed to verify the fluorogenic effect based on the autoquenching substrate as described in Material and Methods (*vide* 2.3.4). The time course of fluorescence intensity change by β-chymotrypsin hydrolysis at every 10 seconds for 1 hour is presented in Figure 2.5A. Cleavage of

the substrate showed a steady increase of the fluorescence intensity. No lags or initial bursts were observed. The fluorescence assay for another autoquenching substrate **2.2** (BODIPY-EAAPA•SLRGK(BODIPY)R-NH_2) that has an Ala residue on P_1 as a negative control substrate was also performed. This substrate contains a cleavage sit for elastase which is not recognized by cymotrypsin. When 2 μM of the elastase autoquenching substrate **2.2** was incubated with 50 μg/ml of elastase in Tris-HCl buffer (pH 8.0), more than 95% of the elastase autoquenching substrate **2.2** was cleaved within 5 min. The same amount of elastase can hydrolyze only less than 5% of the chymotrypsin substrate **2.1** (BODIPY-EAAPY•SLRGK(BODIPY)R-NH_2) in the same period. β-chymotrypsin (0.25 μg/ml) cleaved the chymotrypsin autoquenching substrate **2.1** (2 μM) in 2 min completely while it hydrolyzed only a trace amount of the negative control substrate **2.2**. Prolonged incubation time (2 hours) for both enzymes allowed cleavage of the their respective non-optimal substrates. Elastase showed lower activity to **2.2** compared to chymotrypsin to its substrate **2.1** because the P' residues were designed only for chymotrypsin in both substrates. Elastase has intrinsically low activity for cleavage of the substrate with Ala-Ala-Pro-Ala as P residues (P_1 to P_4). The reported catalytic efficiencies (k_{cat}/K_M) for chromogenic substrates, suc-Ala-Ala-Pro-Ala-*p*NA for porcine elastase and suc-Ala-Ala-Pro-Phe-*p*NA for chymotrypsin, were 2.9×10^5 $M^{-1} \cdot s^{-1}$ and 1.0×10^6 $M^{-1} \cdot s^{-1}$ respectively (DelMar *et al.*, 1979). This preliminary fluorescence assay showed the specificity of the autoquenching substrates.

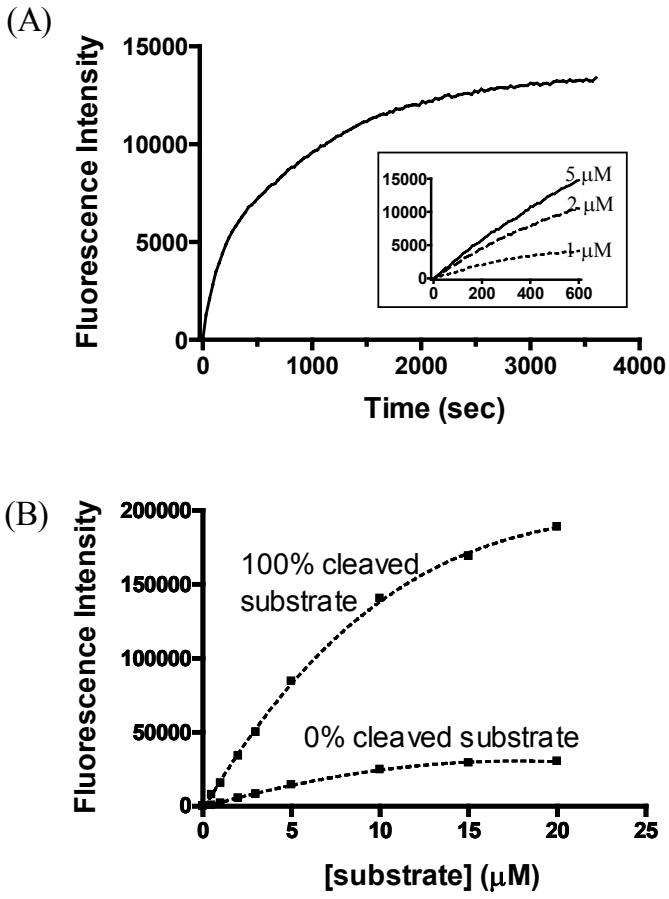

Figure 2.5 Fluorescence assay on a microplate using a microplate fluorescence reader (spectrofluorometer). (A) Continuous fluorescence assay for the hydrolysis of 2 μM of the fluorogenic, autoquenching substrate **2.1** (BODIPY-EAAPYSLRGK(BODIPY)R-NH_2) by 0.1 μg/ml of β-chymotrypsin in Tris-HCl buffer in a volume of 100 μl at 23 ^{o}C. (Insert) Plotting of fluorescence by first 10 min with 5 μM (solid line), 2 μM (dashed line) and 1 μM (dotted line) of the autoquenching substrate. (B) Quenching effect before and after β-chymotrypsin completes digestion.

Very high concentrations of fluorescent dyes may quench each other even if they are not covalently linked. The useful concentration range of fluorescent dyes is limited by the inner filter effect, which has been described for EDANS/DABCYL protease substrates (Holskin *et al*., 1995). After proteolytic hydrolysis of high concentrations of the EDANS/DABCYL substrates, the released fluorescent fragment, EDANS-containing peptide product, becomes quenched by the intact or by released DABCYL peptide. Such an inner filter effect affects the newly designed autoquenching substrates. High concentration of the substrate of the *bis*-BODIPY autoquenching substrate and/or the released two mono-BODIPY peptide products might quench themselves. Hence, the fluorescent intensities of the uncleaved autoquenching substrate as well as completely cleaved mono-BODIPY products with variant concentrations were determined prior to characterization to evaluate the usefulness of the new autoquenching substrate for enzyme kinetics (Figure 2.5B). The autoquenching of the *bis*-BODIPY peptide functioned as a FRET substrate at all tested concentrations (0.5 μM to 30 μM). The fluorescent intensity ratio of the fully cleaved and the intact substrate was more than 8 times even at lower than 1 μM of the substrate. However, the change of fluorescence intensity for completely cleaved products is not linear at concentrations of over 10 μM. This is not problematic for overall substrate sensitivity because the uncleaved substrate also has the same tendency to exhibit the inner filter effect so the entire system can be normalized by a standard curve. High sensitivity of the substrate at very low concentrations allows for activity measurements of enzyme with low K_M value.

2.4.4 Kinetic assay

K_M determinations were made with fluorescence intensity measurements at nine substrate concentrations ranging from 0.7 to 27 μM with 1.9 nM of β-chymotrypsin. The concentration of β-chymotrypsin was estimated by UV

spectroscopy using a Nanodrop microspectrometer at 280 nm calculated with a protein standard (2 mg/ml of bovine serum albumin). The profile of initial rates of hydrolysis versus concentration of the substrate **2.1** (BODIPY-EAAPYSLRGK(BODIPY)R-NH_2) by β-chymotrypsin is shown in Figure 2.6A. Initial time points (2 to 10 min) showed linearity, which corresponded to less than 10% hydrolysis of total substrate as shown in Figure 2.6B. The initial velocities of hydrolysis reaction were obtained from the linear range of data point of the initial stage using the least-squares linear fit of Origin 7.0 of OriginLab Corporation (Northampton, MA). Kinetic parameters of the substrate for β-chymotrypsin were calculated using the nonlinear least squares fit of GraphPad Prizm 4 program (GraphPad Software, San Diego, CA) based on the Michaelis-Menten equation.

The classic Michaelis-Menten equation is expressed as $Vo = V_{max}\cdot[S]/(K_M+[S])$. The initial velocities obtained from fluorescent intensity change and substrate concentration resulted in a typical Michaelis-Menten curve with V_{max} = 4.5 ± 0.3 nM/s and K_M = 3.2 ± 0.6 μM. The V_{max} and the enzyme concentration (1.32 nM) resulted in a catalytic constant of 3.39 ± 0.2 s^{-1} defined as $k_{cat} = V_{max}/[E]_T$. The catalytic efficiency (k_{cat}/K_M) of β-chymotrypsin for the autoquenching substrate was 1.06 x 10^6 $M^{-1}\cdot s^{-1}$. A previous catalytic efficiency of β-chymotrypsin for a chromogenic substrate (suc-Ala-Ala-Pro-Phe-pNA) was reported as 1.0 x 10^6 $M^{-1}\cdot s^{-1}$ with K_M of 43 μM and k_{cat} of 45.0 s^{-1} (DelMar *et al.*, 1979). The enzyme efficiency to the substrate **2.1** was almost the same as the *p*NA chromogenic substrate. The K_M value for the autoquenching substrate was much lower than that for the chromogenic substrate, however. Although *p*NA group itself can also contribute to binding in the S_1' subsitesite, the autoquenching substrate has more than 3 optimized residues corresponding to S_1', S_2' and S_3' subsites of β-chymotrypsin, which might cause an increase of binding energy between the substrate and the enzyme. The k_{cat} value for the chromogenic

substrate is higher than that for the autoquenching substrate. The ability of the good leaving group *p*NA may contribute to this difference.

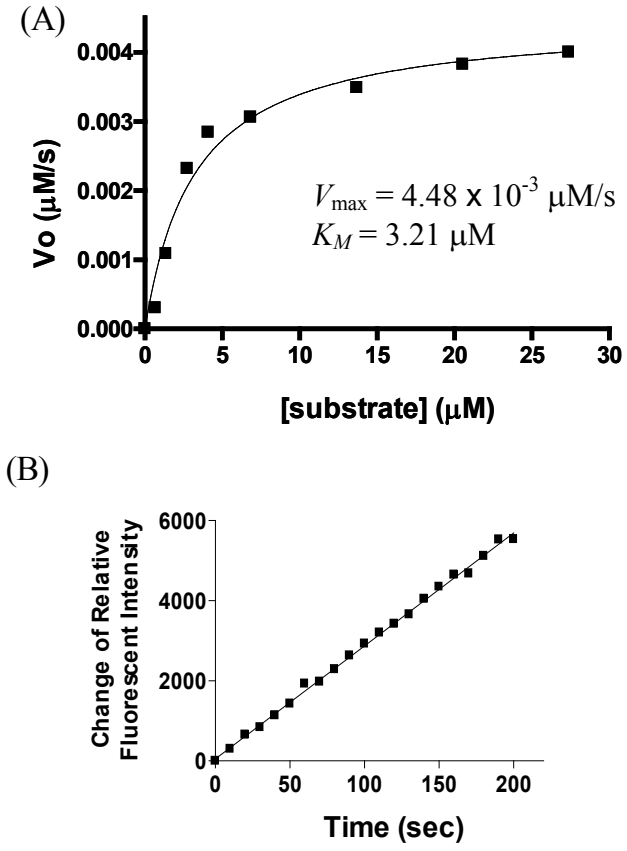

Figure 2.6 Analysis of kinetic parameters. (A) Profile of initial rates of hydrolysis by β-chymotrypsin obtained from fluorescence measurement versus concentration of the substrate **2.1**. (B) Initial stage of the hydrolysis for initial reaction rate determinations. The initial velocities of hydrolysis reaction was calculated from linear range of data point of the initial stage (represented at 14 μM of the substrate as an example).

The new autoquenching substrate demonstrated that the two BODIPY dyes on the autoquenching substrate have no adverse effect in catalytic efficiency. Hence, the *bis*-BODIPY autoquenching substrates can be used for protease assay and kinetics in large screening.

2.4.5 Comparison of quenching effect in FRET substrates

A series of FRET substrate (Figure 2.2) were designed and synthesized for comparison. Three quenchers, TNB, TMR and QSY7, were chosen to compare the autoquenching effect of BODIPY of substrate **2.1**.

TNB is a small non-fluorescent molecule of which the absorbance range is on UV region (λ_{max} = 342 nm). When TNB is covalently coupled with BODIPY FL dye in close proximity, it is known to quench BODIPY FL (unpublished data, Mark Olsen) even though the emission wavelength of BODIPY FL does not match the excitation wavelength of TNB molecule. Similarly the fluorescence of BODIPY is quenched *ca*. 50% at 70 mM of Trp or Tyr in water and DMSO solution (Karolin *et al*., 1994) (Marme *et al.*, 2003, Neuweiler *et al.*, 2003). Those quenching effect by simple aromatic compounds may occur because of direct collisional interaction between the linked two molecules, not by a FRET effect.

TMR was chosen as a quencher of BODIPY FL dye because TMR also quenches fluorescein (Ex/Em = 494/518 nm, Förster radius (R_o) between TMR and fluorescein = 55 Å), which has fluorescent properties that are similar to BODIPY FL (504/513 nm).

Another non-fluorescent dye, QSY7, was selected as an effective quencher because it is reported to have a broad absorption in the visible-light spectrum, with an absorption maximum near 560 nm and high extinction coefficients (ε = 90,000 $cm^{-1}M^{-1}$) to provide a high quenching effect to a green or red fluorescent dye.

A comparison of the hydrolysis of the substrates by chymotrypsin is presented in Figure 2.7. The autoquenching substrate **2.1** reveals a significantly higher fluorescence after full digestion (Figure 2.7A), around 2-fold than other substrates. This makes sense because the autoquenching substrate releases two fluorescent BODIPY FL peptide products, while the other substrates release only one fluorescent BODIPY FL peptide product after cleavage.

In fluorescence assay for proteases with fluorogenic substrates, the effect of the fluorescent dye on the hydrolysis of the substrates has been an issue. The cleavage rate of TNB/BODIPY FRET substrate **2.6** by chymotrypsin was comparable to the cleavage rate of the autoquenching substrate. Unfortunately, the TMR/BODIPY substrate **2.7** and the QSY7/BODIPY FRET substrate **2.8** were not sensitive to hydrolysis with 2 μg/ml of the enzyme. At a higher amount of chymotrypsin (20 μg/ml), the two substrates showed typical curves of enzymatic hydrolysis (Figure 2.7B). The slower cleavage of the TMR/BODIPY and QSY7/BODIPY FRET substrates by chymotrypsin was also demonstrated by HPLC analysis (Figure 2.8). Therefore, the TMR and QSY7 molecules as *C*-terminus quenchers of BODIPY FL apparently cannot be used for the kinetic analysis of chymotrypsin. The TMR and QSY7 molecules are far (as P_6 site) from the cleavage site, making it unclear why these substrates were not cleaved by the enzyme. The quecher molecules possiblely interfere the chymotrypsin activity.

The activity of chymotrypsin with each FRET substrate is very different although peptide sequences of the TNB, TMR and QSY7 labeled FRET substrates are exactly the same. Note that TNB is the smallest quencher group, so that size may be the issue. Unfortunately, the background fluorescence of the TNB/BODIPY substrate is high and only 2 or 3-fold fluorescence intensity increase was observed upon cleavage since the efficiency of quenching effect is probablely lower than others. For comparison, the *bis*-BODPY autoquenching substrate exhibited more than 8 fold increase. From these results above, the *bis*-BODPY autoquenching substrate proved to be the most suitable substrate.

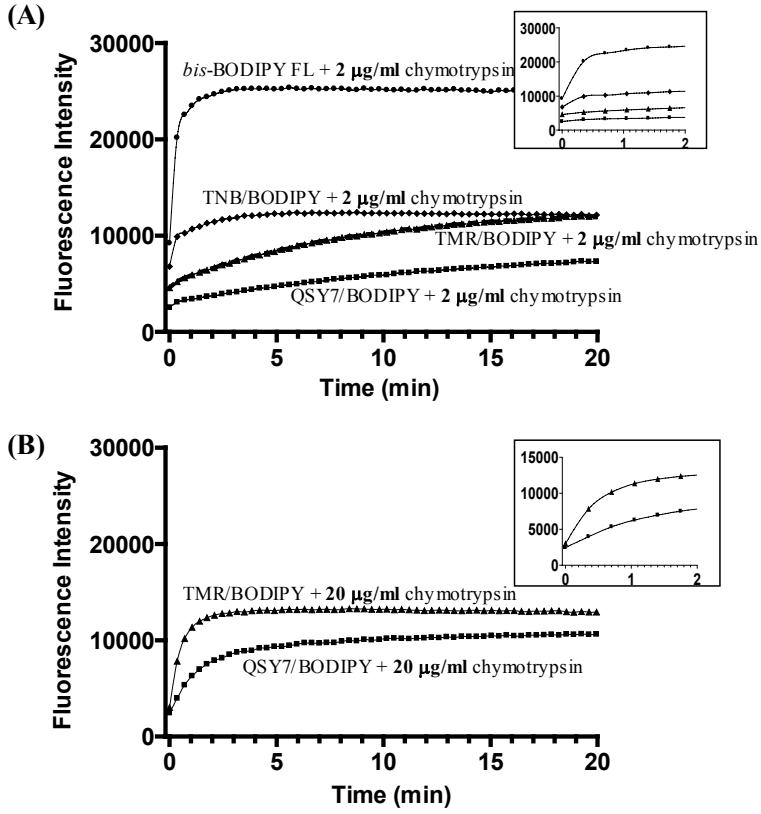

Figure 2.7 Quenching efficiency of the autoquenching substrate and the FRET substrates. (A) Time course fluorescence intensity profile of hydrolysis by 2 μg/ml of β-chymotrypsin. (Insert) First 2 min enlargement. (B) Hydrolysis of FRET substrates and with higher concentration of 20 μg/ml β-chymotrypsin. The *bis*-BODIPY FL autoquenching substrate **2.1** and the TNB/BODIPY substrate **2.6** were almost digested within 0.5 min after addition of chymotrypsin at the high concentration of chymotrypsin (data are not shown). (Insert) First 2 min enlargement; (*bis*-BODIPY FL autoquenching substrate **2.1** (filled circle), TNB/BODIPY substrate **2.6** (diamond), TMR/BODIPY substrate **2.7** (triangle), QSY7/BODIPY substrate **2.8** (square). Ex/Em wavelengths are 490/510 nm with 495 cutoff.

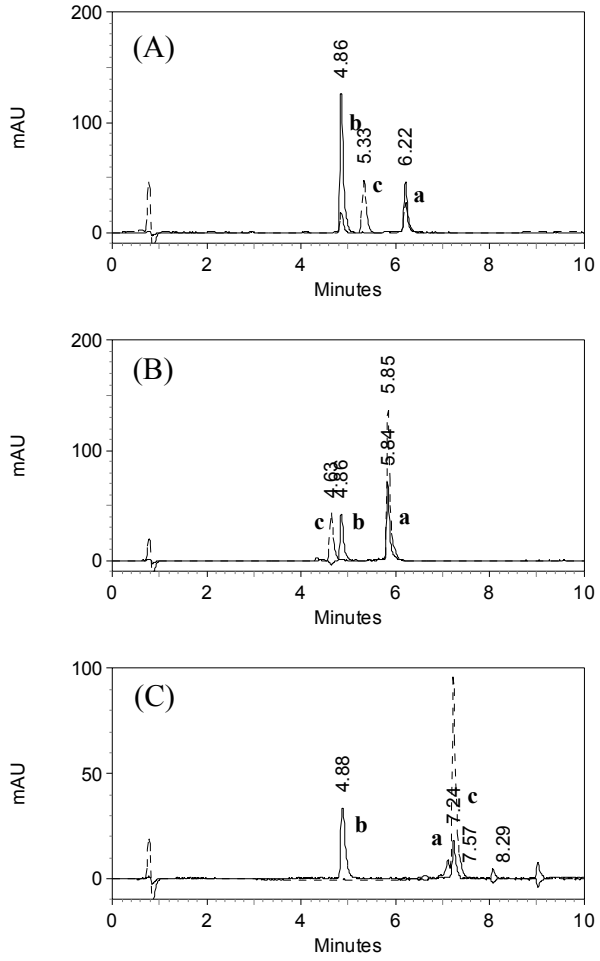

Figure 2.8 HPLC analysis of the FRET substrates after partial proteolytic hydrolysis by β-chymotrypsin at 23°C for 2 min in 20 mM Tris-HCl buffer (pH 8.0). (A) Products of **2.6** (TNB/BODIPY) by β-chymotrypsin (0.32 μg/ml) (B) Products of **2.7** (TMR/BODIPY) by 10 times amount of β-chymotrypsin (3.2 μg/ml) used in TNB substrate. (C) Products of **2.8** (QSY7/BODIPY) by β-chymotrypsin (3.2 μg/ml). Note that 10 times amount of β-chymotrypsin was used for (B) and (C). (Absorbance chromatograms are overlaid; All the solid lines are at 504 nm representing BOIPY FL conjugated peptide and the dotted lines are at 340 nm for TNB in (A), 552 nm for TMR in (B) and 565 nm for QSY7 in (C); **a**, uncleaved substrates; **b**, *C*-terminal BODIPY labeled products; **c**, *N*-terminal quencher labeled products)

Two more *bis*-BODIPY autoquenching substrates (**2.3** and **2.4**) were synthesized to determine the distance dependency of the quenching effect between BODIPY dyes. Both substrates have Phe as a P_1 residue instead of Tyr. The longer substrate (**2.3**, BODIPY-EAAPF•SLRGRK(BODIPY)R-NH_2) has 11 amino acids between the BODIPY dyes. As expected, the cleavage pattern (as shown in Figure 2.9) of the substrate **2.3** was very similar to the previous autoquenching substrate **2.1** (BODIPY-EAAPY•SLRGK(BODIPY)R-NH_2). The shorter substrate **2.4** (BODIPY-AAF•ARK(BODIPY)R-NH_2) was expected to have higher quenching than the longer ones because there is only 6 amino acids between two the BODIPY groups. However, no dramatic change in the quenching effect was observed. Enzyme assays shown in Figure 2.10 demonstrate that all autoquenching substrates can be used in various concentrations of enzymes.

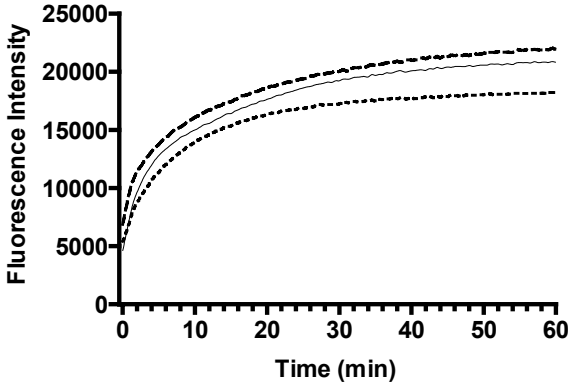

Figure 2.9 Continuous fluorescence profile for the hydrolysis of 2 μM of the fluorogenic, autoquenching substrates by 0.1 μg/ml of β-chymotrypsin in Tris-HCl buffer in a volume of 100 μl at 23 ^{o}C using a microplate fluorescence reader. Solid line, **2.1**; dashed line, **2.3**; dotted line, **2.4**.

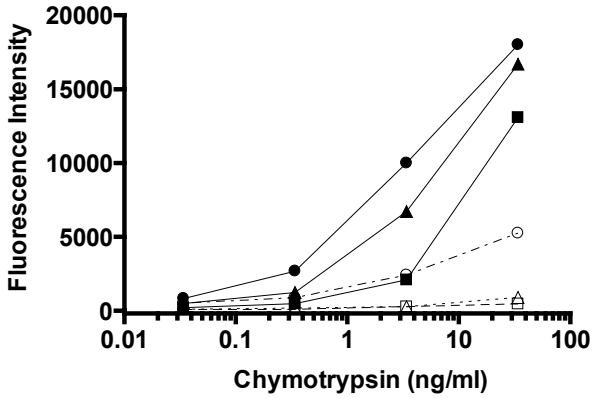

Figure 2.10 Fluorescence versus chymotrypsin concentration. The detection of β-chymotrypsin proteolytic activity using 3 μM of **2.1** (closed circles), **2.3** (closed triangles), **2.4** (closed squares), **2.6** (open circles), **2.7** (open triangles), and **2.8** (open squares) plotting the fluorescence intensities at 490/515 nm (Ex/Em) with 495 nm cutoff. All reactions were incubated for 90 min at 23°C.

2.5 CONCLUSION

The newly designed and synthesized substrates are effective fluorogenic substrates that are useful for enzyme kinetics and sensitive detection of enzyme activity. Best of all, the facile synthesis on a peptide substrate by labeling two BODIPY FL at once made it easy to prepare fluorogenic substrates including amino acid residures at the P' position. Compared to the low yielding multi step synthesis of traditional FRET substrates, the straightforward one-step preparation of *bis*-BODIPY autoquenching substrates gives high yields, which are necessary for high throughput enzyme activity screening. TNB/BODIPY substrate showed a weaker quenching effect compared to *bis*-BODIPY autoquenching substrates. The TMR and QSY7 quenching groups are not effective in our designs because they apparently interfere with chymotrypsin activity.

Chapter 3

A new screening method for high throughput directed evolution in specificity using two-color system

3.1 CHAPTER SUMMARY

3.1.1 Goals

To develop a more flexible high-throughput screening method for isolating enzyme variants with new substrate specificity based on Fluorescence Activated Cell Sorting (FACS).

3.1.2 Approach

A substrate was designed and synthesized, that utilizes a new strategy we call "electrostatic capture" on the bacterial cell surface. The electrostatic capture substrate does not bind on the surface of *E. coli* before enzymatic cleavage, but the product does. This is in contrast to earlier developed FRET substrates, containing two dyes (donor and acceptor molecules), which are pre-loaded on the surface before reaction. The electrostatic capture substrate has only one fluorescent dye on the positively charged *C*-terminus that is neutralized by the negatively charged *N*-terminus. Upon enzyme cleavage, the positively charged fluorescent half is retained on the negatively charged *E. coli* surface. Taking advantage of the multi-parameter capability of a FACS and the electrostatic capture probes, two different substrates with two different colored fluorescent dyes were synthesized. The wild-type substrate contains one fluorescent dye and the desired substrate embodies a different fluorescent dye. This "two-color" substrate approach enables FACS to detect the proteolytic activity of OmpT variants while simultaneously deselecting unwanted wild-type activity.

3.1.3 Results

Using the two-color substrate approach, OmpT variants (1.3.19 and 1.2.19) were isolated with new substrate specificity from a library with a high mutation rate. A relatively non-specific OmpT variant (C5) was used as the parent. The mutants were further characterized using the *bis*-BODIPY autoquenching substrate and HPLC analysis. 1.2.19 and 1.3.19 have evolved from wild-type Arg-Arg activity to have Ala-Arg specificity. This research was done in collaboration with fellow graduate student Mark Olsen.

3.2 INTRODUCTION

OmpT

OmpT (EC 3.4.21.87), the outer membrane protease in *E. coli*, was discovered and partially characterized in 1980 (Grodberg *et al.*, 1988, Leytus *et al.*, 1981). It is a 33.5 kDa protease that is a member of the highly homologous omptin family of proteases. OmpT is involved in the microbial pathogenicity of Gram-negative bacteria (Sodeinde *et al*., 1992), in the breakdown of antimicrobial peptides (Stumpe *et al*., 1998), and in DNA excision repair (Sedliakova *et al*., 1997). The protease is synthesized as a proprotein of 319 amino acids containing a signal sequence of 20 amino acids and the mature protein is 297 amino acids. The protease cleaves the amide bond preferentially between two successive basic amino acids (Arg and/or Lys) of a substrate.

Recently, the substrate specificity of OmpT was studied using synthetic peptides called the SPOT peptide library for P_2, P_1, P_1' and P_2' positions (Dekker *et al*., 2001) as well as protein substrates (Okuno *et al.*, 2002a, Okuno *et al.*, 2002b). OmpT was originally known to cleave the peptide bond between the adjacent basic amino acids (Arg/Lys-Arg/Lys). In contrast to the highly exclusive preference for basic amino acids (Arg or Lys) at the P_1 position, P_1' has less stringent preference. For the P_2' position, there is a clear preference for hydrophobic amino acids (e.g.,

Ala, Ile, and Val). The P_2 position has a broad preference for hydrophobic and neutral amino acids. A negatively-charged residue (Asp or Glu) and a bulky aromatic residue (Trp) are hardly allowed for all positions from P_2 to P_2'.

OmpT is an efficient enzyme. Its hydrolysis efficiency (k_{cat}/K_M) with an optimal peptide substrate, Ac-WGGR•RIKGWGTI-NH_2, is 3.3 x 10^6 sec^{-1} M^{-1} (Leytus *et al*., 1981, Olsen *et al*., 2000). The active site and mechanism of OmpT have been studied (Kramer *et al*., 2000, Kramer *et al*., 2001a) and the X-ray structure has been reported (Vandeputte-Rutten *et al*., 2001). OmpT has a 10-stranded antiparallel beta-barrel structure. The active site of OmpT looks like a groove of a vase at the top of the beta-barrel structure, and protrudes into the extracellular space outside far from the lipid bilayer of outer membrane. A putative binding site for lipopolysaccharide, that is essential for OmpT activity, was discovered. OmpT was proposed to be a serine protease with Ser99 and His212 as active site residues based on site-directed mutagenesis and inhibitor profile data. However, recently a novel proteolytic mechanism, involving a His212-Asp210 dyad and an Asp83-Asp85 couple that activate a putative nucleophilic water molecule based on the active site residues has been porposed (Figure 3.1).

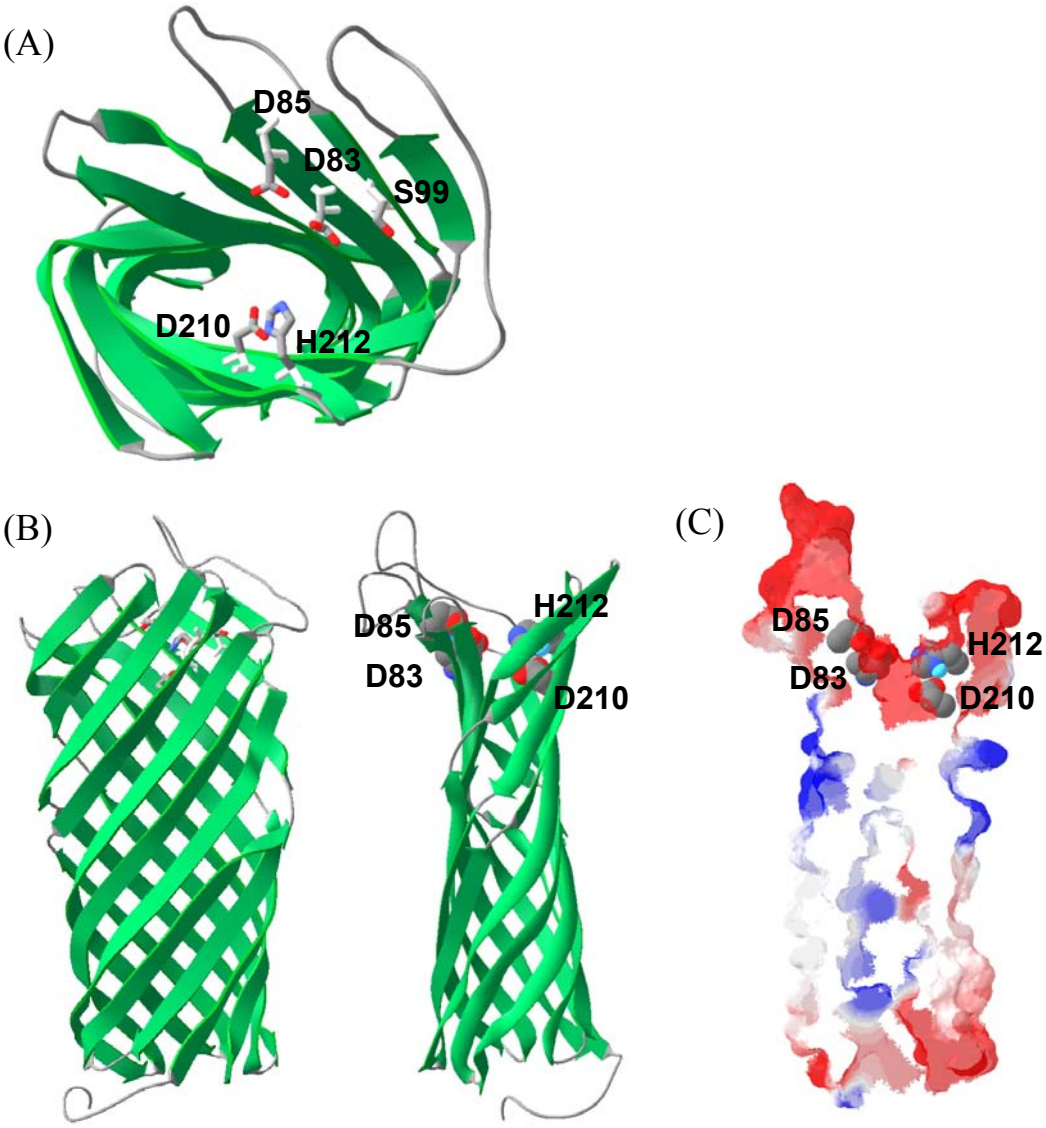

Figure 3.1 (A) Active site cleft of OmpT. (B) Side view of ribbon representation. (C) Cross-section (slab mode) of electrostatic potential surface of the β-barrel (blue = positive charged, and red = negative charged).

FRET-based substrate for directed OmpT evolution study using FACS

Olsen designed FRET-based substrate that yields fluorescent *N*-terminal peptide product with a net +3 charge after OmpT protease digestion (Figure 3.2A) (Olsen *et al.*, 2000). The pre-loaded substrate and product remain on the negatively-charged surface of *E. coli* outer membrane (-25 to -30 mV of ζ potential) (Razatos *et al*., 1998). The intact substrate is labeled with two dyes, tetramethyl rhodamine (TMR) on the *C*-terminus and BODIPY dye on the positively charged *N*-terminus. The intact substrate does not emit fluorescence because TMR (Ex/Em = 540/564 nm) quenches the emission energy of BODIPY-FL (Ex/Em = 502/512 nm) by FRET (Förster Radius (R_0) = 55 Å) (Haugland, 1996) and/or collisional quenching effect. Upon OmpT cleavage of the preferred peptide bond (Arg-Arg of this substrate) in the middle of the FRET substrate, the intermolecular quenching of TMR to BODIPY is disrupted and the *C*-terminus peptide product containing both a net +3 charge and BODIPY-FL emits fluorescent green light and is retained on cell surface as shown in Figure 3.2B. The *N*-terminal peptide product containing the quencher TMR is neutral and diffuses away quickly from the cell. FACS can analyze and rapidly sort the green fluorescent cells having active OmpT from non-fluorescent inactive cells. The electrostatic interaction of positively charged peptides on the surface and FRET quenching is necessary to link the enzyme activity (phenotype) to the cell (genotype).

Based on the FRET substrate design, a substrate **3.1a** was synthesized for enrichment model study. The FACS system with the FRET substrate demonstrated the successful enrichment (> 5000-fold) of cells having OmpT plasmid from OmpT(-) cells as shown in Figure 3.3A. In order to alter the wild-type Arg-Arg activity of Arg-Val specificity, a FRET substrate **3.1b** with Arg-Val sequence was prepared and used to screen a library of 2 x 10^6 OmpT variants. The library was constructed by error-prone polymerase chain reaction (PCR) mutagenesis at different Mn^{+2} concentration (Cadwell & Joyce, 1992). Three clones active toward

the substrate **3.1b** were isolated following FACS sorting (Figure 3.3B) and a secondary enzyme activity assay (Figure 3.3C). One of the collected variants (C5) had 8 point mutations (Table 3.1) and displayed approximately 60-fold increase in catalytic efficiency (k_{cat}/K_M = 1440 $s^{-1}M^{-1}$) for Arg-Val compared to wild-type OmpT (k_{cat}/K_M = 24 $s^{-1}M^{-1}$).

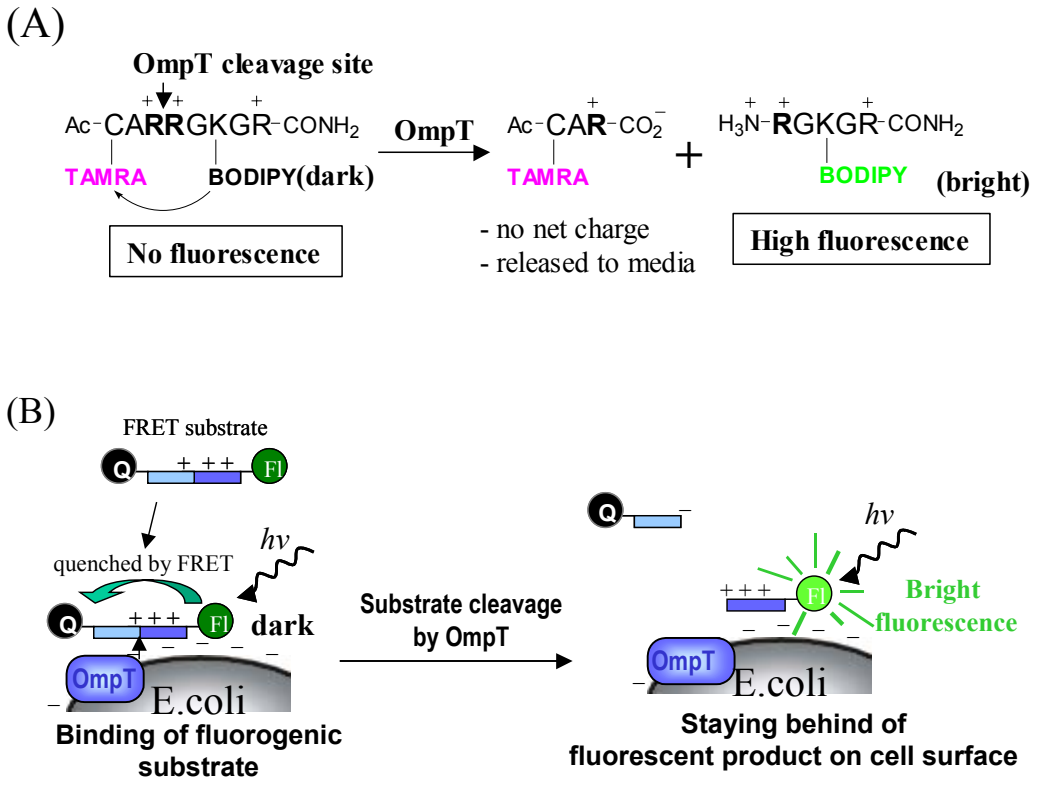

Figure 3.2 The FRET substrates used for flow cytometry-based directed enzyme evolution (Olsen *et al.*, 2000). (A) Cleavage of the FRET-based substrate. The quencher for the fluorophore (BODIPY-FL) is tetramethylrhodamine (TMRA) (B) Strategy for localization of the substrate and the product, and detection of the fluorescent product on the cell surface following cleavage.

(A)

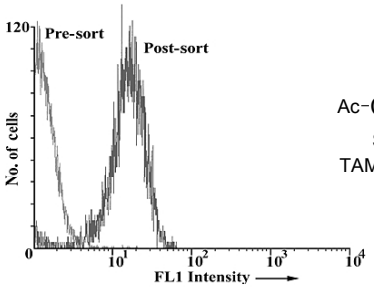

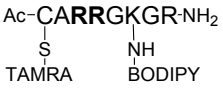

3.1a

(B)

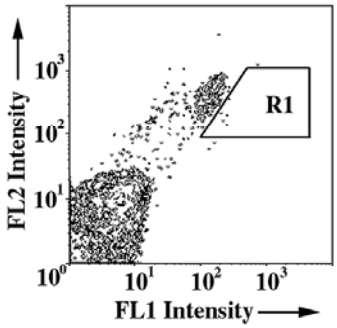

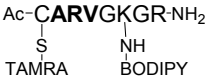

3.1b

(C)

Enzyme	K_{cat}/K_M ($s^{-1}M^{-1}$)	Cleavage site (%)			
		Arg-Val	Val-Val	Val-Gly	Gly-Thr
OmpT	24	100	nd	nd	nd
C5	1440	89	8	1	2

Figure 3.3 Flow cytometry discrimination of *E. coli* on the basis of OmpT activity. (A) Enrichment of cells with expressing wild-type OmpT from excess of negative control cells using FRET substrate **3.1a**. (B) FACS dot-plot of an OmpT library to sort out OmpT variants that can cleave the substrate **3.1b**. (C) Digested peptide products and relative catalytic efficiencies of an unlabeled peptide substrate; H-WGGPGR•V•V•GG•TI-NH_2 by wild-type OmpT and C5 variant isolated by high throughput OmpT evolution with FACS. (nd = not detected) (Olsen *et al*., 2000)

	33	87	111	137	149	186	200	288
WT	Glu	Met	Glu	Ser	Ile	Ser	Tyr	Ile
C5	*Lys*	*Leu*	*Val*	*Asn*	*Val*	*Cys*	*Phe*	*Phe*

Table 3.1 Amino acid mutation in the isolated clones C5. (Olsen *et al*., 2000)

Although variant C5 retains high Arg-Arg cleavage activity, the screening strategy was successful in isolating variants with new specificity from a large library. However, the activity of C5 was actually rather disappointing. In the directed evolution of the OmpT protease, conversion of the wild-type specificity to a new specificity has proven to be more difficult than expected. In this chapter, I will describe a new strategy for isolation of enzyme with altered substrate specificity using a high throughput FACS methodology that is intended to overcome this barrier.

3.3 MATERIALS AND METHODS

3.3.1 General instrumentations and methods for synthesis

Peptides, RR-peptide (Ac-CARRGKGR-NH_2) and RV-peptide (Ac-CARVGKGRGR-NH_2), were purchased from Cell Essentials (Boston, MA). Other peptides were prepared on Rink amide resin without cleavage and deprotection from the Facility in MBB of the University of Texas at Austin. Double coupling steps were performed to increase purity of peptides. Conjugating reagents and characterization methods of new peptides are the same as in the Materials and Methods part of chapter 2.

3.3.2 Synthesis of FRET OmpT substrates (Figure 3.4A and 3.5A)

3.3.2.1 Optimization and general method of coupling the 5-TMRIA to peptide containing a sulfide group

A small scale reaction was performed to optimize thiol conjugation of tetramethylrhodamine-5-iodoacetamide dihydroiodide (5-TMRIA of Molecular Probes) with a series of mild bases, such as 400 mM $NaHCO_3$, 200 mM $NaHCO_3$ + 40 mM Na_2CO_3, 40 mM $NaHCO_3$ + 200 mM Na_2CO_3, 1x PBS, 200 mM Na_2HPO_4, or 200 mM DIPEA. All the reactions were monitored by analytical reverse-phase HPLC using a gradient of acetonitrile/water with 0.1% TFA from 10 to 50% at 545 nm.

After optimization, a preparative scale reaction was followed. TMRIA (5.5 μmole) in DMF was added to a solution containing the RR-peptide (5 μmole) in water, 1 M Na_2CO_3 (100 μl, more than 25 times excess), and 0.5 M $NaHCO_3$ (50 μl). The reaction mixture was shaken intermittently at room temperature for 1 hour and diluted with 5 ml of 0.1 % TFA in water. The product was purified by FPLC using a gradient of acetonitrile/water 0.1% TFA from 10% to 30% as described in the Chapter 2. The pure fractions of the product were lyophilized. The dried product was dissolved in water (0.5 ml) and quantified by a UV-vis spectrophotometer at 552 nm ($\varepsilon = 90000\ cm^{-1}M^{-1}$).

Preparation of TMR-RR-peptide conjugate

5-TMRIA (4.5 mg, 4.87 μmole) in DMF (242 μl) and the RR-peptide (6.79 mg, 4.85 μmole) in water (242 μl) were used as in the general method. The yield after FPLC purification was 3.49 mg (39%) of dark purple powder. ESI MS (m/z); calculated 1384.69 for M, found 1385.6 for MH^+ and 694.0 for $(MH^2)^{+2}$; high MS (m/z); calculated 693.3547 for $(MH^2)^{+2}$ and 750.35114 for $(M\text{-}TFA\text{-}H^2)^{+2}$, found 693.3537 and 750.3515.

Preparation of TMRA-RV-peptide conjugate

5-TMRIA (4.50 mg, 4.87 μmole) in DMF (250 μl) and RV-peptide (Ac-CARVGKGRGR-NH_2, 7.54 mg, 4.85 μmole) in water (250 μl) were used as in the general method. The yield after FPLC purification was 2.15 mg (22%) of dark purple powder. ESI MS (m/z); calculated 1540.78 for M, found 1541.6 for MH^+, 771.8 for $(MH^2)^{+2}$ and 515.2 for $(MH^3)^{+3}$.

3.3.2.2 General method of coupling the BODIPY FL SE or TMR SE to peptide containing a free amino group

A small scale reaction was performed to optimize amide conjugation of 4,4-difluoro-5,7-dimethyl-4-bora-3a,4a-diaza-*s*-indacene-3-propionic acid, succinimidyl ester (BODIPY FL-SE) of the TMR labeled peptides with a series of bases, such as $NaHCO_3$, $NaHCO_3$ + Na_2CO_3, Na_2CO_3, DIPEA, or DMAP. All reactions were evaluated by analytical reverse-phase HPLC with a UV detector at 502 nm and 552 nm.

For a preparative scale reaction, 40 mM BODIPY FL SE (1.1 equivalent for mono-BODIPY, 2.2 equivalent for *bis*-BODIPY) or TMR SE in DMF (40 μl) was added to the mixture of the 40 mM peptide (2 μmole) in water (50 μl) and 1 M DMAP (25 μl). The reaction mixture was shaken intermittently at room temperature for 1 hours and diluted with 5 ml of 0.1 % TFA in water. The yield after FPLC purification was estimated by UV absorbance (ε = 90000 $cm^{-1}M^{-1}$ for TMR at 552 nm).

Preparation of TMR-RR-peptide-BODIPY FRET substrate (3.1a)

BODIPY FL SE (2.61 μmole) in DMF (90 μl), TMR-RR-peptide (1.27 μmole) in water (90 μl) and 1 M DMAP (25 μl) were used as in the general method. The product was purified by FPLC to give a dark purple powder of 0.713 mg (28%). ESI MS (m/z) of TMR-RR-peptide-BODIPY conjugate **3.1a** (Ac-C(TMR)ARRGK(BODIPY)GR-NH_2); calculated 1658.81 for M, found 1659.6 for MH^+, 830.6 for $(MH^2)^{+2}$, 554.5 for $(MH^3)^{+3}$.

Preparation of TMR-RV-peptide-BODIPY FRET substrate (3.1b)

BODIPY FL SE (2.03 μmole) in DMF (70 μl), TMR-RV-peptide (1.02 μmole) in water (70 μl) and 1 M DMAP (20 μl) were used as in the general method. The yield after FPLC purification was 0.720 mg (32%). ESI MS (m/z) of TMR-RV-peptide-BODIPY conjugate **3.1b** (Ac-C(TMR)ARVGK(BODIPY)GRGR-NH_2); calculated 1814.89 for M, found 1815.7 for MH^+, 908.6 for $(MH^2)^{+2}$, 606.5 for $(MH^3)^{+3}$.

3.3.3 Synthesis of electrostatic capture OmpT substrates (Figure 3.4B and 3.5B)

3.3.3.1 General method for glutaric acid coupling on N-terminus of a peptide

An Fmoc protected peptide on resin was prepared using a Rink amide AM or MBHA resin as solid support in 0.25 mmole scale. A portion of the resin (~20 μmol) was swelled up with DMA in a solid phase syringe reactor. The resin was treated with 20% piperidine in DMA for 20 minutes twice to remove the Fmoc group on *N*-terminus. After deprotection of the Fmoc group, a mixture of glutaric anhydride (5 equivalent) and DIPEA (10 equivalent) in DMA (2 ml) was added to the resin. The syringe reactor was shaken for 4 hours at room temperature. Each step was monitored by Kaiser test (Kaiser *et al*., 1970). The peptide was deprotected and cleaved from the resin with 95% TFA/2.5% water/2.5%TIS mixture for 2 hours. The peptide was precipitated with diethyl ether to give white powder.

Preparation of glutaric acid-EEGGRRIGRGGK(BODIPY)-NH_2 (3.2a)

The glutaric acid-peptide was cleaved off from the resin (87mg, 0.72 mmol/g) as above, and dissolved in water to a final stock concentration of 40 mM. ESI MS (m/z) of glutaric acid-EEGGRRIGRGGK-NH_2; calculated, 1383.73 for M, found 1384.7 for MH^+, 693.6 for $(MH^2)^{+2}$. BODIPY FL SE (1.0 eq.) in DMF (50 μl), the glutaric acid-peptide (3.68 mg, 2.0 μmole) in water (50 μl) and 1 M DMAP (20 μl) were used as in the general method to give a dark orange powder with yield of 2.22 mg (60.3%), based on UV absorbance (ε = 82000 $cm^{-1}M^{-1}$ for BODIPY at 504 nm).

ESI MS (m/z) of the conjugate **3.2a** (glutaric acid-EEGGRRIGRGGK(BODIPY)-NH_2); calculated 1657.84 for M, found 1658.7 for MH^+, 830.5 for $(MH^2)^{+2}$.

Preparation of glutaric acid-EEGGRRIGRGGK(TMR)-NH2 (3.2b)

TMR SE (1.0 eq.) in DMF (50 µl), glutaric acid-peptide (1.7 µmole) in water (50 µl) and 1 M DMAP (17 µl) were used as in the general method to give a dark purple powder yield of 1.32 mg (36.4%) based on UV absorbance (ε = 90000 $cm^{-1}M^{-1}$ for TMR at 552 nm). ESI MS (m/z) of the conjugate **3.2b** (glutaric acid-EEGGRRIGRGGK(TMR)-NH_2); calculated 1795.88 for M, found 1796.8 for MH^+, 900.0 for $(MH^2)^{+2}$, 600.7 for $(MH^3)^{+3}$.

Preparation of glutaric acid-EEGGRXGRGK(BODIPY)-NH_2 (3.3)

The glutaric acid-peptide (for X = Arg, glutaric acid-EEGGRRGRGK-NH_2) was cleaved from the resin (254 mg, 0.72 mmol/g) resulting in white powder (76 mg). ESI MS (m/z); calculated, 1213.63 for M, found 1214.7 for MH^+, 608.2 for $(MH^2)^{+2}$. The peptide (glutaric acid-EEGGRRGRGK-NH_2, 2.0 µmole) in water, BODIPY FL SE in DMF and 1 M DMAP (30 µl) were used as in the general method with yield of 2.1 mg. ESI MS (m/z) of **3.3**, calculated 1487.84 for M, found 1488.8 for MH^+, 745.0 for $(MH^2)^{+2}$. (For X = Val, Ala, Leu and Trp, all of mono-BODIPY coupled peptides were synthesized, FPLC purified and analyzed by HPLC and MS as previously described.)

3.3.4 Synthesis of *bis*-BODIPY autoquenching substrate for enzyme assay (Figure 3.4C and 3.5C)

Preparation of BODIPY-ARRIGK(BODIPY)GRGR-NH_2 (3.4)

The peptide (H-ARRIGKGRGR-NH_2) was cleaved from the resin (102 mg, 0.72 mmol/g) to give 35 mg of white powder as above. ESI MS (m/z) of H-ARRIGKGRGR-NH_2; calculated, 1124.71 for M, found 1125.8 for MH^+, 563.7 for $(MH^2)^{+2}$. The peptide (1.4 µmole) in water (35 µl), BODIPY FL SE (2.2 eq.) in DMF (88 µl) and 1 M DMAP (35 µl) were used as in the general method. The

product was a dark brown powder with a yield of 1.2 mg (42%). ESI MS (m/z) of the conjugate **3.4** (BODIPY-ARRIGK(BODIPY)GRGR-NH_2); calculated 1672.93 for M, found 1674 for MH^+, 838 for $(MH^2)^{+2}$, 559 for $(MH^3)^{+3}$.

Preparation of BODIPY-GARRGK(BODIPY)GR-NH_2 (3.5)

The peptide (H-GARRGKGR-NH_2) was cleaved from the resin (148 mg, 0.72 mmol/g) to give 23mg. ESI MS (m/z) of H-GARRGKGR-NH_2; calculated, 855.53 for M, found 857 for MH^+. The peptide (1.6 μmole) in water (40 μl), BODIPY FL SE (2.2 eq.) in DMF (88 μl), and 1 M DMAP (40 μl) were used as in the general method with a yield of 0.9 mg (40%). ESI MS (m/z); calculated 1403.74 for M, found 1406 for MH^+, 703 for $(MH^2)^{+2}$.

Preparation of Ac-K(BODIPY)ARVGK(BODIPY)GRGR-NH_2 (3.6)

The acetylated peptide (Ac-KARVGKGRGR-NH_2) was prepared as above to give a white powder (6.5 mg). BODIPY FL SE (2 μmole) in DMF, the peptide (50 μl) in water and 1 M DMAP were used as in the general method with a yield of 0.6 mg. ESI MS (m/z); calculated 1672.92 for M, found 1673.8 for MH^+, 837.4 for $(MH^2)^{+2}$.

Preparation of BODIPY-EEGGRRGRGK(BODIPY)-NH_2 (3.7)

The unmodified peptide (H-EEGGRRGRGK-NH2) was cleaved from the resin (195 mg, 0.72 mmol/g) to give a white powder (77.8 mg). ESI MS (m/z) of H-EEGGRRGRGK-NH_2; calculated, 1099.60 for M, found 1100.8 for MH^+; MALDI-TOF-MS analysis (m/z); found 1101.52. BODIPY FL SE (2.2 eq.) in DMF, the peptide (3.2 μmole) in water and 1 M DMAP was used as in the general method with a yield of 1.3 mg. ESI MS (m/z); calculated 1647.81 for M, found 1648.7 for MH^+, 825.0 for $(MH^2)^{+2}$. (For X = Val, Ala, Leu and Trp, *bis*-BODIPY peptides were synthesized, FPLC purified and analyzed by HPLC and MS as previously described.)

Preparation of BODIPY-ARVIGK(BODIPY)GRGR-NH_2 (3.8)

The unmodified peptide (H-ARVIGKGRGR-NH_2) was cleaved from the resin (100 mg, 0.72 mmol/g) to give a white powder (34.8 mg). ESI MS (m/z) of the peptide; calculated 1067.68 for M, found 1069.0 for MH^+. BODIPY FL SE (2.2 eq.) in DMF, the peptide (4 μmole) in water and 1 M DMAP were used as in the general method with a yield of 1.0 mg. ESI MS (m/z); calculated, 1615.90 for M, found 1616.8 for MH^+, 809.0 for $(MH^2)^{+2}$.

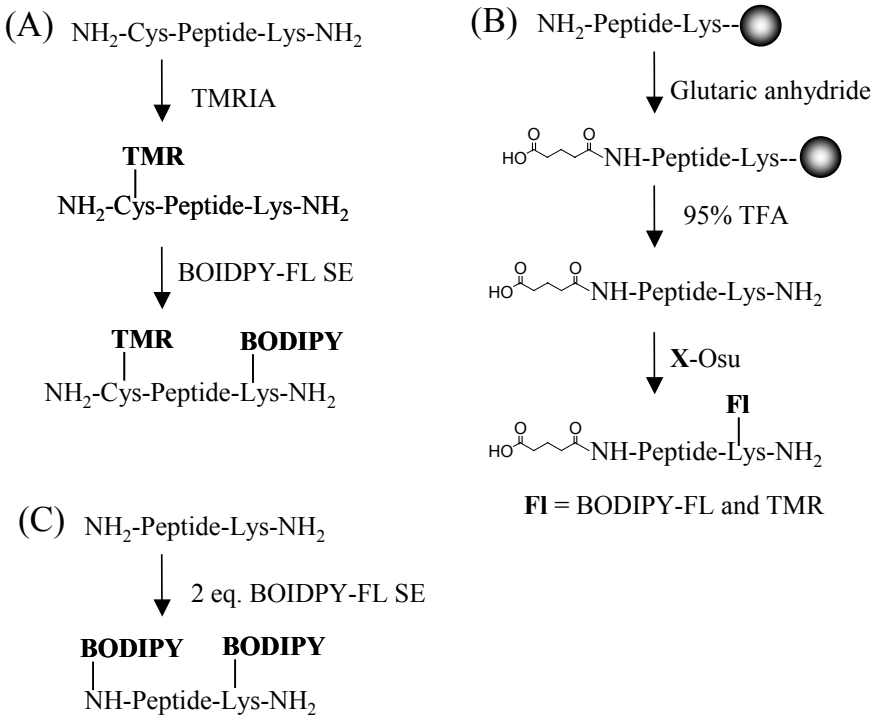

Figure 3.4 Synthetic schemes of the OmpT substrates. (57A) FRET substrates, (B) electrostatic capture substrate, (C) *bis*-BODIPY autoquenching substrates.

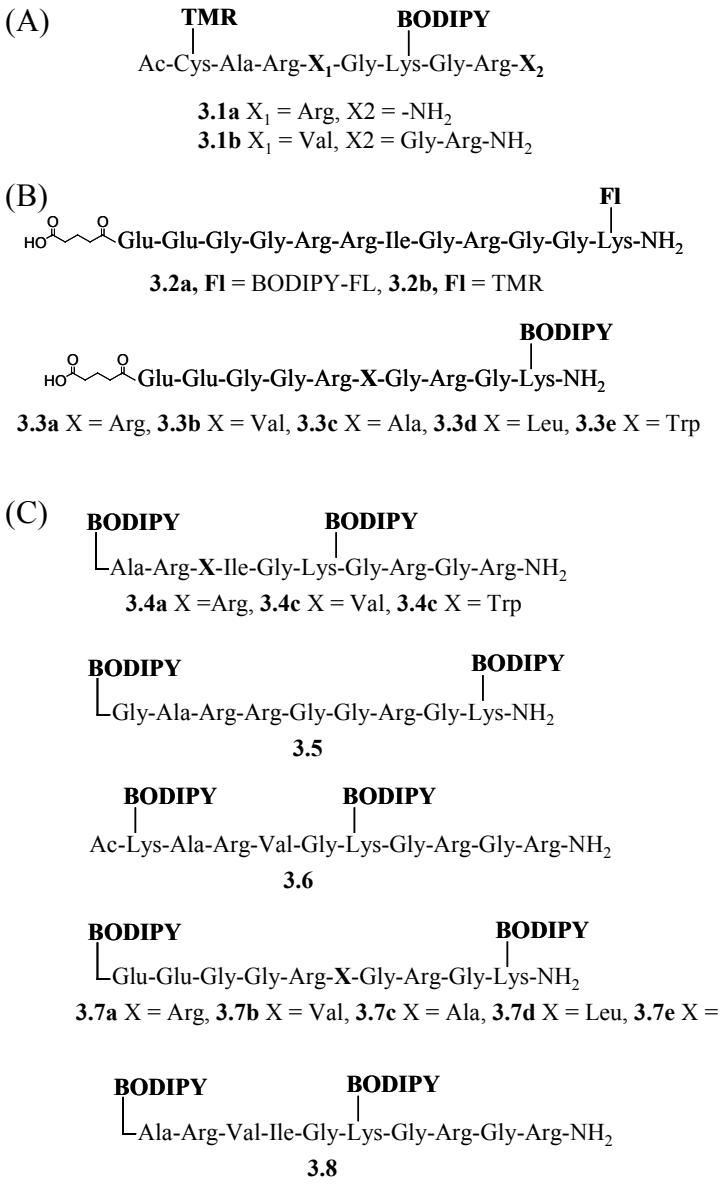

Figure 3.5 Structure of substrates. (A) FRET substrates, (B) electrostatic capture substrate, (C) *bis*-BODIPY autoquenching substrates.

3.3.5 Flow cytometry analysis for evaluation of the new substrates and library screening

UT5600 cells were transformed with the plasmid pML19 that encodes the wild-type OmpT (Olsen *et al*., 2000). UT5600 as a negative control and UT5600/pML19 as a positive control were inoculated from a fresh colony grown on a LB plate and incubated overnight in LB broth medium at 37^{o}C. Growth media were supplemented with ampicillin (100 μg/ml) when necessary. The cell suspensions were subcultured 1:100 in fresh LB broth medium and regrown at 37^{o}C for 6 to 8 hours. At OD_{600} of 1.0 ~ 2.5, the cells (0.5 ml) were harvested and washed with 0.5 ml of 1% sucrose solution. The aliquot (50 μl) of cell suspension in 1% sucrose solution was mixed with 449 μl of 1% sucrose solution. The electrostatic capture substrates were added to the suspension at a final concentration of 100 nM and the mixture was incubated at room temperature for 30 min. The suspensions (10 μl) were diluted with 1 ml of 1% sucrose solution (SIP solution) and analyzed using a Becton-Dickinson FACSort or FACSCalibur without additional washing. The collected data were processed on WinMDI 2.8 program (http://facs.scripps.edu).

3.3.6 Isolation of new OmpT variants using two-color system based on electrostatic capture substrates and FACS

The procedure of library construction and FACS sorting was modified from the previous method (Olsen *et al*., 2000). The C5 OmpT variant was used as a PCR template (enzyme to be evolved) instead of wild-type OmpT. The two-color system was applied by adding two substrates with different fluorescent dyes together with the cell library. The electrostatic capture substrate **3.2b** was used to identify mutants with the desired activity and the FRET substrate **3.1b** was employed for deselection of unwanted wild-type activity. With this approach, two

clones (1.2.19 and 1.3.19) were sorted and then screened with the fluorogenic substrates, **3.1a**, **3.1b** and **3.6** by Mark Olsen in our group.

3.3.7 Post-screening for OmpT activity of whole cell using *bis*-BODIPY autoquenching substrates

UT5600, UT5600/pML19 and OmpT variants (C5, 1.2.19, 1.3.19) were cultured at in LB media at 37^{o}C for 12 hours. The fluorometric assays were performed in a Corning 96-well microplate. The cell culture (1ml) was harvested and spun down by a tabletop centrifuge at 8000 rpm for 1 min. The supernatant was discarded. The pellet was washed and resuspended with 0.5 ml of 0.1 M Tris-HCl buffer (pH 7.5). The cell suspension (20 μl) was added to a solution containing 1 μM of the *bis*-BODIPY autoquenching substrate in 100 mM Tris-HCl buffer (pH 7.5). The fluorescence intensity was measured in a Gemini XS Microplate Spectrofluorometer (Molecular Device Corporation, Sunnyvale, CA) using an excitation wavelength of 490 nm and an emission wavelength of 515 nm with 9 nm bandwidth. The fluorescence intensity of the stirred sample was monitored at every 5 min for 2 hours.

3.3.8 Determination of purified enzyme concentration

The concentrations of the OmpT variants were measured by a BCA (bicinchoninic acid) protein assay kit 23225 (Pierce Biotechnology, Inc., Rockford, IL). Briefly, 1 ml of WR solution, which was a 50:1 mixture of reagent A (sodium carbonate, sodium bicarbonate, bicinchoninic acid and sodium tartrate in 0.1 M sodium hydroxide) and reagent B (4% cupric sulfate), was added to 50 μl of series of the diluted 1.2.19 (20 and 100-fold), 1.3.19 (10 and 50-fold) solutions. BSA standard solutions ranging 0 to 250 μg/ml were also prepared. The reaction mixtures were incubated with at 60 ^{o}C for 30 min and the absorbance was measured at 562 nm. The concentrations were calculated from BSA standard curve fit.

To verify the concentration, micro-scale UV spectrometry (Nanodrop) was performed at 280 nm, which is measuring the absorption of tryptophan in a sample protein. A BSA solution (2 mg/ml) was used as standard. Based on the molecular weights of the proteins and numbers of tryptophans present in the proteins, the concentrations were estimated. In addition, amino acid analysis of the hydrolyzed stock solutions (15 μl) of 1.2.19 and 1.3.19 were also performed by Scientific Reasearch Consortium, Inc (St. Paul, MN) to show the concentrations between the various methods were consistent.

3.3.9 HPLC analysis for enzyme kinetics of OmpT variants

Diluted stock solutions of the OmpT and C5 variant were used at 10 μM (Olsen *et al*., 2000). The 1.2.19 and 1.3.19 variants were prepared at 27.1 μM, and 17.9 μM from previously isolated enzyme stock solution. Stock solutions of two peptide substrates, **3.10** (H-WEEGGRRIGRGGK-NH_2) and **3.11** (H-WCARVGKGRGR-NH_2), were prepared at 5 mM. A series of concentrations of the substrates in 20 mM Tris-HCl (pH8.0) and 1 mM EDTA were incubated with 0.11 μM and 0.36 μM of 1.3.19 variant solution. 0.5 μM and 0.02 μM of C5 variant solutions were used for **3.10** and **3.11**, respectively. The aliquot (100 μl) of hydrolysis reaction was stopped at several time points (0.5 to 20 min) by adding 10 μl of 0.2 M TFA. The products were analyzed on a System Gold® (Beckman Coulter) HPLC system equipped with a 0.5 μm ODS C18(2) Luna(R) column (Supelco). The products were eluted with 0.1% TFA in acetonitrile and 0.1% TFA in water. The UV (absorbance) was monitored at 280 nm, which corresponds to the Trp residue on the substrate; flow rate was 1 ml/min; gradient elution ratio was as follows: 5% acetonitrile:95% H_2O for 2 min, gradually increasing to 40% acetonitrile:5% H_2O by 17 min, 95% acetonitrile:5% H_2O for an additional 5 min, and then returning to initial elution ratio over 5 min, followed by additional 5 min to equilibrate the column. The final concentration of the substrate **3.10** was varied from 50 μM to 300 μM for 1.3.19, and the concentration of **3.11** was ranged from 5

to 30 μM for 1.3.19 and C5. Initial cleavage rates were determined by monitoring the amount of products produced as a function of substrate peptide concentration. The data were fitted to the Michaelis-Menten equation by nonlinear regression using GraphPad Prizm 4 (GraphPad Software, San Diego, CA).

3.4 RESULTS AND DISCUSSION

3.4.1 Optimization of fluorescent dye conjugation and synthesis of substrates

A large-scale synthesis of FRET OmpT substrates of BODIPY-FL/TMR was necessary for screening clones after FACS. The FRET substrates synthesized by the original method could not be used for microplate assays where a relatively large amount is needed. The original protocol from the reagent company (Molecular probes) results in poor purification yields (< 1%). The protocol was designed for conjugation of a fluorescent molecule to a protein, not a small peptide. Furthermore, only limited reagents including the activated fluorescent dyes and peptides were available. To optimize the reaction, small-scale reactions (0.02 μmole) of 5-TMRIA conjugating to Cys thiol in the first step of the FRET substrate synthesis were performed with organic and inorganic bases (Table 3.2). The mixture of sodium carbonate and sodium bicarbonate solution gave the best results (~70% yield in analytical HPLC analysis). Other conditions including 1xPBS as in the manufacturer's protocol for protein conjugation showed multiple peaks on HPLC chromatograph and low product yield of 5% ~ 30% in an analytical HPLC analysis. This reaction left unreacted TMRIA and decomposed form of TMRIA, such as tetramethylrhodamine-5-hydroxyacetamide and tetramethylrhodamine-5-*N*,*N*-dimethylaminoacetamide. In a large scale (5 μmole), the optimized reaction gave an enhanced purification yield (up to 40%).

Optimization of BODIPY-FL SE conjugation on the amino group of the Lys residue of the TMR labeled peptide was also shown in Table 3.3. The yield of BODIPY-FL conjugation significantly increased to more than 95% within 20 min

by using DMAP as an organic base. On the other hand, sodium bicarbonate and DIPEA left the starting peptide at 20 % and 60%, respectively, even after prolonged reaction time. Sodium carbonate also decomposed BODIPY-FL SE quickly to its inactive BODIPY-FL carboxylic acid form. The main advantage of DMAP is that it works as an excellent catalyst for acylation reaction as well as a base. After FPLC purification, I obtained a few μmole (mg scale) of the final FRET substrates, which was enough for microplate assays. The overall yield for the two coupling steps was more than 20 times improved when compared to the previous yield.

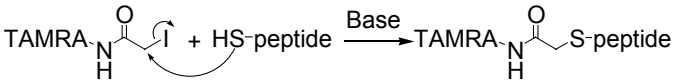

Reaction condition (Base, ~50 eq.)	**Yield estimated by HPLC**	
	1 hour	**10 hours**
$NaHCO_3$	20%	40%
$NaHCO_3$ + Na_2CO_3 (5:1)	**60%**	**75%**
$NaHCO_3$ + Na_2CO_3 (1:5)	**70%**	**85%**
NaOAc (pH ~8.9)	5%	20%
Na_2HPO_4	30%	50%
DIPEA	30%	20%

Table 3.2 Optimization of TAMRA conjugation on thiol group on Cys.

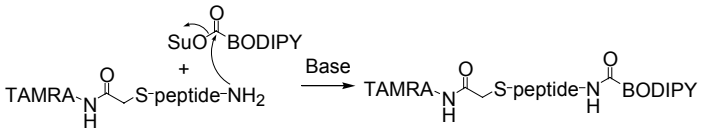

Reaction condition (Base, ~50 eq.)	**Yield estimated by HPLC**
$NaHCO_3$	20 %
Na_2CO_3	75 %
DIPEA	50 %
DMAP	**> 95 %**

Table 3.3 Optimization of BODIPY-FL SE conjugation on amino group of Lys. Prolonged reaction time did not show significant yield increase.

3.4.2 Design and synthesis of the "electrostatic capture" substrate

With the FRET substrates, only limited amounts of the substrate can be pre-loaded to the cell surface, and complications occur when two fluorescent dyes are present on one substrate. In addition, preparation of FRET substrates required multi-step synthesis which can be time consuming.

Design of the electrostatic capture substrate

To improve the problematic surface pre-loaded substrate system, I designed a novel substrate that does not use FRET (Figure 3.6). The new assay is based on "electrostatic capture". The substrate is designed to have no net positive charge to avoid surface pre-loading onto the negatively charged *E. coli* outer membrane in contrast to the previous pre-loaded FRET-based substrate. In general, the *N*-terminus of the electrostatic capture substrate is negatively charged to compensate the positive charges on the *C*-terminus (Figure 3.6A). The negative charges on the substrate prevent binding to the cell surface. To convert the α-amino group on the *N*-terminus to a negatively charged group, the peptide is capped with glutaric anhydride while still on the resin. After cleavage from the resin and deprotection, a *C*-terminal residue (Lys) of the OmpT substrate peptide is covalently labeled with only one fluorescent dye. Once a cleavable site in the middle of the electrostatic capture substrate is cleaved by OmpT on the cell surface, the negatively charged *N*-terminal portion is released back to the reaction medium. The resulting *C*-terminal peptide product, containing three positive charges and a fluorescent dye, is captured by the negatively charged surface of *E. coli* in low-ionic-strength solution through electrostatic attraction as shown in Figure 3.6B. The electrostatic capture of the fluorescent peptide products on the cell displaying active OmpT produces a high signal in FACS. Cells that cannot cleave the substrate give a low signal on FACS analysis because there is no electrostatic interaction between the cell surface and the intact substrate.

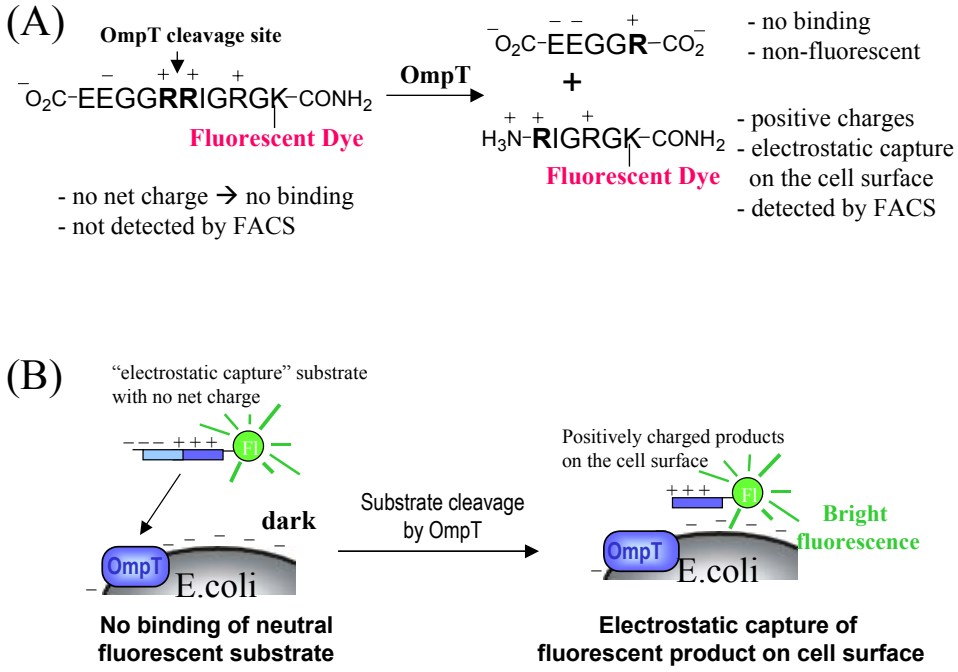

Figure 3.6 Design of "electrostatic capture" substrates used in FACS assays. (A) Cleavage of the electrostatic capture substrate by OmpT. Fluorescent dyes (Fl) are BODIPY for FL1 (530 nm) or TMR for FL2 (588 nm). (B) Strategy for localization of the electrostatic capture substrate. The highly positively charged product stays on the negatively charged cell surface while the uncleaved substrate with no net charge does not bind.

Synthesis of the electrostatic capture substrate

To verify electrostatic capture approach, two substrates **3.2a** (glutarate-EEGGRRIGRGK(BODIPY)-NH_2) and **3.2b** (glutarate-EEGGRRIGRGK(TMR)-NH_2) were synthesized. This straightforward single coupling step is simple and the yield is high and represents a significant advantage compared to the original FRET-based substrates that contained two different fluorophores.

FACS analysis with electrostatic capture substrates

The new substrates were incubated with either UT5600 (OmpT-) or UT5600/pML19 (OmpT+) strains and cell populations were analyzed by FACS at their proper detection wavelength: 530 nm for BODIPY-FL and at 584 nm for TMR, respectively. FACS histograms in Figure 3.7A and B showed excellent differentiations between the positive and negative control cells for both the BODIPY-FL **3.2a** and the TMR substrates **3.2b**. The ratio of positive signal to background signal was 50-fold and 20-fold for the BODIPY-FL and TMR substrates, respectively. In general, only a difference of 5-fold is required for routine isolation of desired cells with FACS.

Replacement of Ile in P_2' to Gly is known to decrease cleavage activity for OmpT considerably (Dekker *et al*., 2001). Substrate **3.3a**, glutaric acid-EEGGR•RGRGK(BODIPY)-NH_2, was synthesized and applied to FACS analysis, where '•' represents the cleavable peptide bond by OmpT. **3.3a** differs from **3.2a** substrate in that the P_2 is occupied by a sub-optimal Gly residue instead of Ile. Nonetheless, this substrate could distinguish between the UT5600 and UT5600/pML19 cells upon Arg-Arg cleavage although the histogram in Figure 3.7C. In order to apply this new substrate to FACS sorting, the cleaved fluorescent peptide product should stay on the surface of the active cells during 10 to 30 min of FACS sorting time. To prove this assumption, the UT5600 and UT5600/pML19 cells were mixed and analyzed on FACS with **3.3a**. The signals of each cell populations in the histograms of Figure 3.7C are distinguishable at any ratio of cell mixtures to prove that the fluorescent peptide product is not transferred form the OmpT active cells to the inactive cells. This substrate (**3.3a**) showed the P2 and P2' are not critical and it can be used for FACS sorting as an electrostatic capture substrate

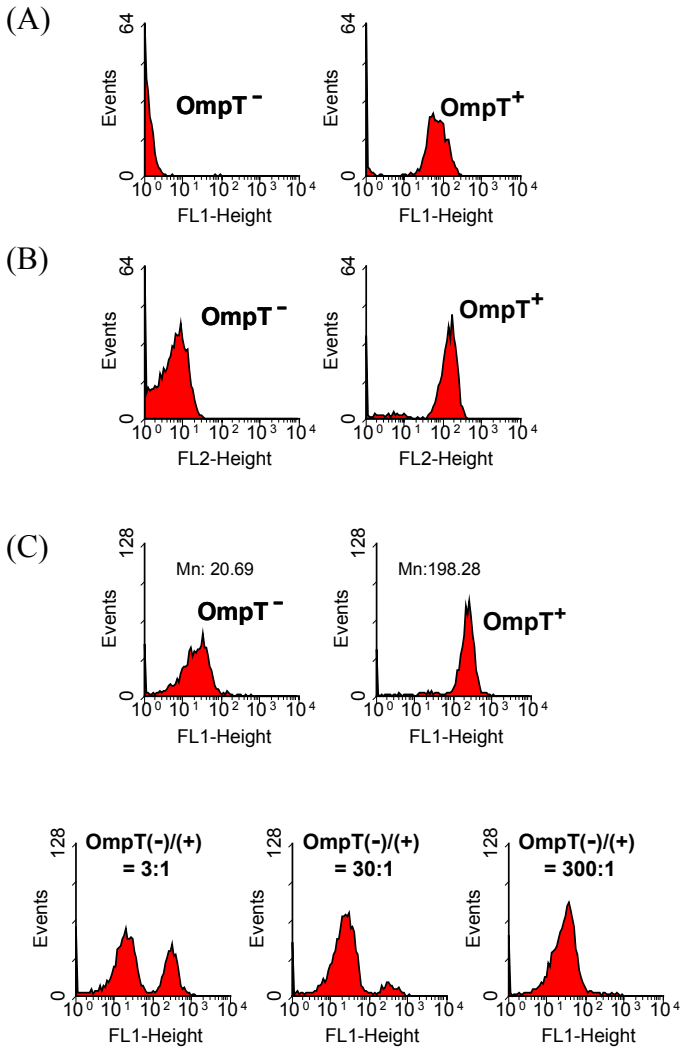

Figure 3.7 FACS assay of "electrostatic capture" substrates (A) FACS histograms of UT5600/pML19 and UT5600(OmpT-) for FL1 at 530 ± 30nm (FL1; for BODIPY) with 100 nM of **3.2a** (glutarate-EEGGR•RIGRGGK(BODIPY)-NH_2) (B) FACS histograms (FL2 for TMR) with **3.2b** (glutarate-EEGGR•RIGRGGK(TMR)-NH_2) (C) Discrimination of FACS signals when the negative cells (UT5600(OmpT-)), positive cells (UT5600/pML19(OmpT+)) are mixed. FACS histograms (FL1) represent the negative cells, positive cells, 3:1, 30:1 and 300:1 mixtures of the two cells with **3.3a** (glutarate-EEGGR•RGRGK(BODIPY)-NH_2)

3.4.3 Two-color system for isolation of specific activity on FACS

Design of two-color system for differentiating specific protease activity from non-specific activity

The successful demonstration of the electrostatic substrate that has only one fluorophore encouraged the design of a new powerful screening approach for discrimination of substrate specificity. Due to the simple design of the electrostatic substrate, two different substrates having differently colored fluorophores could be used for screening simultaneously. This "two-color system" was designed to identify enzymes that are more selective. As shown schematically in Figure 3.8A, each cell of an OmpT library selectively interacts and hydrolyzes its own specific substrate when incubated with a wild-type substrate having TMR (red fluorescence, Em = 564 nm) and a substrate designed with new cleavage sequence containing BODIPY-FL (green fluorescence, Em = 512 nm). For instance, the cells with wild-type OmpT activity cleave the amide bond between only Arg-Arg of the wild-type substrate, and the other substrate remains untouched in the reaction medium. Cleavage of the wild-type substrate results in the positively charged *C*-terminal product being captured on the cell surface, so they become labeled fluorescent red due to TMR emission. A cell with inactive proteases remains dark on FACS analysis. In contrast, a variant with desired substrate specificity would be labeled fluorescent green on FACS analysis due to cleavage of only the desired new substrate and capture of its *C*-terminal product labeled with BODIPY-FL. Non-specific cleavage would result in labeling by both colors. Note that the different emission wavelengths can be discriminated using the different channels of FACS machines (FL1 = 530 nm for BODIPY-FL and FL2 = 588 nm for TMR).

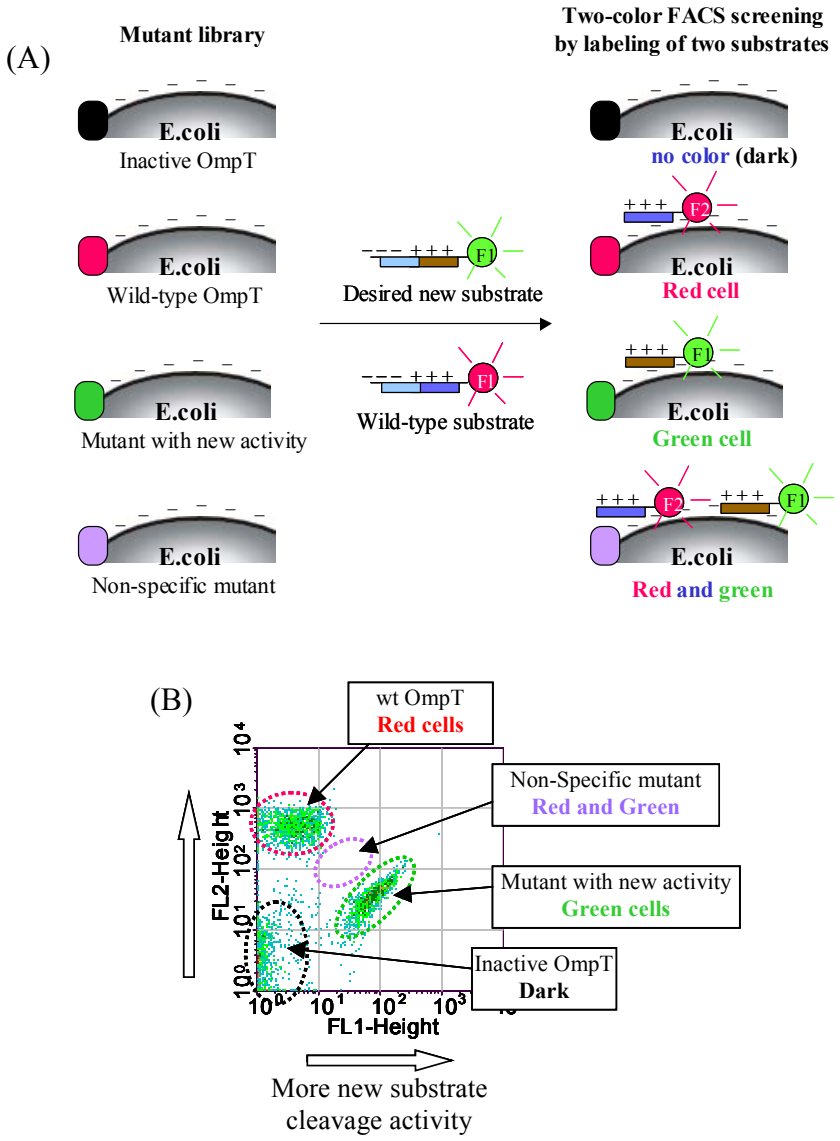

Figure 3.8 Design of two-color FACS sorting based on electrostatic capture substates. (A) Strategy for the two-color system. The cells that have different specificity are labeled with different fluorescent colors. (B) Expected cell population when two-color system is applied. Cell populations on the FACS density-plot were obtained and overlapped from FACS assay of UT5600(ompT-) for the dark cells, UT5600/pML19 with the substrate **3.1a** for the red cells and the substrate **3.1b** for the green cells. The specificity can be discriminated by the different fluorescence channels of FACS.

This approach is a huge improvement over the previous FRET-based substrates. The enzyme library can be quantified by the two-color system. The frequency of clones that gain new specificity, retain wild-type activity, and non-specific variants can be counted by FACS. Hence, this approach can exclude a non-specific variant from the wild-type variant or new variant with desired substrate specificity in FACS sorting. As mentioned above in the introduction, the C5 variant was isolated using the previous FRET-based substrate containing an Arg-Val sequence. It possessed a new substrate activity that was reported to cleave Arg-Val sequence better (k_{cat}/K_M = 1440 $s^{-1}M^{-1}$) than wild-type OmpT (k_{cat}/K_M = 24 $s^{-1}M^{-1}$). However, the C5 variant also inherited wild-type activity from the parent OmpT, and exhibited Arg-Arg cleavage comparable to the wild-type OpmT (k_{cat}/K_M = ~ 1 x 10^{-6} $s^{-1}M^{-1}$) (Olsen *et al*., 2000). In other words, the previous FRET-based method isolated all mutants that can cleave any amide bond within the FRET-based substrate **3.1b** without screening specific cleavage of the Arg-Val amide bond. In the two-color system, the non-specific OmpT variant that cleaves both substrates would be labeled with green and red on the fluorescence channels of FACS. Consequently, non-specific variants can be differentiated from the other cells with a high level of new substrate specificity. As shown in the FACS histogram of Figure 3.8B, the population of non-specific variants is expected to appear somewhere between the populations of the OmpT cells with wild-type specificity and OmpT variant cells with new desired specificity.

Estimation of substrates for two-color system

The two-color system in FACS sorting requires two substrates, the desired substrate for selecting a new activity (substrate specificity) and the other for deselecting the wild-type activity. However, cells expressing C5 did not give a positive signal on FACS analysis when incubated with the BODIPY (**3.3b**) or TMR (**3.3b'**) labeled electrostatic substrates containing the cleavage sequence (-Gly-Arg•Val-Gly-) as a desired substrate for selecting a new activity (Arg-Val cleavage).

Because of low FACS signal of the electrostatic capture substrate **3.3b** (-Gly-Arg-Val-Gly-), the FRET-based substrate **3.1b** (-Ala-Arg-Val-Gly-), which had given a positive signal with the C5 variant, was used for two-color sorting as the substrate having desired cleavage sequence to label the desired variants with fluorescent-green color (BODIPY-FL). For deselection of the wild-type Arg-Arg activity, the electrostatic capture substrate **3.2b** (-Gly-Arg•Arg-Ile-) was used as the wild-type substrate with a fluorescent-red color (TMR). When a mixture of the two substrates was incubated with the cells and analyzed by FACS, three distinguishable populations of UT5600(OmpT-), UT5600/pML19(wild-type OmpT+), and the UT5600/C5 variant appeared in FACS density-plots (Figure 3.9A).

Isolation of specific OmpT variants from a library by FACS using the two-color system

A library of random mutant was constructed as described previously (Olsen *et al*., 2000) sing the C5 gene C5 as a template for error-prone PCR with a mutation rate of 1.1% by fellow graduate student Mark Olsen. The combination of the FRET substrate **3.1b** (-Ala-Arg-Val-Gly-) and the electrostatic substrate **3.2b** (-Gly-Arg•Arg-Ile-) was used at concentration of 100 nM for sorting new variants with the desired activity. Using this two-color approach, the cells with the desired activity from the C5 library of $4x10^5$ protein variants were collected by setting up a sorting gate only on the green (FL1) region (R3 in Figure 3.9B) of the FACS dot plot in order to exclude the non-specific variants (red and green combined emission) and the Arg-Arg cleavage activity (red emission). As expected, preliminarily isolated new variants appeared within the selected R3 region on FACS analysis from an error-prone PCR library where C5 was the parent (Figure 3.9C) (Olsen, 2003a).

(A)

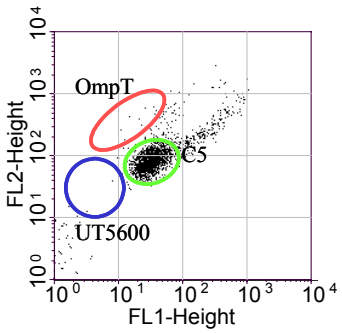

(B)

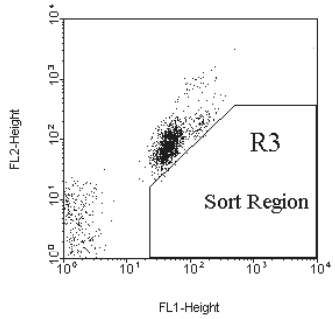

(C)

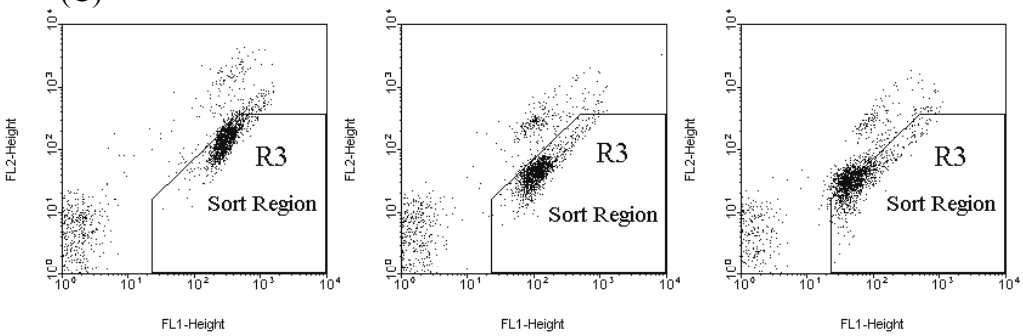

Figure 3.9 Two-color sorting using the mixture of the FRET substrate **3.1b** for isolation of new Ala-Arg activity and the TMR labeled electrostatic capture substrate **3.2b** for deselecting unwanted Arg-Arg cleavage of wild-type substrate activity. (A) Overlapped density-plot of cell population of UT5600(OmpT-), UT5600/pML19(wild-type OmpT+), and UT5600/C5 variant. (B) Sort region of C5 library using two-color system (Olsen, 2003a) (C) Sort region of individual variants isolated using two-color system. FL1 represents more cleavage of new Ala-Arg of **3.1b** and FL2 represents more cleavage of Arg-Arg of **3.2b** (Olsen, 2003a).

The library was re-sorted to recover 99 clones under more strict sort region of FACS desity-plot. After secondary microplates assays of the recovered clones with *bis*-BODIPY autoquenching substrates (**3.7a** and **3.8**), two clones, 1.2.19 and 1.3.19, displayed the desired activity were isolated and sequenced (Table 3.4), working with fellow graduate student Mark Olsen as same procedure as previously described (Olsen *et al*., 2000). Although 1.2.19 and 1.3.19 variants have 4 and 2 amino acid substitutions from C5 (Table 3.4) respectively, only Asp208Gly in 1.2.19 and Ser223Arg in 1.3.19 are located near the active site of OmpT. The 8 point mutation in the variants that come directly from C5 may neutral or have minor effects for the activity (Olsen, 2003a).

	17	200	208	214	223	285
C5	Ser	Phe	Asp	Asp	Ser	Tyr
1.2.19		Tyr	**Gly**	Val		Phe
1.3.19	Gly				**Arg**	
wt*	Ser	Tyr	Asp	Asp	Ser	Tyr

Table 3.4 Amino acid mutations found in the isolated clones 1.2.19 and 1.3.19 compared to C5. Note that only the point mutations in bold font are located near the active sites. C5 has eight different mutation points from wild-type OmpT, which is far from the active sites. (*wild-type OmpT sequence for comparison)

3.4.4 Enzyme activity assay by *bis*-BODIPY autoquenching substrates

A series of *bis*-BODIPY autoquenching substrates for post screening of the OmpT variants were designed and prepared as described in chapter 2.

Total cell activities of the wild-type OmpT and the variants were evaluated by observing the fluorescent intensity in a 96-well microplate assay using the autoquenching substrates (Figure 3.10). Three Arg-Arg substrates, **3.4**, **3.5** and **3.7a**, were cleaved by wild-type OmpT and C5 cells as expected. It is not surprising that the substrate **3.7a** was a poor substrate since it contains two Gly's in the P_2 and P_2' positions and Glu in P_4. Although two consecutive basic amino

acids at the P_1 and P_1' sites are major factors for substrate binding of OmpT, flanking residues are also important for OmpT activity (Dekker *et al*., 2001) (Okuno *et al*., 2002b).

The new clones, 1.2.19 and 1.3.19, cleaved substrate **3.8** (-Ala-Arg-Val-Ile-) specifically. C5 cells also showed considerable activity with that substrate. Interestingly, these new OmpT variants could not cleave substrate **3.7b** (-Gly-Arg-Val-Gly-). These results could not be explained in straightforward manner because **3.7a** (-Gly-Arg•Arg-Gly-) containing the same flanking sequence of **3.7b** was cleaved by wild-type OmpT and C5 cells to some extent in spite of having Gly residues on P_2, P_2' and Glu residue on P_4.

For further characterization of the OmpT variants, the enzymes that were purified by fellow graduate students Mark Olsen and Navin Varadarajan, were assayed with the same substrates. The purified enzymes gave results that were consistent with the total cell enzyme activity assay. In particularly, the purified wild-type OmpT and C5 enzymes cleaved all Arg-Arg substrates (Figure 3.11A, B, and E). The purified OmpT variants showed cleavage activity with substrates **3.6** (-Ala-Arg-Val-Gly-) and **3.8** (-Ala-Arg-Val-Ile-) but not the substrate **3.7b** (-Gly-Arg-Val-Gly-) (Figure 3.11C, D and F). To uncover the variant's new binding of S_1' prefernces at altering P_1' new substrates of the form as Arg-X were prepared (**3.7c** for Arg-Ala, **3.7d** for Arg-Leu, or **3.7e** for Arg-Trp). The variants could not cleave any of these substrates as shown in Fig. 6H, underscoring the highly sequence specific nature of cleavage by these new OmpT variants.

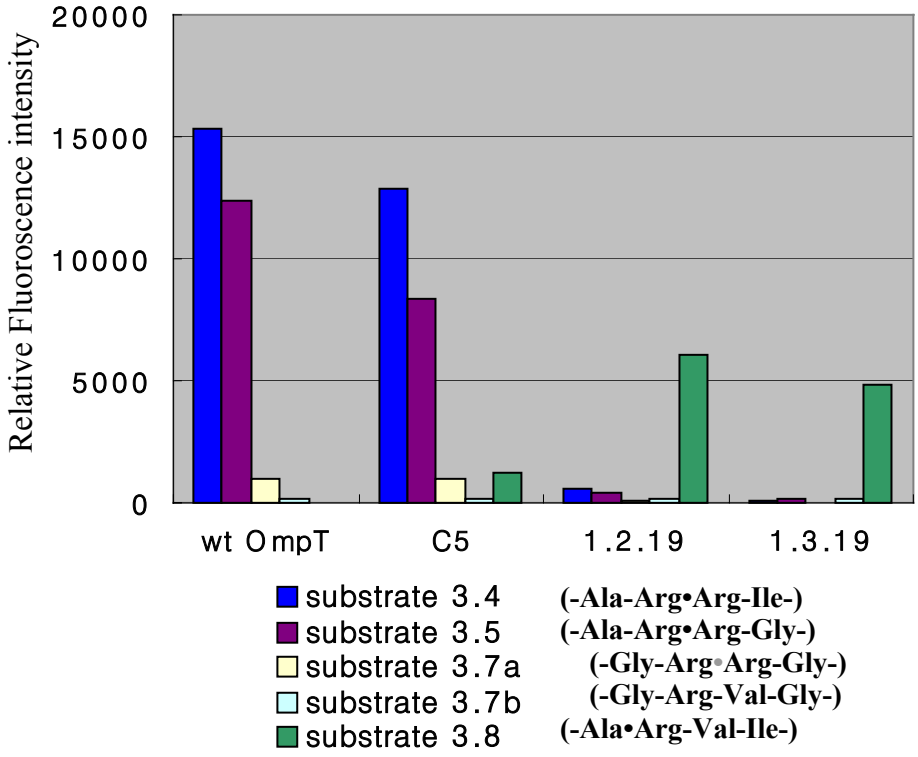

Figure 3.10 Primary fluorometric assay of activity of whole cells. Suspensions of UT5600/pML19, UT5600/C5, UT5600/1.2.19 and UT5600/1.3.19 were incubated with the *bis*-BODIPY autoquenching substrates. The substrate sequences in parentheses are the cleavage site, and • represents a probable peptide bond of cleavage.

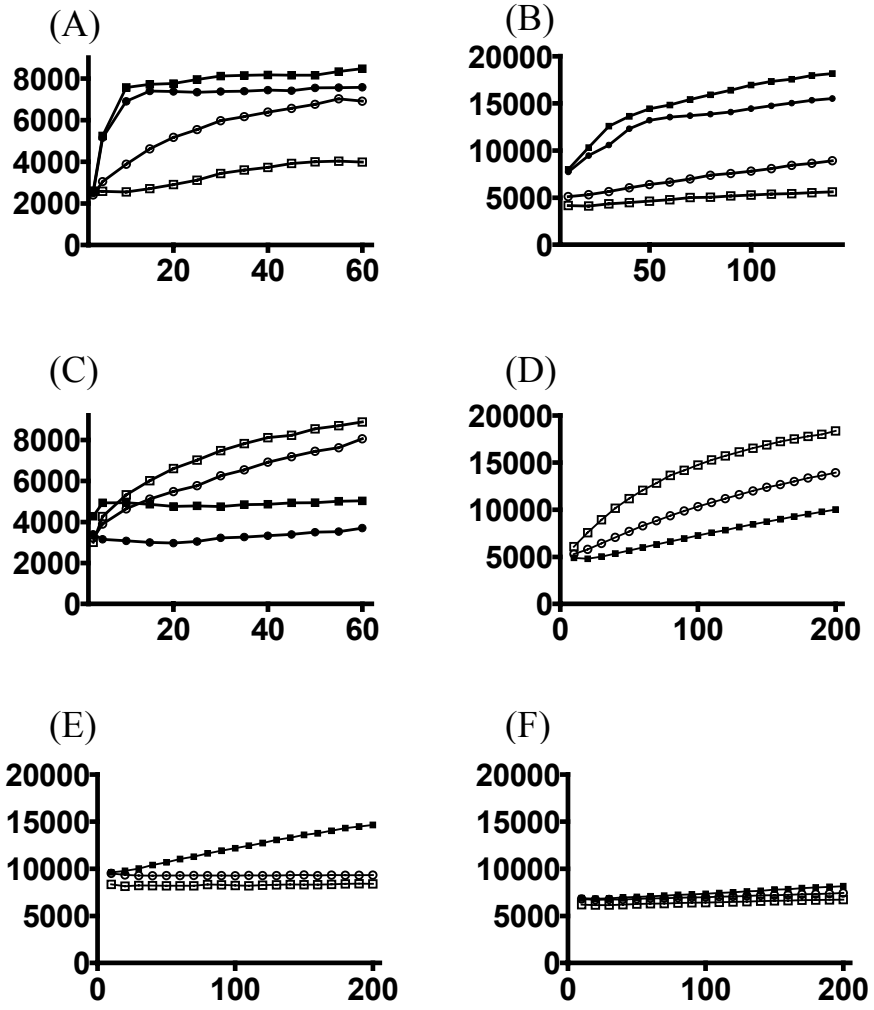

Figure 3.11 Fluorometric enzyme assay of the relative activity for the purified enzymes; wild-type OmpT (close circle), C5 (close square), 1.2.19 (open circle), and 1.3.19 (open square) with the *bis*-BODIPY substrates. (A) substrate **3.4** (-Ala-Arg•Arg-Ile-) (B) substrate **3.5** (-Ala-Arg•Arg-Gly-) (C) substrate **3.8** (-Ala-Arg•Val-Ile-) (D) substrate **3.6** (-Ala-Arg-Val-Gly-) (E) substrate **3.7a** (-Gly-Arg-Arg-Gly-) (F) substrates **3.7b~d** (-Gly-Arg-X-Gly-, when X=Val, Leu or Trp).

3.4.5 Reconsidering of cleavage site and enzyme kinetics

The substrate specificity of OmpT is complicated because it recognizes the substrate from at least P_6 to P_2'. Reconsideration of a completely different cleavage site was thus required. In the enzyme activity assays, any cleavage of peptide bonds in the *bis*-BODIPY autoquenching substrates could give the fluorescent signal, not just cleavage between Arg-Val. Cleaved peptide products were characterized by LC/MS spectroscopy. To simplify the substrate specificity, the same amino acid sequences of the substrates that had been used in FACS sorting were used to verify the cleavage sites of the variants. Two natural peptide substrates, **3.10** (H-WEEGGRRIGRGRK-NH_2) and **3.11** (H-WCARVGKGRGR-NH_2), were prepared for HPLC analysis as analogues of the substrates (**3.1b** and **3.2b**) used in the FACS sorting. Those substrates have the same sequences of the FACS substrates but fluorophores were not labeled to remove potential unnatural fluorphore labeling effects on protease activity. In order to detect the products on the HPLC at 280 nm, a Trp was added to the *C*-teminus of the substrate peptide. These substrates were incubated with the purified OmpT variants and the products were analyzed by HPLC and MS. As expected, the wild-type OmpT and the C5 variant cleaved the peptide bond with similar activity between Arg and Arg of the substrate **3.10** (Figure 3.12A and B). The substrate **3.11** was hydrolyzed by C5 as shown in Figure 3.12C. Surprisingly, major products from fully digested **3.11** by C5, 1.2.19 and 1.3.19 (Figure 3.12D, G and H) were identified as H-WCA-OH and H-RVGKGRGR-NH_2 in LC/MS analysis. The peaks (m/z) identified in ESI-MS were 379.22 (MH^+) and 884.58 (MH^+) and precisely matched with H-WCA-OH and H-RVGKGRGR-NH_2, respectively. The result confirmed the acquired new activity of C5 from the first FACS sorting is Ala-Arg cleavage rather than Arg-Val cleavage, and this was transferred to the more active variants, 1.2.19 and 1.3.19.

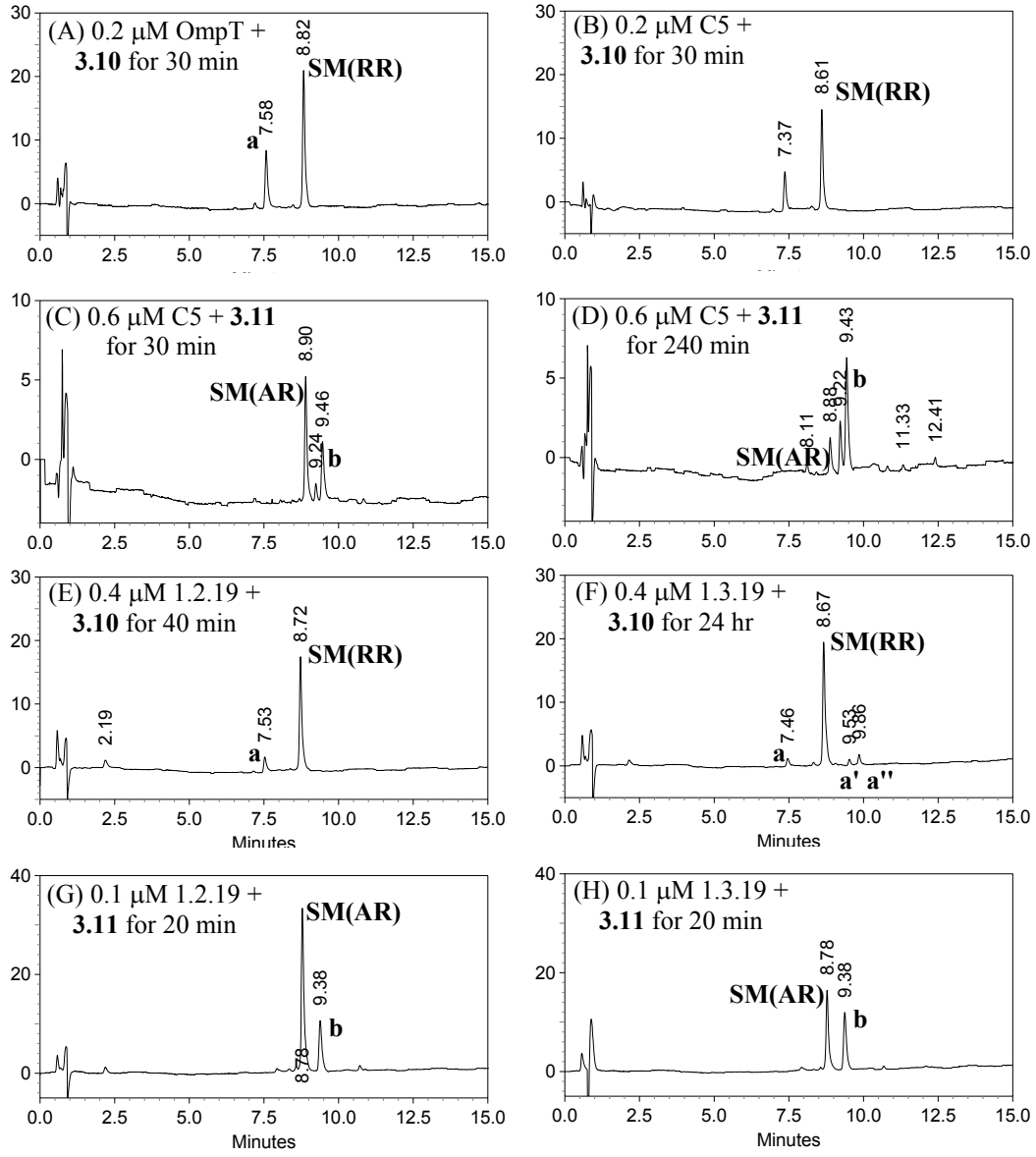

Figure 3.12 HPLC analysis of digested products of substrate **3.10** (0.1 mM) for Arg-Arg cleavage (A, B, E and F), and substrate **3.11** (0.1 mM) for Ala-Arg cleavage (C, D, G and H) with the wild-type OmpT (A), C5 (B, C and D), 1.2.19 (E and G) and 1.3.19 (F and H). (**SM** on HPLC chromatograph represents a remained starting substrates, **3.10** or **3.11**; digested products of the substrate **3.10**, **a**, **a'** and **a''** is H-WEEGGR-OH, H-WEEGGRRI-OH and H-WEEGGRRIG-OH respectively; digested product of the substrate **3.11**, **b** is H-WCA-OH.)

However, the Arg-Arg cleavage activity of 1.2.19 with the substrate **3.10** was significantly lower than parental C5 cleavage. Moreover, 1.3.19 cleaved only trace amounts of the substrate even after 24 hours (Figure 3.12E and F). Lower concentration of 1.2.19 and 1.3.19 were used for HPLC analysis for protease activity for Ala-Arg of **3.11** because of fast hydrolysis (Figure 3.12G and H). In general, the 1.3.19 variant showed much lower activity towards Arg-Arg cleavage of **3.10** and higher activity for Ala-Arg cleavage of **3.11** than 1.2.19. Based on the HPLC analysis, 1.3.19 is highly specific for the Ala-Arg site in **3.11**. Further investigation of the new variants confirmed that the direction of the directed OmpT evolution was shifting from the native specificity of Arg-Arg cleavage toward the completely new specificity of Ala-Arg. The kinetic parameters of the parental C5 variant and the 1.3.19 variant with the new specificity (Table 3.5) were obtained as described in the Material and Methods.

Enzyme	Cleavage site	K_M (μM)	k_{cat}	k_{cat}/K_M ($M^{-1}se\ c^{-1}$)	Ratio of catalytic efficiency (AR/RR)
C5	AR of **3.11**	1.5±1.2	0.017±0.002	1.1×10^4	0.035
C5	(RV)* of **3.11**	8.2±4.5	0.0058 ±0.0011	7.1×10^2	(prefer RR cleavage)
C5	RR of **3.10**	2.2±0.98	0.68±0.053	3.1×10^5	
1.3.19	AR of **3.11**	4.1±1.2	0.56±0.04	1.4×10^5	6.1×10^4
1.3.19	RR of **3.10**	117±30	$2.7x10^{-4}$±$6x10^{-6}$	2.3	(prefer AR cleavage)

Table 3.5 Catalytic efficiencies of C5 and 1.3.19 variants reacting with the substrates **3.10** and **3.11**. (*It is not clear whether a small peak at 9.24 min in Figure 3.12C is the *N*-terminal product (H-WCAR-OH) of **3.11** by Arg-Val cleavage because only a very small peak of the *N*-terminal product was found in LC/ESI-MS at 534.24 $(H\text{-}WCAR\text{-}OH+H)^+$, calculated 533.23 while huge peaks of Ala-Arg cleavage products were found.)

The 1.3.19 variant showed a remarkable 61,000-fold specificity (ratio of catalytic efficiency) for Ala-Arg over Arg-Arg (**3.11** to **3.10**). This number is huge when the very low specificity to Ala-Arg activities of the C5 and the wild-type OmpT (0.036 and 0.013, respectively) are compared. According to this analysis,

the specificity conversion from C5 to 1.3.19 would be more than a million-fold! Notice that this dramatic change of specificity derives from a decrease in Arg-Arg cleavage activity as well as an increase of Ala-Arg cleavage. Our current explanation for this remarkable result is that the unwanted Arg-Arg activity was efficiently avoided by the two-color sorting system used in the FACS isolation of 1.2.19 and 1.3.19.

These results now explain why the electrostatic substrates **3.3b** and **3.3b'** (both have Gly-Arg-Val-Gly-) incubated with C5 cells did not give signals on FACS analysis while the FRET substrate **3.1b** (-Ala-Arg-Val-Gly-) gave the positive signal. The substrates **3.3b** and **3.3b'** for FACS analysis lack an Ala-Arg cleavage site. This specificity is also consistent with the finding that the *bis*-BODIPY substrate **3.7b**, without Ala-Arg sequence, was also not cleaved by 1.2.19 and 1.3.19. A combination of two electrostatic capture substrates (e.g., glutaric acid-EEGG**R•R**IGRGGK(BODIPY) and glutaric acid-EEGG**A•R**IGRGGK(TMR)-NH_2) would have been better to select the desired activity (Ala-Arg) in stead of the combination of the FRET-based substrate and the electrostatic capture substrates because the two electrostatic capture substrates have the same flanking sequences.

Among the most important OmpT recognition sites on the substrate, the basic residue of the P_1 site is extremely restricted. Like the P_1 residue, a basic P_1' residue is also preferred by wild-type OmpT. However, P_1' can be Val, albeit with low activity. Based on the strictly conserved P_1 site, the previous idea, which led us to assume Arg-Val activity was a likely direction for the directed evolution of OmpT specificity. However, C5 was successfully isolated from wild-type OmpT by the FRET substrate **3.1b** with -Ala-Arg-Val-Gly- sequence by cleaving the Ala-Arg peptide bond, not Arg-Val. These results demonstrate that secondary assays for protease activity should be scrutinized very carefully. The previous assumption that OmpT was evolved for from Arg-Arg to Arg-Val cleavage activity was corrected in this work. The same sequence of a substrate in a secondary assay

might reduce the chance of getting a misleading result. Note that we cannot rule out that 1.2.19 and 1.3.19 have other as of yet undetected substrate preferences.

3.4.6 Consideration of specificity on the basis of the structure of the OmpT variants.

Based on the X-ray crystal structure of OmpT (Vandeputte-Rutten *et al*., 2001), the variants C5, 1.2.19 and 1.3.19 were visualized by changing the residues corresponding of point mutations identified by DNA sequencing. The resulting structures were energy-minimized using HyperChem™ (Figure 3.13). In Figure 3.13A, the electrostatic potential surface and ribbon representation of active site cleft with S_1 subsite (dotted circle) of OmpT was rendered using the Swiss-PdbViewer v3.7 program (http://www.expasy.org). The top of the enzyme in the side view contains the active site, which faces the extracellular space while the bottom of the structure is oriented toward the periplasmic space. The proposed active site residues Glu27, Asp83, Asp85, Asp208, Asp210 and H212 in OmpT are shown as stick models.

Although C5 has 8 different point mutations in amino acid sequence from wild-type OmpT, many might be irrelevant to substrate specificity because they are far from the active site and binding groove. However, these point mutations may cause subtle changes in the overall structure of C5 leading to the broadened substrate specificity (Figure 3.13B).

According to the proposed mechanism, the groove that forms the proteolytic site of OmpT is negatively charged due to many acidic residues (Glu residues on 27, 33, 167, and 153, and Asp residues on 83, 85, 97, 158, 159, 208, 210, 214, 274 and 267). The proposed catalytic dyad (Asp210 and His212) is placed in the middle of the groove (Kramer *et al*., 2001a). Asp208 sits on the bottom of the site, and it is expected to interact with the P_1 residue of the substrate. The replacement of Asp208 in C5 with Gly in 1.2.19 reduces the negative charge in the S_1 subsite, which eliminates the putative electrostatic interaction with the positively charged

residue (Arg) of P_1 (Figure 3.13C). The reduced negative charge and smaller amino acid (Asp208Gly) in S_1 of 1.2.19 likely allows large hydrophobic residues to be accommodated in P_1 of the substrate.

The 1.3.19 variant has the highest selectivity for Ala-Arg over Arg-Arg activity among the variants. The point mutation Ser223Arg in the S_1 subsite of 1.3.19 is above and directly contacting Asp208 in the S_1 subsite (Figure 3.13D). This charge serves to neutralize the negative charge of Asp208, eliminating the electrostatic attraction of P_1 (Arg) in the substrate **3.10**. In addition, the positively charged Arg (223) in S_1 of 1.3.19 might be repelling the positively charged P_1 residue (Arg) in the substrate. These explain why 1.3.19 has very little Arg-Arg cleavage activity compared to 1.2.19, which still has some Arg-Arg cleavage activity. The higher preference of Ala at P_1 compared to 1.2.19 could be that the S_1 of 1.3.19 is smaller than that of 1.2.19 as shown in Figure 3.13C and D. In addition, the S_1 of 1.3.19 might not accommodate a large P_1 residue like Arg. The smaller S_1 surface might have more hydrophobic contacts to a small Ala residue of than an Arg residue of P_1.

An OmpT variant with novel specificity at the S_1 subsite can be proposed. For instance, if the Ser208 of OmpT is replaced by Lys or Arg so that the S_1 subsite switches to a positive pocket, the new variants (Ser208Lys or Ser208Arg) will probably have completely new specificity with Glu-Arg and Asp-Arg cleavage activity.

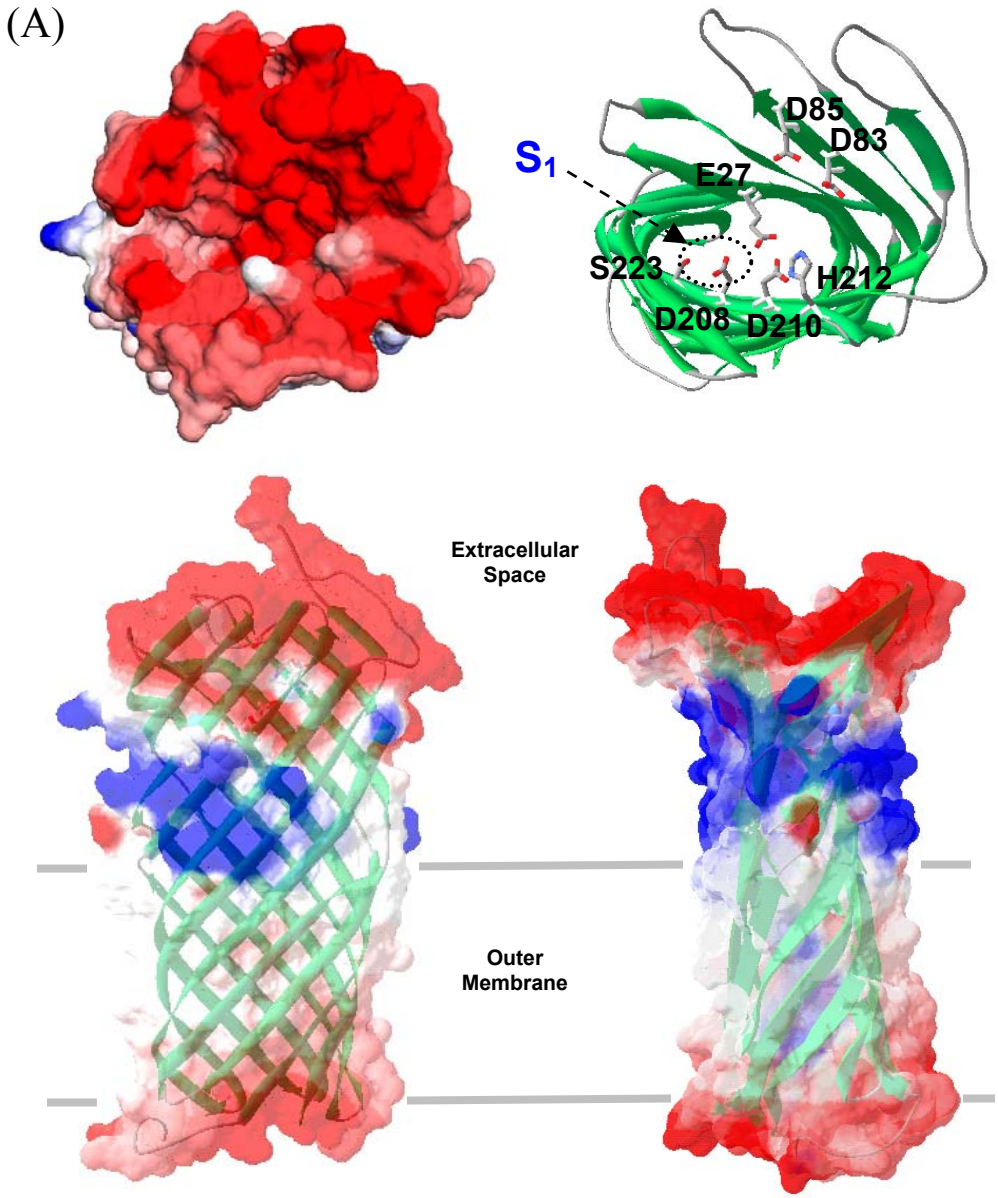

Figure 3.13 (A) Structure of wild-type OmpT. Top view (top) and side view (bottom) of electrostatic potential surface (blue = positive charged, red = negatively charged) and ribbon representation (top right) of active site cleft with S_1 subsite (dotted circle). The proposed active site residues Glu27, Asp83, Asp85, Asp208, Asp210 and H212 in OmpT are shown as stick model (top left).

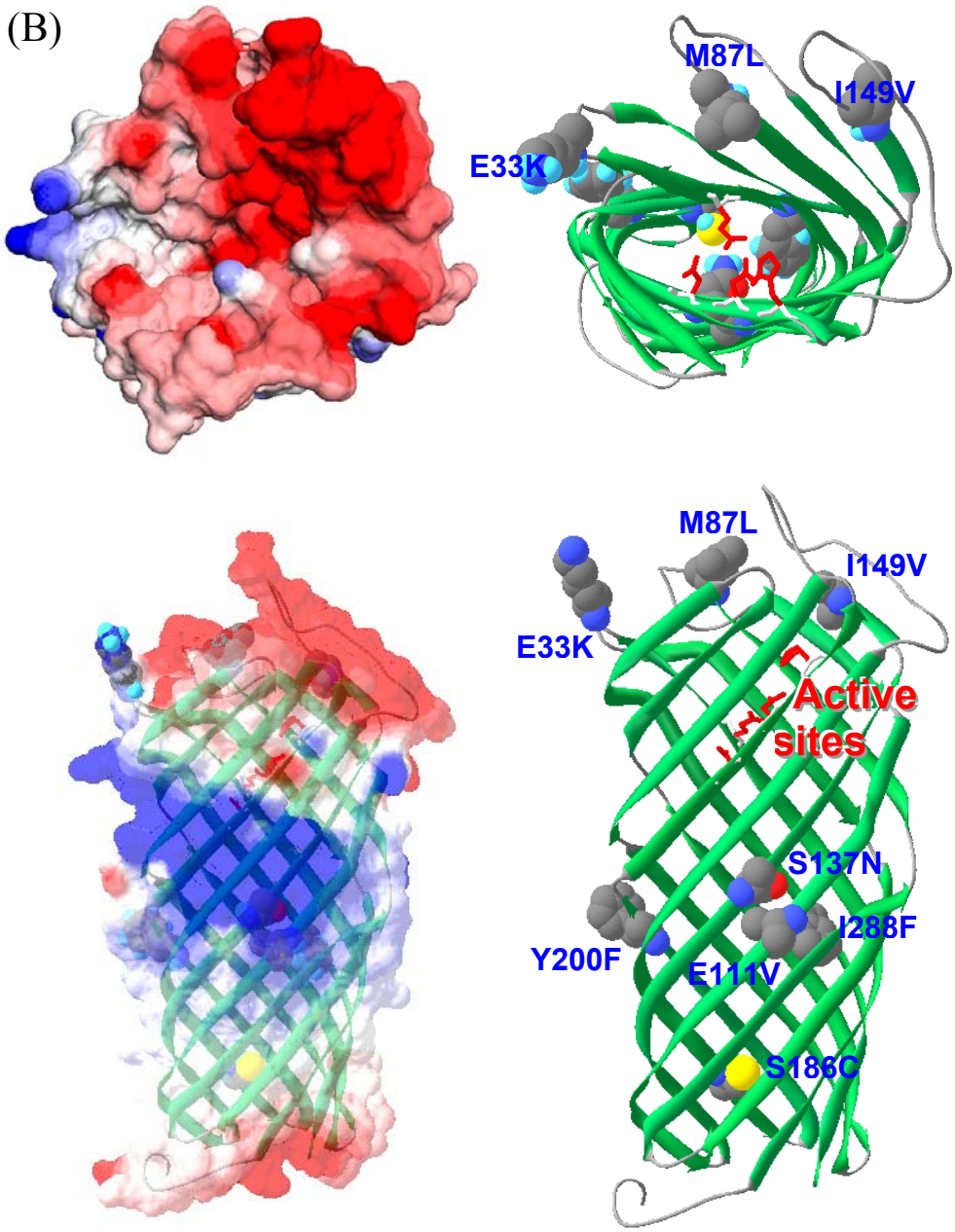

Figure 3.13 (continued) (B) Structure of C5. The proposed active site residues are the same as OmpT (red stick model). The mutation points E33K, M87L, E111V, S137N, I149V, S186C, Y200F and I288F (blue colored letters) are shown in space-fill model.

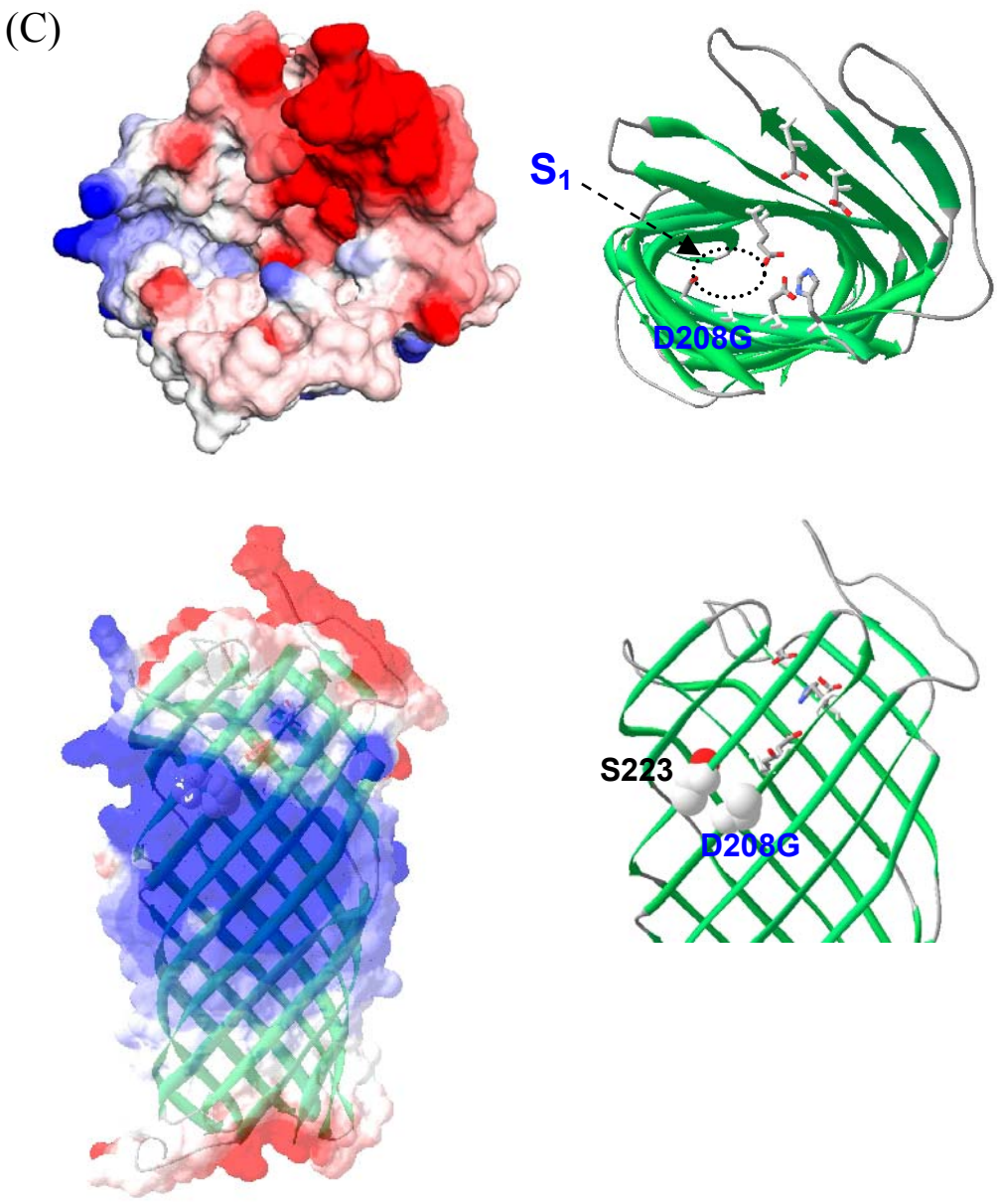

Figure 3.13 (continued) (C) Structure of 1.2.19. The mutation point D208G (blue colored letters) is shown in space-fill model. Amino acid (S223) labeled with black letters is not mutated (same as OmpT) and shown for comparison.

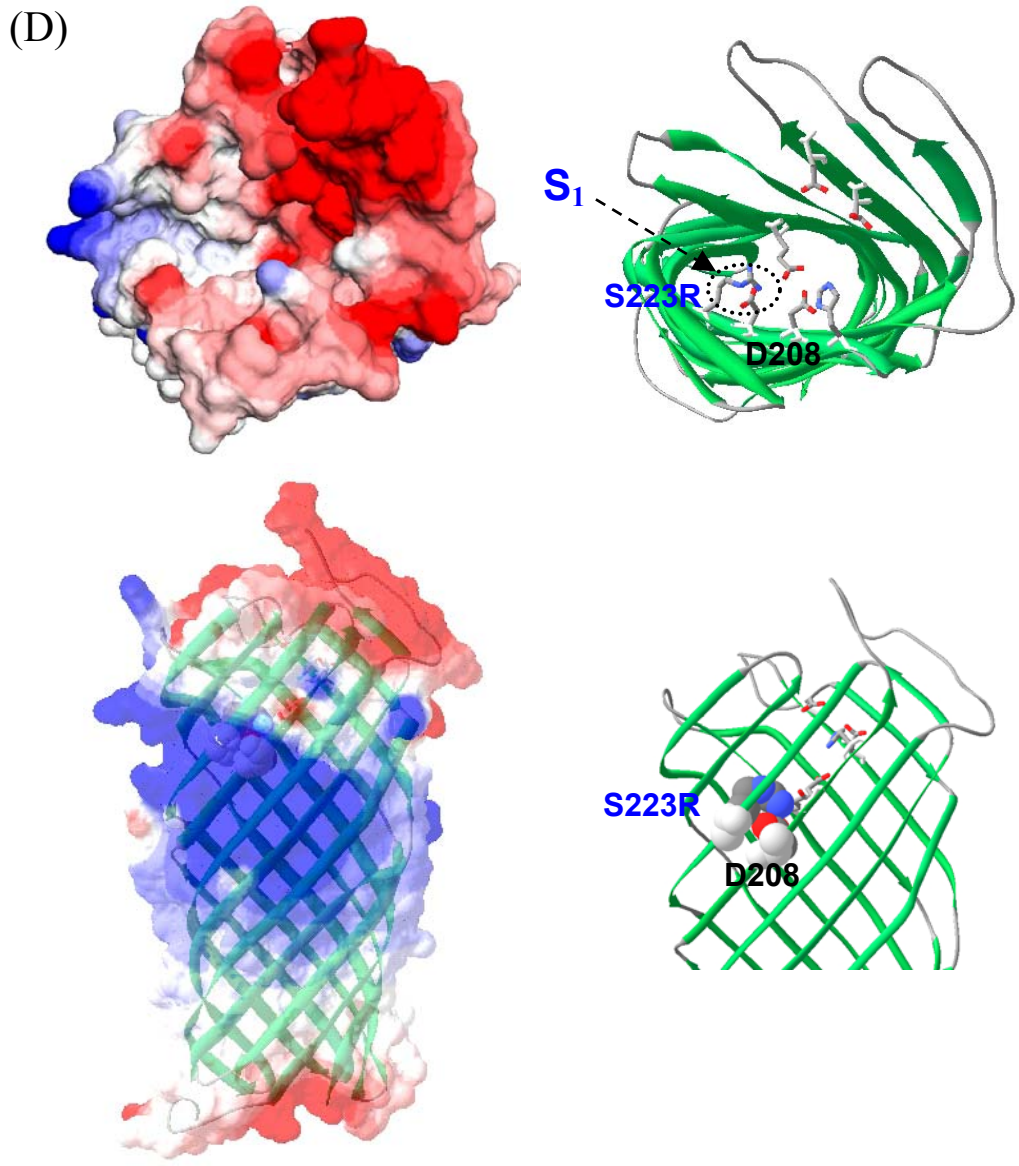

Figure 3.13 (continued) (D) Structure of 1.3.19. The mutation point S223R is shown in space-fill model. Amino acid (D208) labeled with black letters is not mutated (same as OmpT) and shown for comparison in ribbon.

3.5 CONCLUSION

A powerful new strategy for high-throughput screening to alter specificity in directed protease evolution was devised based on FACS. First, substrates releasing electrostatically captured enzymatic products on the negatively charged bacterial cell were designed and tested. The new electrostatic capture substrates contain only one fluorescent dye which enables a strategy using two different substrates with differently colored fluorescent dyes. The two-color system successfully isolated the variants 1.21.19 and 1.3.19, which had totally new selectivity (Ala-Arg cleavage activity) while deselecting the unwanted wild-type activity. This directed evolution of the parental OmpT enzyme to the newly evolved 1.3.19 variant resulted in more than a million-fold change toward Ala-Arg specificity away from Arg-Arg with the two-color system.

Chapter 4

Permeability study of outer membrane of *E. coli* using flow cytometry to detect periplasmic functional proteins

4.1 CHAPTER SUMMARY

4.1.1 Goals

To study the permeability of the *E. coli* outer membrane to detect specific FACS probes designed to periplasmic expressed proteins such as antibodies and enzymes while not sacrificing the bacterial integrity and viability.

4.1.2 Approach

A series of probes composed of a hapten (digoxigenin), a linker and a fluorescent dye (BODIPY) were created. The size and chemical properties of the linker were varied systematically. FACS analysis and sorting was performed with cells expressing periplasmic scFv(anti-dig) antibody that recognize digoxigenin. A variety of known outer membrane permeabilizers were tested. Furthermore, a heptoseless LPS *E. coli* mutant strain (D21f2) with enhanced permeability was also analyzed.

4.1.3 Results

Among the permeabilizers tested, polymyxin B nonapeptide (PMBN) gave the highest outer membrane permeability without sacrificing the cell's integrity and viability. Others were found to be significantly more toxic to the cells. Even the high molecular weight peptide probes can pass through the *E. coli* outer membrane in the presence of PMBN. When Jude1 and ABLEC strains were compared, the Jude1 strain was found to be more robust during FACS analysis when PMBN is

used. Furthermore, without permeabilizers, the D21f2 strain showed high outer membrane permeability to the probes.

4.2 INTRODUCTION

4.2.1 Probes used in the permeabilizer studies

To examine the permeability of the *E. coli* outer membrane, several probes have been used including lysozyme, detergents, hydrophobic antibiotics, 1-*N*-phenylnaphthylamine (NPN), and hydrophobic 3-oxosteroids.

Lysozyme can diffuse in and exert its lytic activity when the outer membrane is permeabilized by polymyxins, thereby allowing periplasmic enzymes to leak out (Warren *et al*., 1957). Limitation of using lysozyme as a general permeability probe includes the fact that lysozyme cannot detect the change in composition of the outer membrane such as formation of phospholipid bilayer patches in the outer membrane. Permeabilization effect of polycationic permeabilizers that weakly bind LPS also cannot be detected by this method (Ohno & Morrison, 1989a, Ohno & Morrison, 1989b).

Bacteriolytic anionic detergents (deoxycholate, or dodecyl sulfate) have also been used as probes with similar mechanism of the lysozyme probes. Bacteria that are treated with outer membrane damaging agents are more susceptible to the detergents that cause lysis (Vaara, 1981, Vaara, 1990).

Additionally, permeability of outer membrane has been measured using **hydrophobic antibiotics**. Hydrophobic antibiotics in particular are not efficient at killing Gram negative bacteria because they cannot diffuse through the outer membrane. When effective permeabilizers, such as PMBN or EDTA, are applied to sensitize the outer membrane, the bacteria become susceptible (Kimura *et al*., 1992). Permeability of the outer membrane is indirectly measured as the mean inhibition concentration (MIC) of the antibiotics.

Hydrophobic **1-*N*-phenylnaphthylamine (NPN)** can also be used as a spectroscopic probe by measuring uptake (Helander & Mattila-Sandholm, 2000). NPN is barely fluorescent in aqueous environments. The intact outer membrane does not allow the entry of the very hydrophobic NPN. However, NPN becomes highly fluorescent when it enters into the phospholipid environments through a permeabilized or damaged outer membrane (Traeuble & Overath, 1973). NPN has been used to study lactic acid or EDTA-based permeabilizers that cause LPS release (Helander & Mattila-Sandholm, 2000).

Hydrolysis of **a chromogenic β-lactam probe** by periplasmic β-lactamase in whole bacteria has also been used to assess outer membrane permeability. Chromogenic probes include the β-lactams, nitrocefin and cephalosporin (PADAC) (Hancock & Wong, 1984, Lehrer *et al*., 1988). However, the method is limited because β-lactamase can be released from the some periplasm when the permeabilizers are used. The activity of β-lactamase remaining in periplasm competes with the released β-lactamase in the medium, adding error to the measurements.

Along similar lines, the outer membrane permeability rates of **hydrophobic steroids** are assessed by following enzymatic conversion by 3-oxosteroid Δ1-dehydrogenase using a small redox indicator dye. In general, the more hydrophobic and uncharged steroids diffuse through the outer membrane better than amphiphilic, negatively charged steroids. These results are consistent with those obtained from hydrophobic antibiotics (Plesiat & Nikaido, 1992).

The above studies serve as important background for our permeabilization studies using FACS probes. In this chapter we will use probes of various molecular weights and use FACS to screen for binding to a periplasmically expressed antibody.

4.2.2 periplasmic expression with cytometric screening (PECS)

Recently, Chen and co-workers in our laboratory have described the "display-less" approach for screening scFv antibody libraries using FACS (Chen *et al.*, 2001). This methodology is intended to complement previously reported surface display systems on *E. coli* (Daugherty *et al.*, 1998) (Figure 4.1A). In this approach, a soluble scFv antibody or scFv library is expressed in the periplasmic space of *E. coli* (Chen *et al.*, 2001). Next, fluorescently labeled hapten diffuses through the outer membrane, where it can bind a complementary scFv (Figure 4.1B). The resulting fluorescent cells are isolated by FACS (Figure 4.1C). In this periplasmic expression with cytometric screening (PECS) approach, the periplasmic space provides a compartment for holding the protein-probe complexes while preserving the genetic information of the target protein inside of the inner membrane.

The PECS approach overcomes several limitations of other protein display technologies and may be a more widely applicable tool for directed protein evolution. For example, protein display on biological particles, generally requires anchoring systems such as g3p (pIII) protein of M13 bacterial phage, Aga2p mating adhesion receptor of yeast (Boder & Wittrup, 1997, Kieke *et al.*, 1997) and Lpp-OmpA' of outer membrane of *E. coli* (Daugherty *et al*., 1998) that are fused on either *N*- or *C*-termini. This use of fusion can mask downstream expression problems that are often encountered when the intact selected scFv is produced (no fusion). PECS uses free target protein thereby selecting for highly expressing intact protein. In addition, dimeric or mutimeric protein complexes would hardly be applied to surface display in *E. coli*, yet are amenable to PECS.

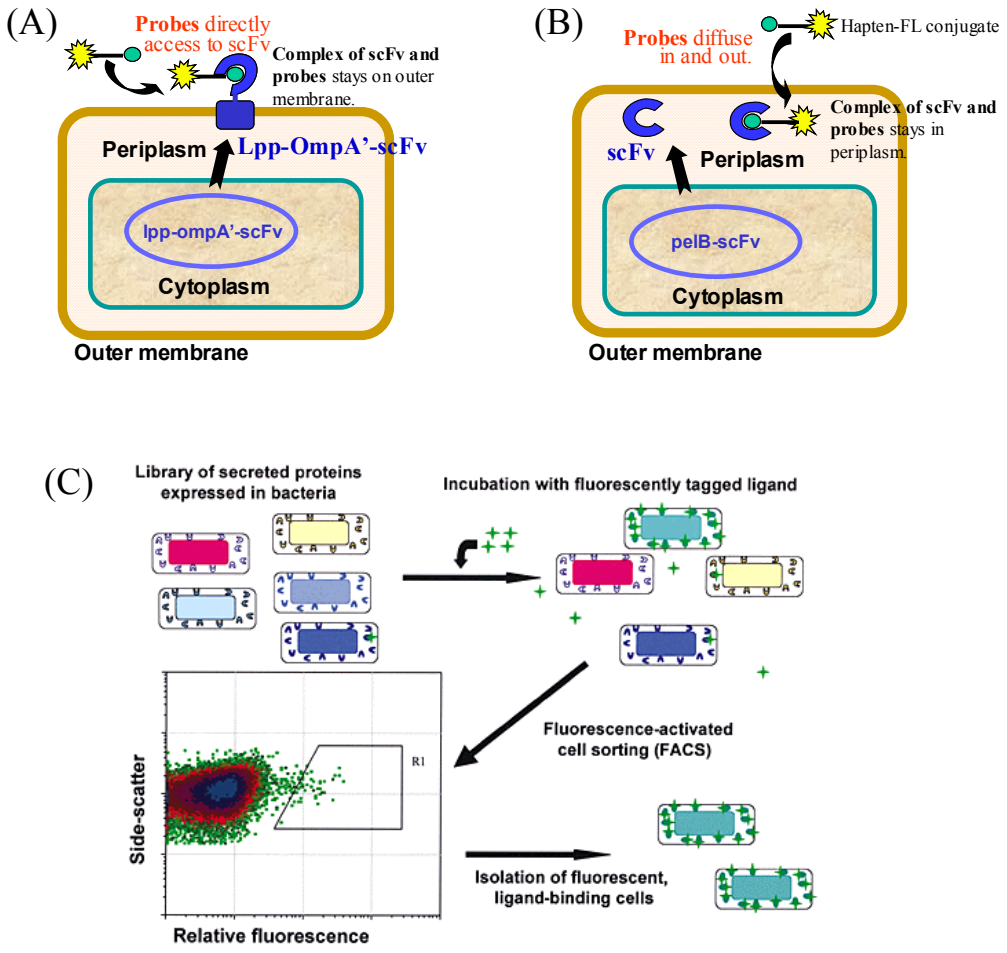

Figure 4.1 Comparison of (A) surface displayed scFv and (B) periplasmic scFv for PECS. (C) A schematic diagram showing the principle of periplasmic expression with cytometric screening (PECS). FACS can isolate the cells expressing protein species with the desired ligand-binding characteristics using defined region parameter (R1) on cell density profile during the FACS sorting. (Chen *et al.*, 2001)

The major issue of PECS is the outer membrane permeability, since probes must enter the periplasmic space in order to interact with the target protein. Generally, the untreated outer membrane of *E. coli* only allows diffusion of molecules that are smaller than about 650 Da (Decad & Nikaido, 1976). Using an 800 Da probe, partial osmotic shock of the ABLEC *E. coli* strain harboring periplasmic scFv with 10x PBS buffer increased the mean fluorescence intensity by 3-fold FACS signal over the signal of the same cell treated with 1x PBS. However, the higher ionic strength caused a decrease in cell viability. Phage infection using phage M13KO7 also improved outer membrane permeability of ABLEC strain. However, phage infected cells grew much slower than uninfected cells.

In order to facilitate the practical usage of PECS approach, analysis of the size limit of probes should be studied systematically. Such systematic studies to develop a method of permeabilizing the outer membrane by increasing the access of larger probes such as a peptide hapten or protease substrate, without compromising cell permeability are reported in the rest of this chapter.

4.3 MATERIALS AND METHODS

BODIPY-FL EDA (4,4-difluoro-5,7-dimethyl-4-bora-3a,4a- diaza-*s*-indacene-3-propionyl ethylenediamine, hydrochloride), BODIPY-FL SE, BODIPY-FL IA (*N*-(4,4-difluoro-5,7-dimethyl-4- bora-3a,4a-diaza-*s*-indacene-3- propionyl)-*N*'- iodo-acetylethylenediamine), Dig-NHS (3-amino-3-deoxydigoxigenin hemisuccinamide, succinimidyl ester) were purchased from Molecular Probes, (Eugene, OR). *Bis*-amino polyethyleneglycol 2000 and 4,7,10-trioxa-1,13-tridecanediamine (NH_2-$(CH_2)_3(OCH_2CH_2)_3CH_2$-$NH_2$) were purchased from Fluka. EDTA, PMBN (polymyxin B nonapeptide) and PEI (poly(ethyleneimine)) were purchased from Sigma. Conjugating reagents and characterization methods of the probes are the same as in the Materials and Methods part of chapter 2.

4.3.1 Chemical synthesis of fluorescent probes (Figure 4.2)

Preparation of BODIPY-EDA-Dig (4.1)

Dimethylaminopyridine (5 μmol in 50 μl of DMA) was added to a mixture of BODIPY-FL EDA (2 μmol in 50 μl of DMA) and Dig-NHS (4 μmol in 50 μl of DMA) at room temperature. After 1 hour incubation, the conjugate was purified by FPLC to give 0.8 mg (55%). ESI MS (m/z), calculated 805.44 for M, found 828.6 for $(M+Na)^+$.

Preparation of BODIPY-EG3-Dig (4.2)

BOIPY FL SE (4 μmol) was added to a mixture of 4,7,10-trioxa-1,13-tridecanediamine (40 μmol) and dimethylaminopyridine (10 μmol) in DMA. After incubation for 1 hour, the intermediate (BODIPY-EG3-NH_2) was purified by FPLC to give 0.86 mg (45%) as described in chapter 2. ESI MS (m/z) of BODIPY-EG3-NH_2, calculated 494.29 for M, found 495.5 for MH^+, 517.5 for $(M+Na)^+$, 475.5 for $(M-F)^+$.

The purified intermediate (0.87 μmol in 50 μl of DMA) was reacted with Dig-NHS (0.87 μmol) and 1M DMAP (8.7 μmol) in DMA. After 1 hour incubation, the probe **4.2** (BODIPY-EG3-Dig) was purified by FPLC to give 0.59 mg (70%). ESI MS (m/z); calculated 965.55 for M, found 966.5 for MH^+, 988.7 for $(M+Na)^+$, 946.7 for $(M-F)^+$.

Preparation of BODIPY-peptide-Dig (4.3)

A protected peptide on resin (H-CEEGPFGRSALVRRK-Rink amide resin) was capped with acetic anhydride on *N*-terminal amino group in the presence of DIPEA. The peptide was deprotected and cleaved from the Rink amide resin with 95% TFA/2.5% water/2.5%TIS mixture and precipitated with chilled diethyl ether to give 33 mg of the peptide (Ac-CEEGPFGRSALVRRK-NH_2) as a white powder. ESI MS (m/z) of the peptide; calculated 1744.92 for M, found 1746 for MH^+, 874 for $(MH^2)^{+2}$ and 583 for $(MH^3)^{+3}$.

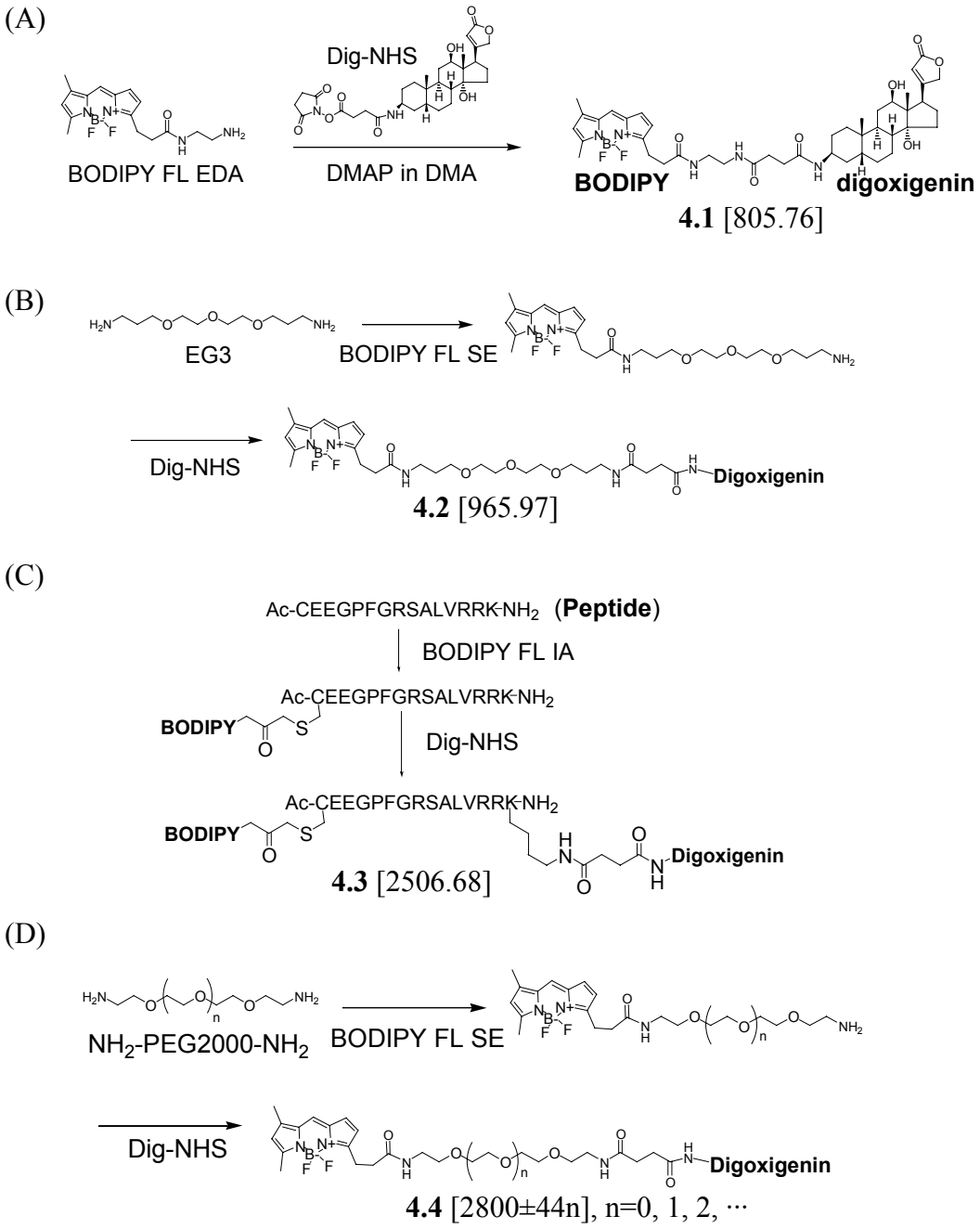

Figure 4.2 Synthetic scheme of BODIPY coupled digoxigenine probes for detection of scFv(anti-dig) antibody. (A) the EDA probe **4.1**, (B) the EG3 probe **4.2** with, (C) the peptide probe **4.3** and (D) the PEG2000 probe **4.4.**

BOIPY FL IA (0.8 μmol in 50 μl of DMA) was added to a mixture of the peptide (2 μmol), $NaHCO_3$ (20 μmole) and Na_2CO_3 (20 μmole) in water. After incubated for 3 hour at room temperature, an intermediate peptide (Ac-C(BODIPY)EEGPFGRSALVRRK-NH_2) was purified by FPLC to give 0.66 mg (37%). ESI MS (m/z) of the intermediate peptide; calculated 2034.04 for M, found 1018.2 for $(MH^2)^{+2}$.

The purified intermediate (0.225 μmol in 150 μl of water) was reacted with Dig-NHS (0.8 μmol) and 1M DMAP (5 μmol) in DMA. After incubation for 2 hours at room temperature, the probe **4.3** (Ac-C(BODIPY)EEGPFGRSALVRRK(Dig)-NH_2) was purified by FPLC to give 0.36 mg (64%). ESI MS (m/z) of the probe **4.3**; calculated 2505.30 for M, found 1253.9 for $(MH^2)^{+2}$.

Preparation of BODIPY-PEG2000-Dig (4.4)

BODIPY-FL SE (2 μmole) was added to a mixture of *bis*-amino polyethyleneglycol 2000 (40 mg, 20 μmole) and 1M DMAP (5 μmole) in DMA. After incubation for 2 hours at room temperature, an intermediate (BODIPY-PEG2000-NH_2) was purified by FPLC to give 1.48 mg (32%) of dark orange powder. ESI MS (m/z) (The peaks display broad distribution between 800 and 1400 for $(MH^2)^{+2}$ and between 650 and 900 for $(MH^2+Na)^{+3}$, which correspond to the calculated molecular weights for n = 30 to 50, where n is the number of ethyleneglycol units in the polyethyleneglycol linker.); calculated 2271.49 (n = 41) for M as one of middling molecules weights, found 1049.2 for $(MH^2)^{+2}$ (n = 37), 1071.0 for $(MH^2)^{+2}$ (n = 38), 1093.6 for $(MH^2)^{+2}$ (n = 39), 1114.8 for $(MH^2)^{+2}$ (n = 40), 1137.5 for $(MH^2)^{+2}$ (n = 41), 1159.7 for $(MH^2)^{+2}$ (n = 42), 1181.2 for $(MH^2)^{+2}$ (n = 43), 736.5 for $(MH^2+Na)^{+3}$ (n = 38) and 780.4 for $(MH^2+Na)^{+3}$ (n = 41).

The purified intermediate (0.32 μmol in 50 μl of water) was added to a mixture of Dig-NHS (0.4 μmol) and 1M DMAP (1 μmol) in DMA. After

incubation for 1 hour at room temperature, the probe **4.4** (BODIPY-PEG2000-Dig) was purified by FPLC to give 0.56 mg (60%). ESI MS (m/z) (The peaks display broad distribution between 1050 and 1500 for $(MH^2)^{+2}$ and between 700 and 1050 for $(MH^2+Na)^{+3}$, which correspond to the calculated molecular weights for n = 30 to 50); calculated 2698.72 (n = 40) for M as one of middling molecules weights, found 1262.0 for $(MH^2)^{+2}$ (n = 36), 1328.5 for $(MH^2)^{+2}$ (n = 39), 1651.4 for $(MH^2)^{+2}$ (n = 40), 1372.7 for $(MH^2)^{+2}$ (n = 41), 1394.6 for $(MH^2)^{+2}$ (n = 42), 1461.7 for $(MH^2)^{+2}$ (n = 45), 864.2 for $(MH^2+Na)^{+3}$ (n = 36), 879.0 for $(MH^2+Na)^{+3}$ (n = 37), 908.1 for $(MH^2+Na)^{+3}$ (n = 39), 937.9 for $(MH^2+Na)^{+3}$ (n = 41), 981.5 for $(MH^2+Na)^{+3}$ (n = 44), 996.5 for $(MH^2+Na)^{+3}$ (n = 45) and 1040.2 for $(MH^2+Na)^{+3}$ (n = 48).

4.3.2 Strain and plasmids

The *E. coli* strain ABLEC was purchased from Stratagene (La Jolla, CA). D21f2, a heptoseless K-12 mutant (CGSC#: 5162; F-, *proA23*, *lac-28*, *tsx-81*, *trp-30*, *his-51*, *rspL173(strR)*, *rfa-1*, *rfa-31*, *ampCp-1*), was obtained from the *E. coli* Genetic Stock Center in the Department of Biology at Yale University, New Haven, CT (Boman & Monner, 1975). Jude1 (*mcr*A, Δ(*mrr-hsd*RMS-*mcr*BC) ϕ80 d*lac*Z ΔM15 Δ*lac*X74 *deo*R *rec*A1 *end*A1 *ara*D139 Δ(*ara*, *leu*)7697 *gal*U *gal*K λ^- *rps*L *nup*G/F' proAB$^+$ *lac*I^{q}ZΔM15 Tn*10* Tet^r) was obtained from Andrew Hayhurst in our group.

The plasmids pDillo-pelB-scFv and pDillo-lpp-ompA'-scFv, which were modified from the pIMS100 vector with scFv (anti-dig-2610), scFv (anti-atr), or scFv (anti-TNB) DNA fragments (Hayhurst & Harris, 1999), were kindly provided by Andrew Hayhurst. scFv (anti-atr) and scFv (anti-TNB) antibodies were used as negative controls for the digoxigenin probes. In the PECS expression plasmid, a [P*tac*]-pelB-scFv-His^6 fusion was used in the pDillo-pelB-scFv plasmid, and a [P*tac*]-lpp-ompA'-scFv-His^6 was used for the pDillo-lpp-ompA'-scFv plasmid. The plasmids are also controlled using a P*tac* promoter and LacI^q, they use ColE1 as a replication origin with high copy number, and amp^R (ampicillin resistant gene) as

a selection marker. Plasmid purifications were performed using the QIAprep Spin Miniprep kits (QIAGEN). The electro-competent cells of ABLEC, Jude1 and D21f2 *E. coli* strains were transformed with the purified plasmids encoding pDillo-scFv's by the electroporation method (Shamrock *et al*., 1989).

Growth media were supplemented with ampicillin (100 μg/ml) when necessary. Bacteria containing plasmids were grown overnight in TB broth containing 2% glucose at 30°C. They were subcultured in fresh 2xYT media containing 2% glucose and re-grown at 37°C for 2 hours until an OD_{600} of 0.5-0.8 was reached. The cells were induced with IPTG (0.2 mM) for an additional 4 hours at 25°C to express the scFv antibodies in the periplasm or on outer surface of the *E. coli* strains.

4.3.3 Flow cytometeric screening with the series of probes

50 μl of the induced cell cultures were incubated in 950 μl of 1xPBS at room temperature for 1 hour with the digoxigenin-BODIPY conjugates (0.2 μM). The incubation was performed with or without permeabilizers. The resulting cell suspensions (10 μl) were diluted with 1 ml of 1xPBS before FACS analysis. 10^4 events were analyzed on a Becton Dickinson FACSCalibur (San Jose, CA). Sheath flow was 1xPBS to all of the screens. Cell viability was judged using the propidium iodide (PI) staining method (1 μg/ml) (Chen *et al*., 2001).

4.3.4 Enrichment test

Jude1/pDillo-pelB-scFv(anti-Dig) and Jude1/pDillo-pelB-scFv(anti-TNB) were induced with 0.2 mM of IPTG and cultured at 25°C for 3 hours until OD_{600} reached between 3.9 and 4.4. Next, the cell cultures were mixed at the ratio of 1:200 of Jude1/pDillo-pelB-scFv(anti-Dig) and Jude1/pDillo1-pelB-scFv(anti-TNB). The mixture was incubated with 5 μg/ml of PMBN and 0.2 μM of the peptide probe **4.3**, (Ac-C(BODIPY)EEGPFGRSALVRRK(Dig)-NH_2) in 1 ml of 1xPBS at room temperature for 30 min. The cell suspension was diluted into 1 ml

of 1xPBS in a SIP tube, analyzed and then sorted on Becton-Dickinson FACSCalibur for 15 min under the same condition as cytometric screening. 30 ml of fluid containing all events inside of R1 in Figure 4.10A and R2 region in Figure 4.10E were collected in 50 ml collecting tubes that already contained 20 ml of 2xYT medium. The sorting procedure was performed twice to collect more cells. The collected cells were harvested by filtering the media through 0.22 μm-filters and then the filters were placed on LB agar plates with 150 μm/ml ampicillin for 24 hours at 37^{o}C. The colonies that appeared on the plate were re-grown and verified by performing FACS analysis with the small probe **4.1** and a PCR reaction with two different primer sets that are designed to amplify scFv(anti-dig) and scFv (anti-TNB). The PCR products were visualized on a 1% agarose gel.

4.4 RESULTS AND DISCUSSION

4.4.1 Design of outer membrane permeability assay using PECS

The 26-10 scFv(anti-dig) antibody binds with high affinity to cardiac glycosides such as digoxin (K_D = 0.9 x 10^9) and digoxigenin (K_D = 2.4 x 10^9) (Chen *et al*., 1999). The plasmids, pDillo-pelB-scFv and pDillo-lpp-ompA'-scFv, were used for *E. coli* expression of periplasmic scFv(anti-dig) and surface displayed scFv(anti-dig). The pectate lysase leader peptide (first 24aa) was positioned on the *N*-termini of the scFv sequences for the periplasmic expression of soluble scFv antibody using the Sec pathway (Economou, 1999). Braun's lipoprotein leader peptide (first 19aa) with Lpp anchoring domain (9aa) were fused to the *N*-termini of scFv sequences used for surface display in the Lpp(1-9aa)-OmpA'(46-159aa)-scFv systems. The plasmids are also encoded with the P*tac* promoter and $LacI^q$ for induction control and the ColE1 as a replication origin with a high copy number.

When the scFv antibody (pDillo-pelB-scFv) is expressed in the periplasm, only small probes (< 650 Da) can diffuse freely through the outer membrane (Figure 4.1A) (Decad & Nikaido, 1976). Once the freely diffusing fluorescent digoxigenin

probes bind to the periplasmic scFv(anti-dig) antibody, the scFv(anti-dig)-digoxigenin probe complex remains within the cell. Due to the fluorescence of the probe, the cells containing the complexes can be analyzed and isolated by FACS from negative control cells that lack the 26-10 scFv(anti-dig) antibody. The FACS fluorescent intensity is proportional to amount of the probe retained in the periplasm. Formation of complexes is directly correlated to the amount of the probe that reaches the periplasmic space because of the high affinity of the scFv antibody to the hapten. The scFv(anti-atr) and scFv(anti-TNB) antibodies are good negative controls because they cannot bind the fluorescently labeled digoxigenin probes. For comparison, surface displayed scFv antibodies (pDillo-lpp-ompA'-scFv) were tested in parallel (Figure 4.1B). To understand of the size effect of probes, a series of probes were designed and prepared by coupling a fluorescent dye (BODIPY-FL).

4.4.2 Design of probes for detecting scFv(anti-dig) on FACS

The development of a method to detect outer membrane permeability is critical to development of the PECS system for screening antibodies and activities of enzymes in *E. coli*. Molecular size and hydrophobicity of probes are the major factors that determine outer membrane permeability. A series of digoxigenin-BODIPY derivatives with different linkers were designed and synthesized in order to determine which probes are able to interact with scFv(anti-dig) antibody expressed in periplasm or on outer surface by FACS analysis. The linkers were attached to digoxigenin on one end as the hapten for scFv antibody binding and BODIPY on the other end as the fluorescent dye for FACS analysis. Ethylenediamine (EDA) was used in the probe **4.1** for the shortest length and lowest molecular weight linker. The ethylene glycol diamine (EG3), which is longer than EDA with three units of ethylene glycol, was used as the medium size linker in the probe **4.2**. A peptide (15 amino acids) was used in the probe **4.3** as a high molecular weight peptide linker that represented peptide haptens or protease

substrates. *Bis*-amino polyethyleneglycol (PEG2000 with ~ 40 of average units of ethylene glycol) was used in the probe **4.4** as a very long and hydrophilic linker, basically an extended form of the EG3 in **4.2** yet with a similar molecular weight to the peptide linker in **4.3** (Figure 4.2).

4.4.3 Preparation of probes for scFv(anti-dig) antibody

The previously optimized reaction condition was used for each coupling of the linkers to fluorescent dye or hapten to prepare the probes **4.1**, **4.2** and **4.4**. The structure of products were verified with HPLC and ESI MS. For preparation of the peptide probe, solid phase coupling of Dig-NHS to the *N*-terminal amino group of the peptide on the Rink amide resin was performed, following by cleavage from the resin with a TFA treatment. However, ESI MS characterization revealed that the hapten on the peptide was a dehydrated product. Digoxigenin may be unstable under strongly acidic condition. BOIDPY dye cannot be used for solid phase assembly because it is decomposed to a non-fluorescent compound under acidic conditions (95% TFA). Hence, the peptide probe **4.3** was prepared in the solution phase by coupling BODIPY-FL IA to the sulfide group of Cys on the *N*-terminus followed by conjugating Dig-NHS to the amino group of Lys on the *C*-terminus as shown in Figure 4.2B.

4.4.4 FACS analysis of antibodies in ABLEC strain

The 26-10 scFv(anti-dig) antibody was expressed in the *E. coli* periplasm using pelB leader sequence in the plasmid pDillo-pelB-scFv(anti-dig). As the negative control antibody, scFv(anti-atr) was also expressed. To compare the probe accessibility to the periplasmic scFv(anti-dig) antibody, surface displayed scFv antibody was encoded in the plasmids, pDillo-lpp-ompA'-scFv(anti-dig). Electrocompetent ABLEC cells were transformed with these plasmids. The ABLEC strains expressing scFv antibodies were labeled with the probe **4.2**, **4.3** and **4.4** with or without a permeabilizer and analyzed by FACS.

Detection of periplasmic and surface displayed scFv antibodies in ABLEC

The permeability was expressed as the ratio of fluorescence intensity at 530 ± 30nm (FL1 for BODIPY) of the positive control ABLEC/scFv(anti-dig) to the negative control ABLEC/scFv(anti-atr) measured in the FACS histogram (Figure 4.3A). When ABLEC/pDillo-pelB-scFv(anti-dig) expressing periplasmic scFv (anti-dig) was labeled with 200 nM of the probe **4.2** (EG3 linker, MW = 965.97) in 1xPBS solution, the FACS analysis shows only a 3-fold higher fluorescence intensity compared to that of the negative control cells, ABLEC/pDillo-pelB-scFv(anti-dig). The small probe can reach the periplasmic slowly, but the large probes (**4.3** and **4.4**) do not diffuse in the periplasm at all because of polysaccharide barrier of highly ordered LPS structure (Figure 4.4A). The signal in 5xPBS enhanced the fluorescence intensity ratio (6x) that is consistent with the previous paper (Chen *et al*., 2001). For the bigger probe **4.3** (peptide linker, MW = 2506.68) and **4.4** (PEG linker, average MW = 2800), the ionic strength effect (5xPBS) did not increase permeability (Table 4.1). In general, a ratio of more than 5-fold is necessary for practical FACS sorting because a higher ratio of fluorescence intensity gives better resolution upon FACS sorting.

ABLEC strain	pelB-scFv			Lpp-OmpA'-scFv		
Incubation conditions	**4.2** EG3	**4.3** Peptide	**4.4** PEG	**4.2** EG3	**4.3** Peptide	**4.4** PEG
1x PBS (0.2 mM IPTG)	3 x	1 x	1 x	**10**	4	1
5x PBS (0.2 mM IPTG)	**6**	1.5	1	**11**	**6**	1
1 ~ 10 % sucrose	3 (6)	n.d.	n.d.	**11**	n.d.	n.d.
0.5 ~ 2% DMSO in	3	n.d.	n.d.	**10**	n.d.	n.d.
1 or 5 % PEG2000	3	n.d.	n.d.	n.d.	n.d.	n.d.
0.5 M urea	2 (3)	(-)	n.d.	5 (7)	- (4)	n.d.
3 M urea	2	2 (6)	n.d.	**6**	4	n.d.
50 μM IPTG in 1xPBS	2.5	1.5	n.d.	**8**	4	n.d.
0.5 mM IPTG in 1xPBS	3 (4)	1 (2)	n.d.	(20)	**5**	n.d.
5 mM IPTG in 1xPBS	3 (8)	1 (3)	n.d.	(28)	(8)	n.d.
0.05mM IPTG in 1% sucrose	4	3 (-)	n.d.	8 (12)	5	n.d.
0.5 mM IPTG in 1% sucrose	5 (13)	1 (3)	n.d.	(23)	5	n.d.
5 mM IPTG in 1% sucrose	6 (26)	1 (4)	n.d.	(28)	4	n.d.
0.2 μg/mL PMBN in 1xPBS	3	1 (2)	1	**8**	4	1
0.5 μg/mL PMBN in 1xPBS	(12)	(10)	(8)	**15**	**6**	3
1 μg/mL PMBN in 1xPBS	(14)	(10)	(8)	**20**	**15**	**7**
2 μg/mL PMBN in 1xPBS	(16)	(13)	(8)	**20**	**18**	**11**

Table 4.1 The ratio of mean fluorescence of ABLEC/scFv(anti-dig) over the mean fluorescence of the negative control cell, ABLEC/scFv(anti-atr), that does not recognize the digoxigenin probes. The ratios in parenthesis were the more than 50% damaged cells that were stained with PI (FL2). The standard sample with 200 nM of the small probe **4.2** in 1x PBS for every batch of FACS analysis was performed to normalize the ratios. (n.d. = not determined)

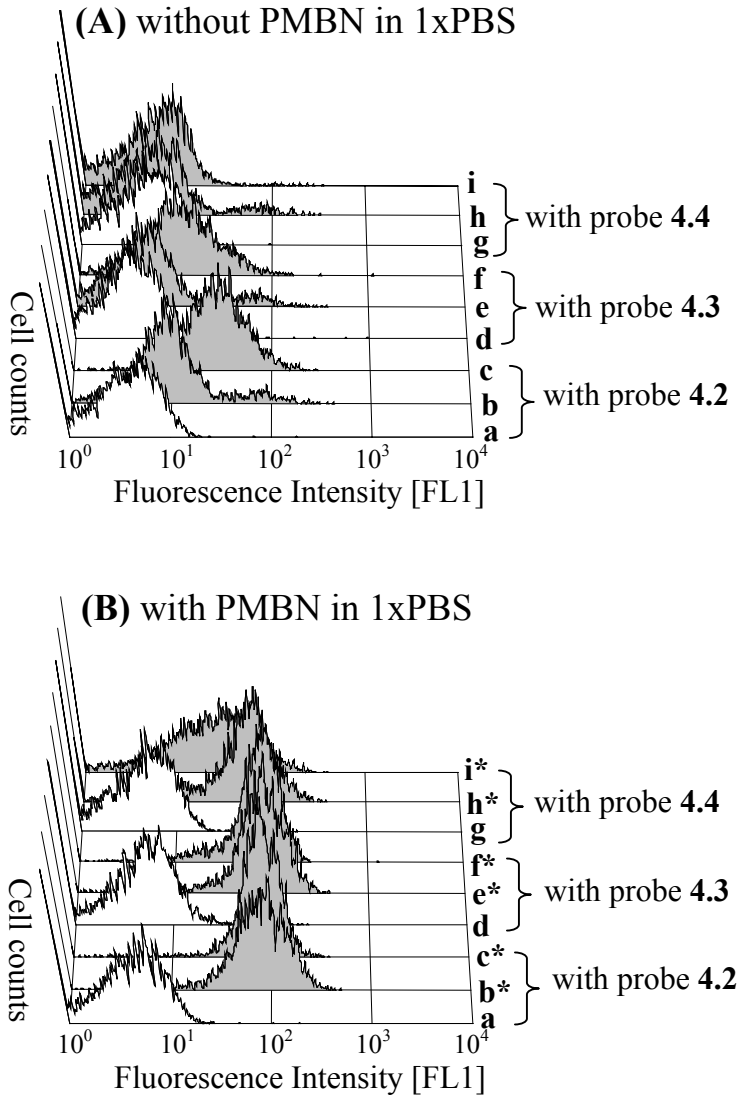

Figure 4.3 Fluorescent detection of scFv(anti-dig)/ABLEC (gray filled histogram) over negative control cell scFv(anti-atr)/ABLEC (empty histogram) which cannot recognize the digoxigenin probes on FACS. (A) without PMBN in 1xPBS and (B) with 2 μg/ml PMBN in 1xPBS. Histogram **a**, **d** and **g** are negative control (pelB-scFv(anti-atr)); Histogram **b**, **e** and **h** are pelB-scFv(anti-dig); Histogram **c**, **f** and **i** are lpp-OmpA'-scFv(anti-dig). All cells were incubated with 200 nM of probes at room temperature for one hour. (* Mostly dead cells identified by PI staining).

On the contrary to periplasmic scFv in ABLEC cells, the strain displaying scFv(anti-dig) antibody on the surface of the outer membrane (ABLEC/pDillo-lpp-OmpA'-scFv(anti-dig)) showed a higher fluorescence intensity ratio (10x) with the probe **4.2** because there is no outer membrane barrier. ABLEC/pDillo-lpp-OmpA'-scFv(anti-dig) labeled with the probe **4.3** gave a low fluorescence intensity ratio compared to the probe **4.2**. The surface displayed scFv(anti-dig) antibody has apparently an accessibility problem although there is no outer membrane permeability issues. The binding pocket faces the outer membrane because the *C*-terminus of bulky Lpp-OmpA' is fused to the *N*-terminus of the scFv antibody which is very close to the binding site of the scFv antibody. Hence, it is possible that only small probes have access to the binding pocket for the steric reason. In addition, the antibody fused to Lpp-OmpA' is thought to be buried in a "jungle" of lipopolysaccharides in highly ordered quasicrystalline LPS structure (Figure 4.4B). The PEG2000 probe **4.4** barely increased fluorescence intensity ratios for periplasmic and surface displayed scFv antibodies (Figure 4.3A-i) presumably because polyethylene glycol is too hydrophilic and large to approach even the surface displayed scFv.

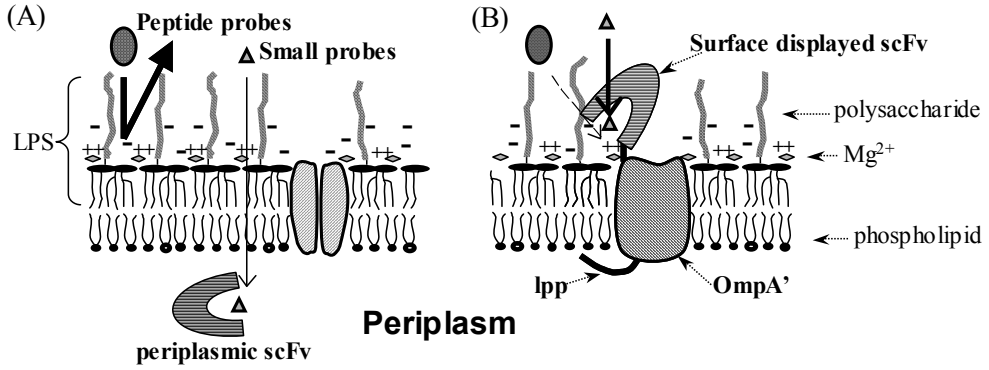

Figure 4.4 Hypothetical structure of outer membrane in wild-type *E. coli* (ABLEC or Jude1) expressing scFv antibodies. (A) Probe permeability to periplasmic scFv antibody. (B) Probe accessibility to surface displayed scFv antibody.

Effect of high expression level of scFv antibody in ABLEC strain

Higher concentration (0.5mM and 5mM) of IPTG increased the expression level of the periplasmic scFv antibodies, which resulted in an increased permeability (FL intensity ratio). However, FACS analysis revealed two cell populations implying that some of cells were killed by the harsh conditions. High expression of surface displayed scFv also increased the fluorescence intensity ratio, but FACS analysis did not show two populations. However, FACS analysis showed that greater than 50% of the surface expression cell population is stained with propidium iodide (PI) indicateing they are not viable.

Sucrose, DMSO, polyethylene glycol 2000, or urea solutions did not increase the fluorescent signal significantly. In fact, 1% ~ 10% sucrose solutions and urea solutions showed adverse effects such as peak splitting on FACS histogram, which caused by dead cells according to PI staining.

PMBN effects on the outer membrane of ABLEC

The strain expressing periplasmic scFv antibody (ABLEC/pDillo-pelB-scFv(anti-dig)) incubated with the probes (**4.2** or **4.3)** in the presence of polymyxin B nonapeptide (PMBN) (Figure 4.5) displayed exceedingly high permeability based on the FACS signal (Figure 4.3B). However, PI staining revealed most of the cells were not viable, despite of fact that PMBN has been known as a non-toxic permeabilizer of the outer membrane of gram(-) bacteria (Viljanen *et al*., 1991). It is not clear that the increased signal is genuine or an artifact from dead cells.

Figure 4.5 Chemical structure of polymyxin B nonapeptide (PMBN) for permeability test with FACS in this study (Dab: α,γ-diaminobutyric acid).

Permeability of ABLEC/pDillo-lpp-OmpA'-scFv(anti-dig) with probe **4.3** was also evaluated using 5xPBS, sucrose, urea and an increase of expression level. However, only small improvements of the ratios (5x) were found. On the other hand, PMBN displayed large fluorescent increase (18x) without adverse effect as evidenced by minimum PI staining. In addition to the outer membrane permeabilizing effect, PMBN also may enhance accessibility of surface displayed antibodies by altering the lipopolysaccharides that act as a blockade. From this analysis, PMBN has emerged as the most promising permeabilizer of the outer membrane for PECS. However, the adverse viability effects observed in the ABLEC strain must be overcome.

4.4.5 FACS analysis of scFv antibody in Jude1 strain with and without permeabilizers

Over expression of scFv or treatment of permeabilizer in the ABLEC strain made the cells very fragile. Alternatively, the Jude1 strain is known to be a more robust cell, so it was selected for study. Plasmids pDillo-pelB-scFv(anti-TNB), pDillo-pelB-scFv(anti-dig), pDillo-lpp-ompA'-scFv(anti-TNB), and pDillo-lpp-ompA'-scFv(anti-dig) were purified from ABLEC strains and used to transform Jude1 cells by electroporation.

Detection of scFv antibody in Jude1 with the small probes

The periplasmic scFv(anti-dig) antibody with the smallest probe **4.1** resulted in an increase of fluorescence (6x) over the negative control cell which expressed the periplasmic scFv(anti-TNB) antibody (Figure 4.5A and B). However, the probe **4.2** gave only less resolution (x3), even though it is only slightly larger (MW = 965.97) than **4.1** (MW = 805.76). The surface displayed Lpp-OmpA'-scFv(anti-dig) antibody with the small probes **4.1** and **4.2** also displayed useful resolution of 9x and 6x, respectively. Without permeabilizer, the Jude1 strain showed similar tendency of the ABLEC strains, not to be detected with the larger probes **4.3** and **4.4** based on FACS.

PMBN effect on periplasmic scFv antibody

As in FACS analyses of ABLEC cells, PMBN increased permeability of the outer membrane of the Jude1 strain. However, Jude1 had greater cell viability, which allowed a higher concentration of PMBN to be used. The periplasmic scFv(anti-dig) cell incubated with PMBN showed much higher fluorescent intensity ratio (Figure 4.6C compared to Figure 4.6A) for the small probes (**4.1** and **4.2)**.

	pelB-scFv				**Lpp-OmpA'-scFv**			
Incubation conditions	**4.1** EDA	**4.2** EG3	**4.3** Pept.	**4.4** PEG	**4.1** EDA	**4.2** EG3	**4.3** Pept.	**4.4** PEG
1x PBS	**6**	3	1	1	**9**	**6**	2	1
0.5 μg/mL PMBN	**10**	4	1.2	1	**9**	**6**	2	1
1 μg/mL PMBN	**13**	**10**	**5**	1.5	**11**	**12**	**6**	1.5
2 μg/mL PMBN	**20**	**13**	**6**	1.5	**18**	**15**	**9**	2
5 μg/mL PMBN	**27**	**26**	**9**	2	**17**	**16**	**11**	3.5
10 μg/mL PMBN	**32**	**30**	**12**	2.5	**18**	**18**	**12**	**5**
1 mM EDTA**	**34**	**20**	2 (5)	1.3 (2)	**16**	**17**	3	1.5 (3)
5 mM lactic acid*	**11**	**5**	4	1	**9**	**6**	**5**	1
10 mM Tris-HCl	1.7	1.5	1	1	4	3	3.5	1
20 μg/mL PEI	(18)	(12)	(11)	n.d.	(22)	(13)	(10)	n.d.

Table 4.2 The ratio of mean fluorescence of Jude1/scFv(anti-dig) over the mean fluorescence of the negative control cells, Jude1/scFv(anti-TNB). The ratios in parenthesis were the damaged cells. The standard sample with 200 nM of the EDA probe **4.1** in 1x PBS analysis was performed to normalize the ratios for every batch of FACS. (*in 10 mM Tris-HCl buffer (pH 7.5), **10 min incubation in 10 mM Tris-HCl buffer, n.d. = not determined)

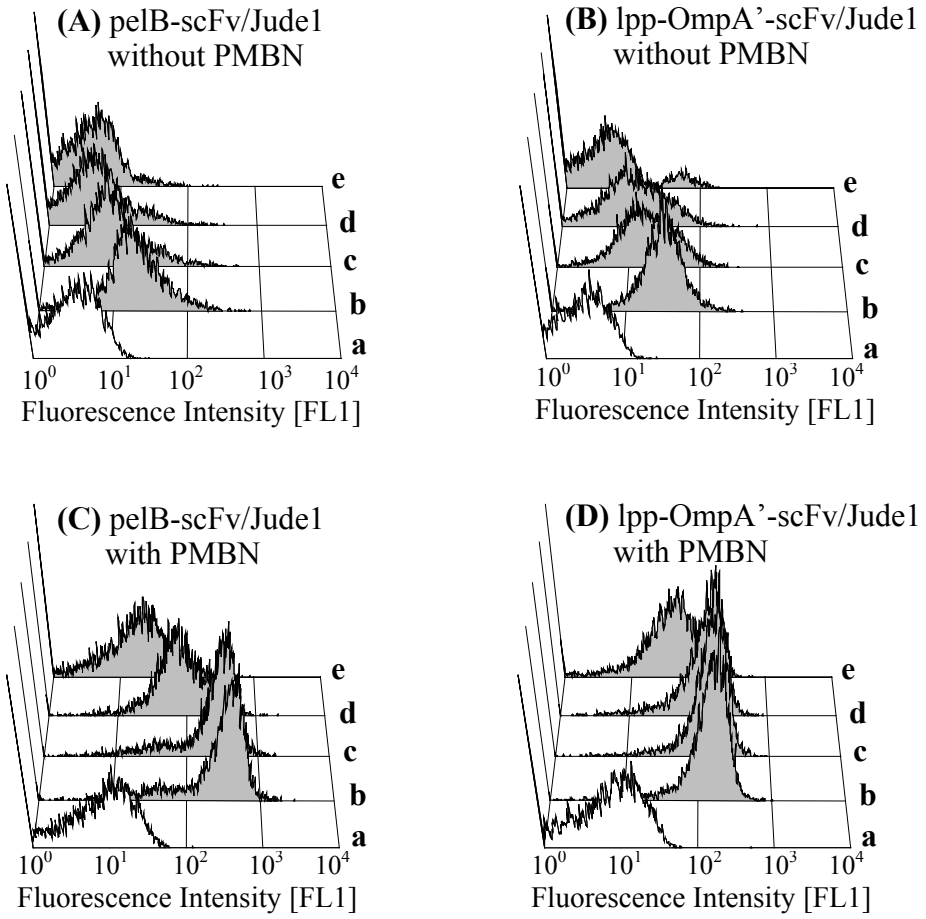

Figure 4.6 Fluorescent detection of scFv(anti-dig)/Jude1 (gray filled histogram) over a negative control cell scFv(anti-TNB)/Jude1 (empty histogram) which cannot recognize the digoxigenin probes on FACS. (A) Periplasmic scFv/Jude1 without PMBN in 1xPBS, (B) Surface display scFv/Jude1 without PMBN in 1xPBS, (C) Periplasmic scFv/Jude1 with 10 μg/ml PMBN in 1xPBS. (D) Surface display scFv/Jude1 with 10 μg/ml PMBN in 1xPBS. Histogram **a** is background negative scFv(anti-TNB)/Jude1 cell labeled with 200 μM of **4.1**; Histogram **b**, **c**, **d**, and **e** are scFv(anti -dig)/Jude1 cells labeled with **4.1**, **4.2**, **4.3** and **4.4**, respectively.

There were no difference in the fluorescence intensity ratio for the small probes **4.1** and **4.2** (32x and 30x with 10 μg/ml of PMBN), probablely due to the saturation of scFv antibodies, which also means that the probes diffuse in and out freely through outer membrane. PMBN was also effective with the peptide probe **4.3** (12x with PMBN and 1x without PMBN) and the polyethylene glycol probe **4.4** (2.5x with PMBN and 1x without PMBN) all without adverse effects. It should be noted that the peptide probe **4.3** (MW = 2506.68) could not enter the periplasm without PMBM at all. In up to 10 μg/ml PMBN, the cells were more than 95% viable when FACS-analyzed by PI staining. This implies that peptides can be used as antibody probe expressed in periplasm for PECS sorting by using PMBN, a nontoxic permeabilizer that allowed passage of large probes across the outer membrane.

PMBN effect on surface displayed scFv antibody

PMBN was also effective for the surface displayed Lpp-OmpA'-scFv(anti-dig) constructs with all four probes (Figure 4.6D). The probes **4.1** and **4.2** with 10 μg/ml PMBN showed a large increase of the fluorescence intensity ratio (both are 18x). The same fluorescence intensities imply that antibodies were almost saturated with 200 nM of the probes. The probe **4.1** and **4.2** labeled cells with different fluorescence intensities (6x and 3x, respectively) without PMBN although the size difference is not significant (MW = 805.75 and 965.97). Note that the fluorescence intensity of the surface displayed scFv(anti-dig) (18x) with the small probe **4.1** in the presence of PMBN is lower than a similar treatment of the periplasmic scFv(anti-dig) antibody (32x). This difference in signal is due to the amount of expressed antibody. The periplasm is believed to provide more space and a better folding environment for expression than protein transported to the outer membrane. The effect of PMBN on the surface displayed scFv cells was more significant with the bigger probes (12x). Even though the small probes, **4.1** and **4.2,** gave very high fluorescence intensity ratios with PMBN, the ratio without

PMBN was already high (9x). The fluorescence intensity of Lpp-OmpA'-scFv(anti-dig) cells with the probe **4.3** (Figure 4.6D-d) was comparable to those with the small probes **4.1** and **4.2** (Figure 4.6D-b and c). On the other hand, the periplasmic pelB-scFv(anti-dig) antibody cells with the probe **4.3** (Figure 4.6C-d) showed relatively lower fluorescence intensity than those with the small probes (Figure 4.6C-b and c). The probe **4.4** had similar results to the probe **4.3**. PMBN disturbs the highly ordered LPS arrangement and may alter accessibility of the binding pocket of the surface displayed scFv antibody that normally faces the outer membrane.

Effect of EDTA and other permeabilizers on the outer membrane of Jude1

Adding EDTA was more effective for the smaller probes **4.1** (34x) and **4.2** (20x) than for the larger ones, probes **4.3** (2x) and **4.4** (1x) in contrast to the PMBN effects with the small probe **4.1** (27x) and the large probe **4.3** (12x). Cells were incubated with 1mM EDTA for only 10 minutes because prolonged exposure (1 hour) resulted in cell damage. The outer membrane permeabilizing mechanism of EDTA is different from PMBN. Divalent cations bind the lipid A domains and contribute intermolecular LPS interactions to the outer membrane stability (Labischinski *et al*., 1985). Chelation of the cations by EDTA disrupts intermolecular interaction of the lipid A domains, which causes perturbation of the LPS arrangement. The increased lateral movement of the LPS by EDTA treatment increases permeability. The increased permeability by 1 mM EDTA in periplasmic scFv antibody cells may not be enough for the larger probes (**4.3** and **4.4**) to permeate the outer membrane. Fluorescence intensity enhancements of Lpp-OmpA'-scFv(anti-dig) may be also caused through LPS perturbation by EDTA treatment for the small probes as the periplasmic scFv antibody cells. High concentrations of EDTA are known to liberate LPS patches and lipoproteins, causing irregularly shaped pits and exposing the peptidoglycan surface as seen in

high-resolution atomic force microscopy (AFM) studies (Amro *et al.*, 1999, Amro *et al.*, 2000). A high concentration of EDTA may therefore be too toxic to *E. coli* cells for use as a permeabilizing agent for PECS.

Lactic acid also increased the outer membrane permeability slightly for the periplasmic scFv(anti-dig) strain, but it did not effect the fluorescent intensity ratio of surface displayed scFv(anti-dig) with small probes (Table 4.2). Lactic acid, an additive to foods, is known to cause sublethal injury to *E. coli* as a natural antimicrobial reagent (Roth & Keenan, 1971) although the mechanism is not clear so far. The permeabilizer effect of lactic acid treatment may be involved in liberation of the LPS layer, like EDTA and HCl solutions (Alakomi *et al*., 2000). 10 mM Tris-HCl buffer (pH 7.5) solution itself was evaluated using FACS in order to see the influence on outer membrane permeability (Table 4.2). It was less effective than 1xPBS, which shows that high salt buffers such as 1x PBS or 5x PBS are thought to increase permeability for the small probes. PEI (Helander *et al*., 1997) seemed to increase the ratio, but it gave a non-uniform cell population in the FSC and SSC analysis by FACS. High concentrations of Ca^{2+} also resulted in similar effects analyzed by FACS (data not shown).

4.4.6 FACS analysis of scFv antibody in D21f2 strain without permeabilizers

D21f2 *E. coli* strain is a outer membrane heptoseless LPS (*waaC*, formerly *rfaC*) strain (Boman & Monner, 1975, Hirvas *et al.*, 1997, Yethon *et al.*, 1998). This strain does not have the normal core LPS components including the O-antigen and core polysaccharides. Removal of the entire O-antigen and the distal portion of the core polysaccharide (the outer core in Figure 4.7) in LPS does not increase permeability of the outer membrane (Nikaido & Vaara, 1985). However, mutants lacking the sugars in the inner core (chemotype Rd1 and Re in Figure 4.7) become dramatically more sensitive to hydrophobic dyes, detergents and antibiotics (Parker *et al*., 1992, Schnaitman & Klena, 1993). The D21f2 strain has an advantage over using the PMBN permeabilizer for PECS in that PMBN can cause cell toxicity

especially with high levels of antibody expression. In addition, the PMBN cannot be used for electrostatic capture system when it is applied to detection of the enzyme activity in chapter 3 (data is not shown) because the highly charged PMBN interferes with electrostatic interaction of the positively charged peptide products to the negatively charged cell surface. Therefore, D21f2 strain appears to be a reasonable choice of a high permeable strain to be evaluated for PECS.

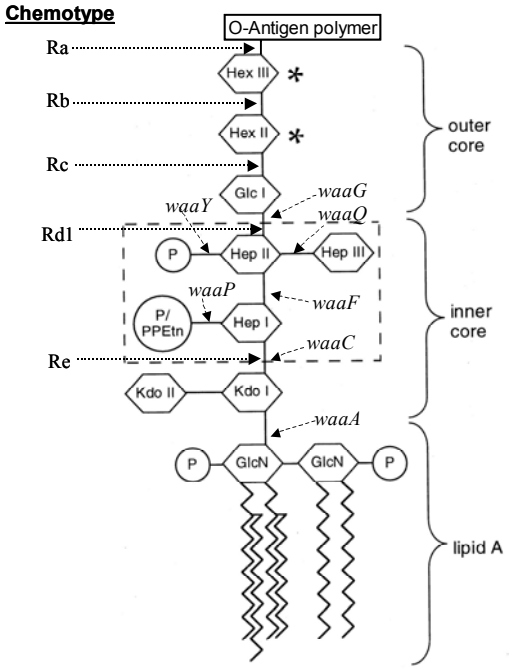

Figure 4.7 Generalized structure of the lipid A and core oligosaccharide of LPS common to *E. coli* and *S. enterica*. Genes (*waa*, formerly *rfa*) encoding the enzymes thought to be responsible for the generation of each linkage are indicated by the genetic symbols. P, phosphate; Hep, L-glycerol-D-manno-heptose; PPEtN, 2-aminoethyl diphosphate. *, structures vary between strains. The scheme is modified from figure in *J. of Biol. Chem*. **1998** p.26311 (Yethon *et al*., 1998)

Electrocompetent D21f2 cells were transformed with the plasmids pDillo-pelB-scFv(anti-TNB), pDillo-pelB-scFv(anti-dig), pDillo-lpp-ompA'-scFv(anti-TNB), and pDillo-lpp-ompA'-scFv(anti-dig). As shown in Table 4.3 and Figure

4.8A, the D21f2 strain that expressed periplasmic scFv(anti-dig) antibody showed relatively high fluorescence intensity ratios (54x) for the small probes **4.1** and **4.2** in 1xPBS without any added permeabilizer (Figure 4.8A). The small hydrophobic probes are thought to pass through phospholipids in the outer leaflet in D21f2.

High fluorescence intensity ratios (25x) were also seen with the surface displayed system of D21f2/pDillo-lpp-ompA'-scFv(anti-dig) (Figure 4.8B). The fluorescent ratios of the small probes **4.1** and **4.2** are almost identical for either periplasmic or surface displayed scFv, which implies free diffusion and high accessibility of these probes. The signal ratio of D21f2/pDillo-pelB-scFv(anti-dig) strain with the small probes (54x in Table 4.3) was higher than that of Jude1 strain with 10 μg/ml PMBN (32x in Table 4.2), but this difference is probably due to different expression level of antibodies between the strains.

The peptide probe **4.3** gave a similar signal in the PMBN/Jude1 (12x) and D21f2 system (11x), while the largest hydrophilic probe **4.4** was slightly better with PMBN/Jude1 (2.5x vs. 1.5x). The disturbed hydrophobic lipid A-phospholipid bilayer of the outer membrane by PMBN treatment maybe allows the large probes to penetrate the outer membrane (Figure 4.9B). However, neither of these two signals are likely to be strong enough to sort libraries.

	pelB-scFv				**Lpp-OmpA'-scFv**			
Incubation conditions	**4.1** EDA	**4.2** EG3	**4.3** Pept.	**4.4** PEG	**4.1** EDA	**4.2** EG3	**4.3** Pept.	**4.4** PEG
1x PBS	**54**	**53**	**11**	1.5	**25**	**25**	**8**	2

Table 4.3 The ratio of mean fluorescence intensity of D21f2/scFv(anti-dig) over the mean fluorescence intensity of the negative control cells, D21f2/scFv(anti-TNB).

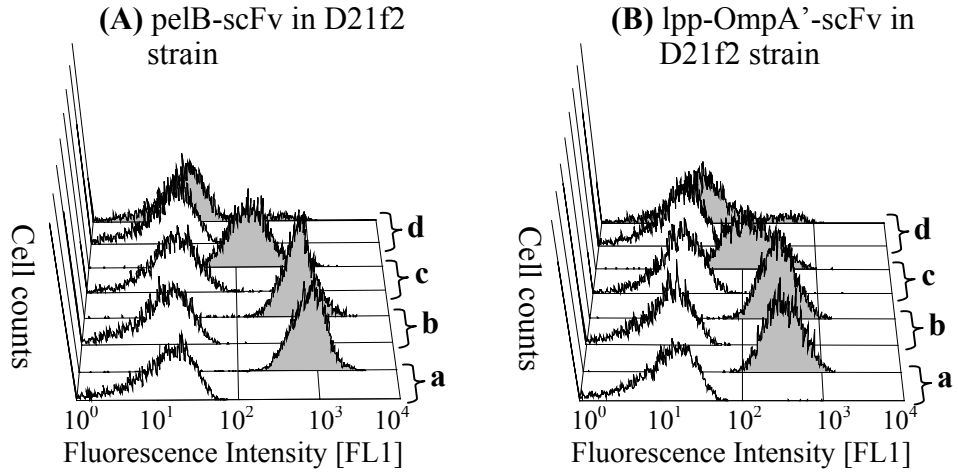

Figure 4.8 Fluorescent detection of scFv(anti-dig)/D21f2 (gray filled histogram) over negative control cell scFv(anti-TNB)/D21f2 (empty histogram) which cannot recognize the digoxigenin probes on FACS. (A) Periplasmic scFv/D21f2 in 1xPBS and (B) Surface display scFv/D21f2 in 1xPBS. Histogram **a**, **b**, **c** and **d** are labeled with **4.1**, **4.2**, **4.3** and **4.4**, respectively.

Interestingly, the D21f2 strain showed significantly higher FACS signals with the surface expressed Lpp-OmpA'-scFv(anti-dig) construct compared to all other strains investigated without permeabilizers (25x for the small probes). In fact, the D21f2 values of surface displayed scFv with the small probes were slightly higher than those seen with PMBN/Jude1 (25x vs 18x), the latter showing a slight advantage with the largest probe **4.4**. This result is consistent with our hypothesis that intact LPS interfering with antigen binding to surface expressed scFv on wild-type *E. coli* strain. The disturbed LPS of Jude1 by PMBN is more efficient in exposing the binding site of the surface displayed scFv than the heptoseless LPS of D21f2 (Figure 4.9).

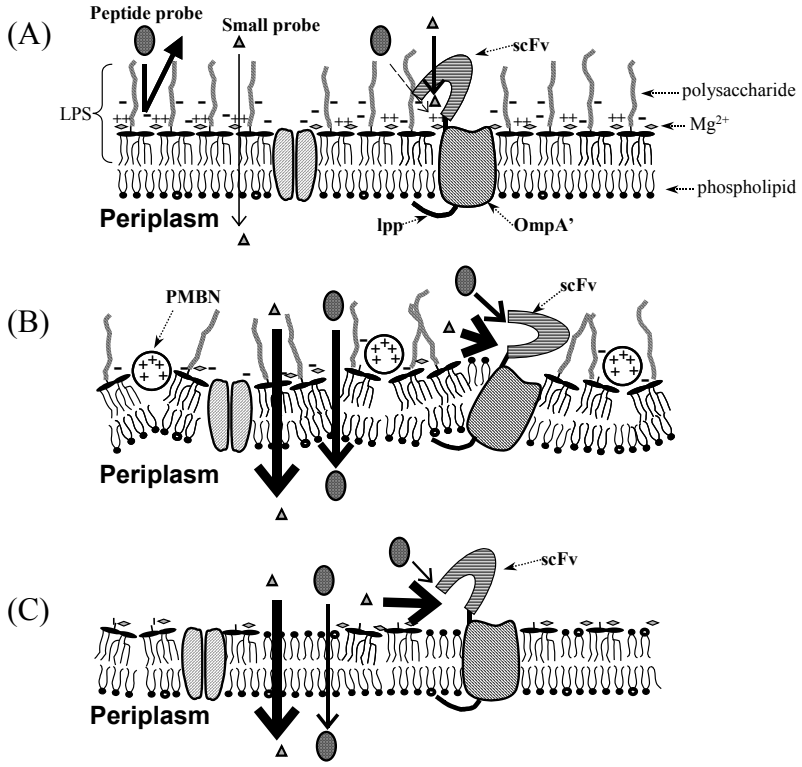

Figure 4.9 Proposed mechanism of small or large probes for accessibility of periplasmic and surface displayed scFv. (A) Intact outer membrane of *E. coli*; Small probes can reach periplasmic and surface displayed scFv slowly but large probes cannot diffuse in periplasm. Large probes also cannot bind surface displayed scFv presumably because of the polysaccharide barrier and low accessibility of binding pocket of scFv that faces down. (B) PMBN treated outer membrane; Highly positive charged PMBN molecules may specifically bind negatively charged inner core and lipid A to disturb supramolecular structure of LPS. (C) Outer membrane of deep rough mutant, D21f2; Lack of lipopolysaccharide structure allows outer membrane to be exposed to media facilitating diffusion into periplasm as well as access to scFv binding site.

4.4.7 Practical enrichment of cells expressing scFv antibody by PECS using the peptide probe 4.3 with PMBN

A signal ratio of greater than 5x is required to sort libraries. Only the small probe **4.1** (MW = 805.76) for PECS is suitable for sorting the positive antibodies in

ABLEC and Jude1 strains in 1xPBS using either periplasmic or surface expression. Although the molecular weight of the probe **4.2** (MW = 965.97) is slightly larger than **4.1**, the resolution of **4.2** (3x) in 1xPBS is not practical for FACS sorting with periplasmically expressed scFv. The peptide probe **4.3** (MW = 2506.68) cannot be used FACS sorting with either the periplasmic and surface displayed scFv antibodies.

PMBN showed dramatic improvement of outer membrane permeability and provided the highest overall signal ratios with the large probes (12x fluorescence intensity ratio for **4.3**). To verify practical use of high molecular weight probe like the peptide probe **4.3** for detection and sorting of periplasmic scFv in *E. coli* strain (Jude1) on FACS, antibody enrichment experiments in the presence of PMBN were performed. IPTG induced cultures of Jude1/pDillo-pelB-scFv(anti-dig) and Jude1/pDillo1-pelB-scFv(anti-TNB) were prepared. Although a shorter induction time (2 hours vs. 4 hours) gave lower expression levels of scFv, cell viability was increased. Collection into 2xYT culture medium (20 ml) in a 50 ml collection tube also increased viability of recovered cells compared to 1xPBS alone during FACS sorting. The positive cells expressing scFv(anti-dig) antibody in the high fluorescent region (R2) were isolated from the 1:200 mixture of scFv(anti-dig):scFv(anti-TNB) cells in the presence of the peptide probe **4.3** (200 nM) and PMBN (5 μg/ml) (Figure 4.10). The twenty eight colonies collected on the filter from FACS sorting were recovered on LB plates containing 200 μg/ml of ampicillin. Each recovered clone was subcultured in 2xYT, induced, and re-screened with the small probe **4.1**. Twenty four out of the twenty eight colonies displayed high FACS signals, verifying that they were the Jude1/pDillo-pelB-scFv(anti-dig) construct. An enrichment factor of over 1200-fold was seen. The plasmids pDillo-pelB-scFv(anti-dig) in the collected cells were confirmed by a PCR reaction using mixture of two primer sets for the scFv(anti-dig) and scFv (anti-TNB) constructs.

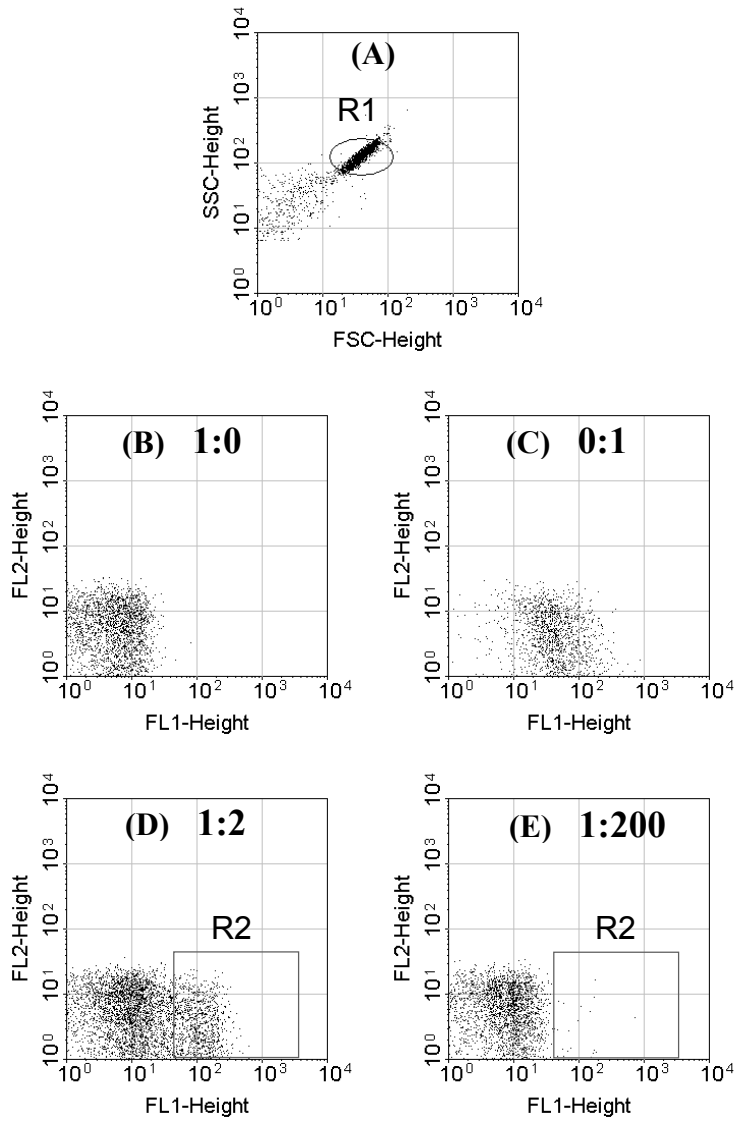

Figure 4.10 Dot plot of pelB-scFv(anti-TNB)/Jude1 as a negative control cell which cannot recognize digoxigenin hapten and pelB-scFv(anti-dig)/Jude1 as a positive control cell. All cells were labeled with 200 nM of the peptide probe **4.3** and 5 μg/ml of PMBN (A) FSC-SSC dot plot, (B) 1:0, (C) 0:1, (D) 1:2 and (E) 1:200 mixture of pelB-scFv(anti-dig)/Jude1 and pelB-scFv(anti-TNB)/Jude1. Region (R2) was used for enrichment.

4.5 CONCLUSION

A successful PECS experiment requires that probes enter the periplasm allowing binding to the target proteins (scFv). Hence, several permeabilizing approaches were evaluated. The permeability studies for PECS revealed that PMBN increases permeability of the outer membrane of ABLEC and Jude1 effectively. However, the Jude1 strain is more amenable for PECS since it is more robust than ABLEC when the scFv is over-expressed. The large peptide probes (~2500 Da) are able to enter the periplasm of Jude1 strain in the presence of PMBN. Enrichment of positive cells was accomplished, demonstrating that PMBM is useful for PECS. Finally, the heptoseless mutant strain D21f2 proved to be a very effective alternative expression system for the PECS or surface displayed approaches, and has the advantage of not requiring any exogenous permeabilizer.

Importantly, this permeabilization study for PECS might provide useful background information of periplasmic enzyme activity detection using FACS. FACS sorting could be used in enzyme directed evolution experiments. In particular, PECS is not limited to relatively small probes, but larger peptide substrates for periplasmic expressed proteases should work as well with either the presence of PBMN or the D21f2 strain.

Chapter 5

Toward high throughput directed enzyme evolution using PECS

5.1 CHAPTER SUMMARY

5.1.1 Goals

To provide the background information required to apply PECS (Periplasmic Expression with Cytometric Screening) for high throughput directed evolution of exogenous proteases that are toxic to *E. coli*.

5.1.2 Approach

Chymotrypsin B or elastase1 was expressed in the periplasmic space based on the pectate lysase leader peptide (pelB). In order to detect activity in the PECS system, an electrostatic capture peptide substrate was synthesized that has a chymotrypsin cleavage site. The substrate is able to diffuse into the periplasm to access the enzyme, and the resulting proteolytic product is designed to be captured in the periplasm and/or on outer membrane as in the OmpT evolution study. Sorting of enzyme libraries would then be carried out using FACS.

5.1.3 Results

Active chymotrypsin was expressed in the periplasmic space by removing the prepeptide sequence of the inactive chymotrypsinogen. Positive control cells expressing active chymotrypsin in the periplasm showed specific activity and high fluorescence intensity in FACS analysis using the fluorescent substrate. On the other hand, negative control cells lacking chymotrypsin activity gave a very low signal. However, when the positive and negative control cells were incubated with the electrostatic capture peptide substrate, only one peak on the FACS histogram

was observed, not the expected two peaks. Our current explanation for these disappointing results is that the single population is due to leakage of the periplasmic chymotrypsin out of the cell to the medium. Hence, the released enzyme cleaved the substrate in the medium, which resulted in electrostatic capture of the product on the cell surface of negative control cells as well as enzyme expressing cells. To prevent leakage, chymotrypsin was anchored to the inner membrane by fusing it to the gene III minor coat protein (gIIIp) (McCafferty *et al*., 1990, Rakonjac *et al*., 1999). However, FACS analysis of the new constructs did not improve resolution on FACS analysis although the enzymatic activity of released enzyme in medium was significantly reduced. Further study to improve the resolution is underway by considering factors for successful application of toxic proteases to the PECS system.

5.2 INTRODUCTION

Enzymes have unique properties that distinguish them from most chemical catalysts. Most impressive is their ability to catalyze specific, and often difficult, chemical reactions in water at room temperature and atmospheric pressure. However, enzymes are often only poorly active towards non-natural substrates and cannot tolerate normal process conditions, including organic solvents. Hence, enzymes have been targeted for directed evolution to overcome the shortcomings of natural enzymes. We expect that high throughput screening of protein libraries using FACS will be a powerful tool for directed evolution (Daugherty *et al*., 2000b, Francisco *et al*., 1993). To extend application of directed evolution beyond the OmpT protease in *E. coli* (Chapter 3), an exogenous protease was considered.

Chymotrypsin family

The serine protease family has been intensively studied for more than 40 years by kinetic, physical and chemical methods. Serine proteases have an essential Ser residue required for enzymatic activity. Trypsin, chymotrypsin and elastase are the

best-characterized enzymes among the serine proteases. The catalytic triads of the active site residues of these proteases are similar and consist of three essential amino acids (Ser 195, His57 and Asp102) for activity. These three enzymes are digestive enzymes that are produced by the pancreatic cells and secreted as larger inactive precursors known as zymogens or proenzymes with very low enzymatic activity. For example, chymotrypsinogen, the proenzyme of chymotrypsin, is expressed then specifically cleaved at the peptide bond between Arg15 and Ile16 by trypsin. Consequently, the product is further processed by autolysis to yield a mature active chymotrypsin. The liberated *N*-terminal Ile16 is critical for activity of serine proteases (Huber & Bode, 1978).

Although the chymotrypsin, trypsin and elastase have sequence homology and similar tertiary structures, they show very different substrate specificities. Chymotrypsin prefers Tyr/Phe in the P_1 position of substrates because the S_1 binding pocket of chymotrypsin is formed by hydrophobic residues and is large enough to accommodate an aromatic group (Cohen *et al*., 1981). On the other hand, trypsin is specific for Lys/Arg in the P_1 site of the substrate. The S_1 binding site contains an anionic residue (Asp189) at the bottom that can form an ion pair with a substrate P_1 residue (Huber & Bode, 1978). Although elastase does not show unique specificity, it prefers substrates containing Ala/Val in the P_1 position. The S_1 binding pocket of elastase is formed by residues of Val216 and Thr226 instead of Gly in trypsin or chymotrypsin (Shotton & Watson, 1970, Watson *et al.*, 1970).

Application of the high throughput FACS technology

Since the x-ray crystal structures are available, rational design methods have been applied to the chymotrypsin family to understand the details of substrate recognition and activity. The substrate specificity of trypsin was converted to that of chymotrypsin or elastase using site-directed mutagenesis. However, the overall activity of the mutants were sacrificed (Hedstrom *et al.*, 1992, Hedstrom, 1998,

Hung & Hedstrom, 1998). Engineering enzymes by rational design methods is very difficult because of they are extremely complicated systems containing a catalytic (turn over rate) and a substrate recognition component. On the other hand, scFv antibodies engineering is less complicated because the key properties are only binding affinity and specificity, not catalysis. To understand protease substrate specificity, a high throughput directed enzyme evolution approach might be more appropriate since the point mutations that improve the properties of the enzyme may be unpredictable at this point. When the mutations have a long ranged effect (far from the active site) or the active site is unclear, it is still very difficult to predict and engineer the key mutations using rational design methods.

A directed evolution applied to the chymotrypsin protease family should lead to a better of understanding the details of substrate recognition. However, expression of the active eukaryotic protease in bacteria might be quite challenging because of expected toxicity. Usually, the chymotrypsin family is expressed as an inactive zymogen in *E. coli* for protein engineering studies (Hung & Hedstrom, 1998, Shirasu *et al*., 1986). However, for a successful directed evolution experiment, activity of the enzyme must be compartmentalized so that phenotype and genotype can be linked. In the case of surface displayed natural OmpT in *E. coli*, it is expressed as an active form without activation and it has its own outer membrane-anchoring domain. However, the exogenous protease, chymotrypsin, will require an anchoring fusion protein, but a fusion that does not interfere with activity.

Chymotrypsin requires the formation of six-disulfide bonds for activity. Proper folding is not expected in the cytoplasm of *E. coli* because it is a reducing environment. Furthermore, an active chymotrypsin in the cytoplasm would be deadly in *E. coli* because it would digest the essential proteins of the cytoplasm. In addition to the folding and toxicity problems of the active protease, inefficient removal of initiator methionine (^{f}Met) is an additional difficulty for engineering the protease in cytoplasm.

The obvious alterative choice is expression in the periplasm of *E. coli,* which is amenable to high throughput FACS technology. Rat anionic trypsin was functionally expressed by removing the activation hexapeptide of the zymogen. It was expressed in periplasmic space of *E. coli* by using bacterial signal peptides such as the *phoA* signal peptide or *his* J signal peptide (Higaki *et al*., 1989, Vasquez *et al*., 1989). We chose to adopt this system for chymotrypsin expression anticipation of PECS screening (Figure 5.1).

A small peptide substrate is expected to penetrate the outer membrane and reach the periplasm based on our PECS study (Chen *et al*., 2001). Once a neutral electrostatic capture substrate is present in the periplasm, chymotrypsin has access to the substrate. The resulting positively charged peptide product would remain associated with the negatively charged membrane and detected by FACS. This system would allow the active protein to be expressed without being toxic to the cytoplasm, and the enzyme would be compartmentalized. Application of high throughput FACS technology combined with the two-color system would overcome the limitation of protein display technologies. This chapter provides background information for the directed evolution of exogenous protease substrate specificity.

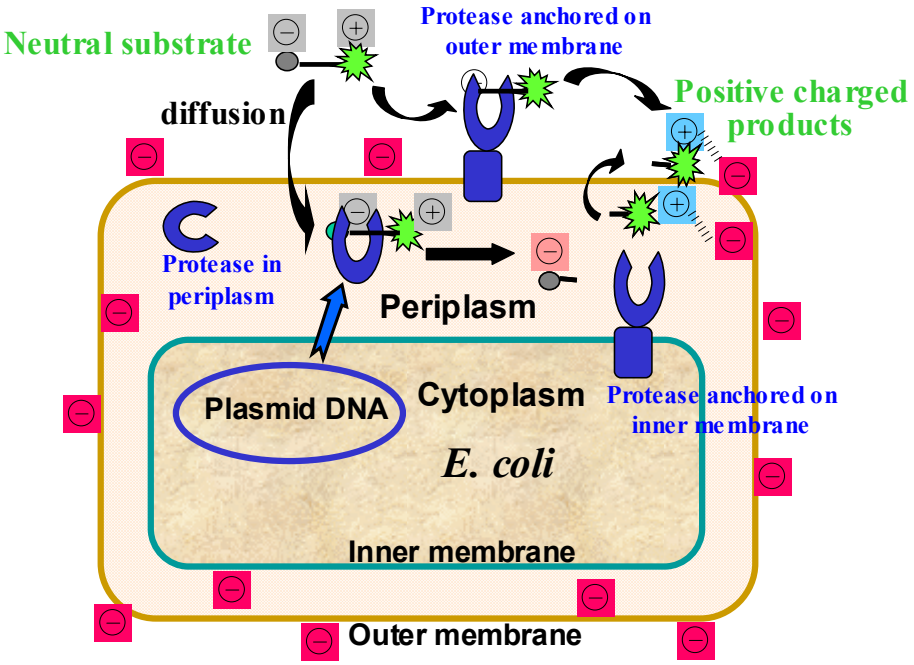

Figure 5.1 Design of periplasmic enzyme expression for cytometric screening using an electrostatic capture substrate. Expression in periplasmic space and anchorage on inner or outer membrane are considered. Proteases are depicted in blue. Surface displayed protease has no outer membrane barrier like OmpT. Periplasmic protease as a soluble form or anchored on the inner membrane need PECS system. An electrostatic capture substrate with net zero charge (⊖ ⊕) can diffuse into the periplasm to access to protease and the resulting substrate product that has 3 positive charges (⊕) is expected to stay on the negatively charged (⊖) periplasm or outer membrane.

5.3 MATERIALS AND METHODS

Reagents, conjugation procedure, and characterization of enzyme probes are generally the same as in the Materials & Methods part of chapter 2. Peptides on Rink amide resin were prepared and capped with glutartic anhydride as in chapter 3.

E. coli strain D21f2 and Jude1 were used for all experiments as in chapter 4. Plasmids pCE-chyB and pCE-ela1 bearing rat chymotrypsin B and porcine pancreatic elastase-1 genes without pre- and pro-sequence were kindly provided from Prof. Stephen Benkovic at the Pennsylvania State University. pAK200 (gIIIp(250-406) and pMopac vectors, which were modified from pAK400 vector (Krebber *et al*., 1997), were obtained from Andrew Hayhurst in our group. pMoPac 2, 10 and 30 that have lpp-OmpA', pectatate lyase (pelB) leader sequence and *malE* gene in upstream of the first *Sfi*I site were used for target protein expression (surface displayed, periplasmic and mbp fusion chymotrypsin, respectively). Restriction enzymes were obtained from New England Biolabs (Beverly, MA) and used with the supplied buffers. Primers for PCR were obtained from Integrated DNA technology (Coralville, IA). Electrocompetent cells were prepared using a published protocol (Sharma & Schimke, 1996). Two chromogenic substrates, succinyl-AAPF-*p*NA and succinyl-AAPA-*p*NA were purchased from Bachem (Torrance, CA).

5.3.1 Chemical synthesis of fluorescent probes for FACS analysis

Preparation of glutaric acid-EAAPYSLRGK(BODIPY)R-NH_2 (5.1)

BODIPY FL SE (1 eq.) in DMF, the peptide (4 μmole) in water and 1 M DMAP (60 μl) were used. The yield after FPLC purifications was 3.0 mg (49%) of dark orange powder. ESI MS (m/z) of glutaric acid-EAAPYSLRGK(BODIPY)R-NH_2 conjugate; calculated 1633.83 for M, found 1634.8 for MH^+, and 818.3 for $(MH^2)^{+2}$.

Preparation of glutaric acid-EAAPASLRGK(BODIPY)R-NH_2 (5.2)

BODIPY FL SE in DMF, the peptide (4 μmole) in water and 1 M DMAP were used. The yield after FPLC purifications was 2.4 mg (36%) of dark orange powder. ESI MS (m/z) of glutaric acid-EAAPASLRGK(BODIPY)R-NH_2 conjugate; calculated 1541.81 for M, found 1542.8 for MH^+, and 772.2 for $(MH^2)^{+2}$.

5.3.2 Method for plasmid constructs

Construction of plasmid for periplasmic chymotrypsin expression (Figure 5.2)

Mature rat chymotrypsin B gene of residues 34-263 (chymotrypsinogen numbering) was amplified from plasmid pCE-chyB with primers (ChyB-f: 5'-GCAAAGGCCCAGCCGGCCATGGCGATCGTCAACGGAGAGGATGC-3' and ChyB-r: 5'-GCTTAGGCCCCCGAGGCCGAGTTGGCTTCCAAGATCTGCTG-3', underlined sequence for *Sif*I site) and digested by *Sfi*I restriction enzyme. Mature porcine pancreatic elastase-1 gene of residues 27-266 was cloned from plasmid pCE-ela1 parallel with chymotrypsin cloning using same method. The Tet^r gene was removed from vector pMoPac10 (Hayhurst *et al*., 2003) by digestion with *Sfi*I. The digested PCR product was ligated into the 4-kb large fragment of the vector with T4 DNA ligase (Stratagene) at room temperature for 3 hours to construct pMoPac10-chyB for periplasmic expression plasmid (where leader peptide is 24 amino acid residues of pelB signal peptide in Figure 5.2). The resulting plasmid (1 μl) was electroporated into frozen Jude1 cell or D21f2 (40 μl), and plated on LB plates supplement with ampicillin. Next, a single colony was cultured in TB+2% sucrose medium with 150 μg/ml of ampicillin and incubated at 37 ^oC at 250 RPM for 12 hours. The plasmid was purified using QIAgen Miniprep kit and sequenced at ICMB DNA-Core Facility in University of Texas at Austin. A 30 % glycerol frozen stock of the culture was also prepared.

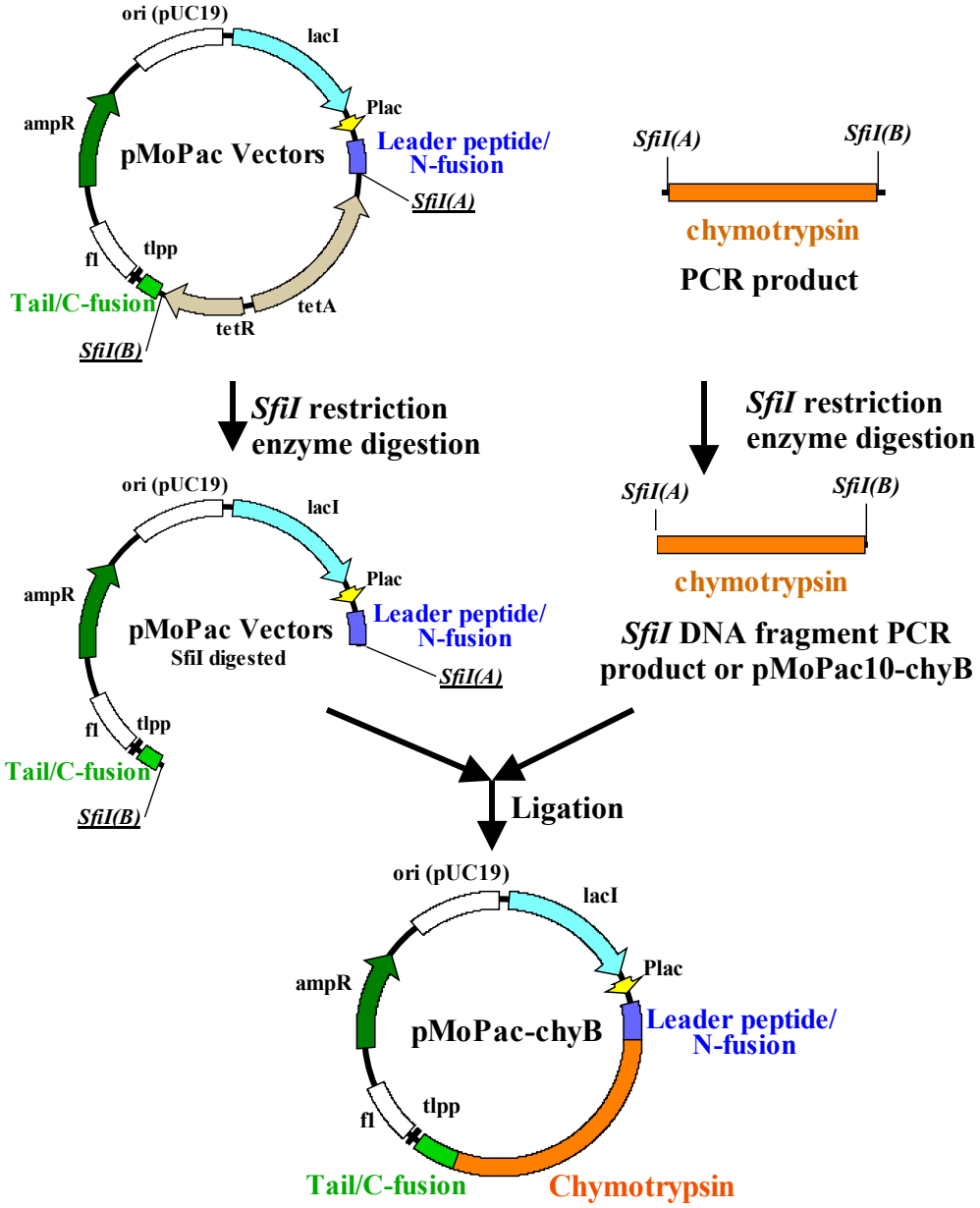

Figure 5.2 Construction of plasmid for chymotrypsin expression. (pMoPac2 has chloramphenicol resistant gene instead of ampicillin resistant gene.)

Correction of chyB

Based on the sequence of Rattus norvegicus (rat) Chymotrypsinogen B (Ctrb) mRNA in NCBI database, point mutation Ile199Ser of chymotrypsin in pCE-chyB was found during sequencing of pMoPac10-chyB and repaired to Ser199 by the QuickChange™ site-directed mutagenesis kit (Stratagene) with primers (ChyB-rep-f; GATCACCGATGTGATGACCTGCGCAGGCGCTAGC and ChyB-rep-r; GCTAGCGCCTGCGCAGGTCATCACATCGGTGATC) according to the manufacturer's protocol.

Construction of chyB plasmids for alternative targeting location

The chymotrypsin gene (0.7 kb) *Sfi*I DNA fragment from the pMoPac10-chyB (chymotrypsin B) was ligated into large *Sfi*I DNA fragment of pMoPac30 and pMoPac2 vectors to construct plasmids to express periplasmic maltose binding protein (MBP) fused chymotrypsin and surface display on outer membrane with same procedure as pMoPac10-chyB construction. For *N*- and *C*-terminal anchoring on the periplasmic face of the inner membrane, pAPEx1 (Harvey, 2003), a derivative of pMoPac1 vector, and pAK200 were used, respectively. 1 μl of ligation mixture was used to transform the Jude1 strain. pMoPac10-chyB and pAk200-chyB were purified from the Jude1 strains and transformed to electrocompetent D21f2 cell.

Cell culture and induction

Growth media were supplemented with ampicillin (150 μg/ml) or chloramphenicol (35 μg/ml) if required. Jude1 or D21f2 containing the plasmids were grown overnight in TB broth containing 2% glucose at 37^{o}C. They were subcultured in fresh TB media and re-grown at 37^{o}C for 2 hours until O.D. is 0.5-0.8. The cells were induced with IPTG (0 to 0.5 mM) for an additional 3 hours at 25^{o}C to express the chymotrypsin in *E. coli* strains. The cells were harvested and resuspended in 1xPBS. The cell suspensions were subjected to electrophoresis on

4-20% SDS polyacrylamide gels. Western blotting was performed through electrophoretic transfer to a PVDF membrane at 150 mA for 40 min. After blocking with 5% non-fat dry milk, the membrane was incubated with a 1:50000 dilution of rabbit anti-His tag antibody conjugated to horseradish peroxides in TBST (0.154 M NaCl, 0.1% Tween-20 and 10 mM Tris-HCl (pH 7.6)) and developed with Supersignal West Pico Chemiluminescent Substrate (Pierce, Rockfort, IL).

5.3.3 Activity assay

Enzyme activity assay on spectrometry

The induced cell cultures (0.5 ml) were washed with 0.5 ml of 1% sucrose. For the microplate assay, 10 µl of the cell suspension was added to 190 µl of 0.8 mM succ-AAPF-*p*NA in 20 mM Tris-HCl (pH 8.0) and 0.5 mM EDTA. The release of *p*-nitroanilide was measured at 405 nm. Negative control cells were used, comprised of the same strain the without the plasmid or IPTG induction.

Cytometric analysis with FACS

The induced cell cultures (0.5 ml) were harvested and washed with 0.5 ml of 1% sucrose. The aliquot (50 µl) of cell suspension was mixed with 449 µl of 1% sucrose and the electrostatic capture substrates **5.1** or **5.2** at a final concentration of 200 nM. The resulting solution was incubated at room temperature for 30 min. The resulting cell suspensions (10 µl) were diluted with 1 ml of 1% sucrose solution (SIP solution) and applied to a FACSCalibur (Becton-Dickinson) without additional washing. Settings of FACS screening was as following; Forward scatter E01, Side scatter trigger 400volts, FL1 800volts. The collected data were processed on WinMDI 2.8 program (http://facs.scripps.edu) and depicted in the form of histograms showing 10,000 cellular events from each population.

5.4 RESULTS AND DISCUSSION

5.4.1 Protease expression

A bacterial expression system for active rat chymotrypsin B and porcine elastase 1 were constructed (Figure 5.2). The chymotrypsin and elastase genes were ligated into pMoPac10, 30, and 2 (Table 5.1). These vectors allow for exploration of a number of different expression strategies. In all cases, expression is controlled by a *lac* promoter (Plac), which is induced with IPTG. The pelB leader peptide and maltose-binding protein (MBP) with natural *malE* signal sequences (Di Guan *et al*., 1988) were used for periplasmic expression of target enzymes as soluble and MBP fused forms with pMoPac10 and 30. When the target pelB-ChyB peptide is excreted to periplasm via Sec pathway (Economou, 1999), leader peptidase 1 of the bacterial *lep* gene cleaves off the pelB leader peptide to give *N*-terminal free protease (Tschantz & Dalbey, 1994). MBP is known to facilitate expression and folding of fusion proteins. pMoPac2-chyB plasmid was designed to express chymotrypsin on the surface of outer membrane with lpp-OmpA' as an anchor protein.

Vector	Leader peptide	N-fusion protein	C-fusion protein	Target protein location
pMoPac10	pelB	–	6xHis tag	Periplasm
pMoPac30	malE	MBP	6xHis tag	Periplasm
pMoPac2	lpp	Lpp-OmpA'	6xHis tag	Outer surface of outer membrane
pAPEx1	NlpA	CDASS	6xHis tag	Anchored on inner membrane (periplasm)
pAK200	pelB	–	gIIIp'	Anchored on inner membrane (periplasm)

Table 5.1 Representation of leader peptide and fusion proteins. Leader peptide; PelB (24aa), malE (26aa), lpp(19aa), and NlpA (25aa). N-terminal fusion protein; MBP (366aa), lpp-OmpA'(133aa), and CDASS (the first Cys is modified with a lipophilic anchor). C-terminal fusion peptide; 6xHis tag (36aa with c-myc tag) and gIIIp' (52aa).

The cells transformed with the plasmids were grown, and induced with IPTG. The cell suspensions were washed and resuspended to assay activity. The expression level was analyzed by Western blotting after SDS polyacrylamide gel electrophoresis. When probed with anti-His tag antibody, pMoPac2, 30 and 10-chyB gave 41 kDa of lpp-OmpA'-ChyB, 68 kDa of MBP-ChyB and 29 kDa of ChyB, respectively, as shown in Figure 5.3. These are the expected sizes of the fusion proteins. However, the expression levels were too low to be detected with Coomassie blue staining.

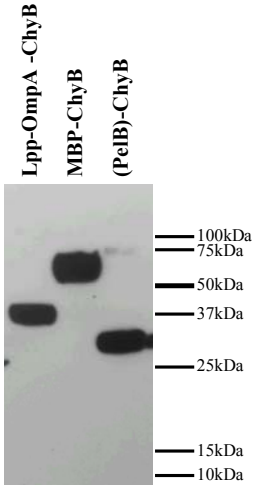

Figure 5.3 SDS PAGE gel (4-20% Tris-Glycine gel) of the total cell extracts from Jude1 strain blotted with HRP conjugated anti-6xHis antibody.

5.4.2 Detecting activity of periplasmic chymotrypsin

Activity assay of proteases

The enzymatic activities of the proteins were examined by measuring the absorbance at 405 nm with chromogenic substrates in Tris-HCl buffer (pH 8.0) and 0.5 mM EDTA. Chrmotrypsin and elastase activity was measured using the substrates suc-AAPF-*p*NA and suc-AAPA-*p*NA, respectively. The elastase

substrate can be a negative control substrate for chymotrypsin. The activity was measured using whole cells since the FACS assay will also use whole cells. Table 5.2 showed that only (pelB)-ChyB could hydrolyze the chymotrypsin substrate while the *N*-terminal fusions of chymotrypsin, lpp-OmpA'-ChyB and MBP-ChyB, exhibit no such activity. The *N*-terminal Ile-16 (numbering in zymogen) might be also important to chymotrypsin activity as the liberated *N*-terminal Ile16 of trypsin is known to be critical for activity (Huber & Bode, 1978). The (pelB)-ChyB cell was specific for the chymotrypsin substrate, suc-AAPF-*p*NA, and showed no activity for the elastase substrate, suc-AAPA-*p*NA. None of the elastase fusions showed activity for suc-AAPA-*p*NA except lpp-OmpA'-Ela1 protein. However, this fusion only showed very week activity. It is not clear that the poor activity of the elastase fusions expressed in periplasm is due to improper folding.

Protease activity	**Suc-AAPA-*p*NA**	**Suc-AAPF-*p*NA**
(pelB)-Ela1	–	–
Lpp-OmpA'-Ela1	+	–
MBP-Ela1	–	–
(pelB)-ChyB	–	+++
Lpp-OmpA'-ChyB	–	–
MBP-ChyB	–	–

Table 5.2 Microplate assay of enzymatic activity of total cell with chromogenic substrates. The reaction is performed in 20 mM Tris-HCl. pH 8.0 and 0.5 mM EDTA.

Detecting activity of periplasmic chymotrypsin on FACS

As a preliminary experiment, Jude1 *E. coli* cells containing the plasmids were grown and induced with IPTG. The electrostatic capture substrate **5.1** (1.6 kDa) for detecting chymotrypsin activity is expected to permeate the outer membrane because it is much smaller than the peptide probe **4.3** (2.5 kDa) used for the permeabilization experiments in chapter 4. Prior to a reaction with the electrostatic

capture substrate, the cells were washed with 1% sucrose solution to remove all ionic salts and resuspended with the same solution. The step is critical because high concentrations of ionic salts impede charge-charge interactions between the positively charged product of substrate and the negatively charged outer membrane of the cell. For example, the FACS signal in a histogram was gradually decreased by increasing the concentration of Tris-HCl buffer (pH 7.5).

Histograms of Jude1/pMoPac10-ChyB showing the FL1 (BODIPY-FL fluorescence emission) are depicted in Figure 5.4. The IPTG-induced Jude1/pMoPac10-chyB and Jude1 cells as positive and negative controls were incubated with chymotrypsin substrate **5.1** (glutaric acid-EAAPY•SLRGK(BODIPY)R-NH_2). Elastase substrate **5.2** (glutaric acid-EAAPA•SLRGK(BODIPY)R-NH_2) was used as a negative control.

Chymotrypsin expressing cells displayed high fluorescence intensity with only the substrate **5.1** as expected. It is important to compare the mean fluorescence intensity generated of the positive control substrate (**5.1**) to that of the negative control substrate (**5.2**) for evaluation of positive fluorescence signal detected in histogram as chymotrypsin activity (Figure 5.4A top right), because non-specific binding of substrate can conceivably occur due to possible surface property changes in over-expressed *E. coli*. Using **5.2** also reduces the likelihood of isolating chymotrypasin variants with non-specific proteolytic activity that can cleave any peptide bond within the electrostatic substrate **5.2**. No positive signal on histogram was observed as in histogram when the positive cell was incubated with an unoptimized peptide (glutaric acid-EGFNFPQVTRGK(BODIPY)GR-NH_2) as another negative control substrate (data not shown). Hence, the activity recorded from FACS signals appears to be specific to chymotrypsin. When EDTA (0.5mM) was added during incubation to increase permeability, the positive cells showed higher mean fluorescence intensity (34x over negative control cell) (Figure 5.4B top left) than that of non-EDTA treated cells (18x over negative control cell). The EDTA-treated cells also showed a relatively small coefficient of variation (CV),

which is a measurement of the uniformity of the cell population (sharp peak in the histogram). A small CV implies that the substrate is more accessible to the expressed enzyme with EDTA. Other Lpp-OmA and MBP fused chymotrypsin did not show any positive signal at all.

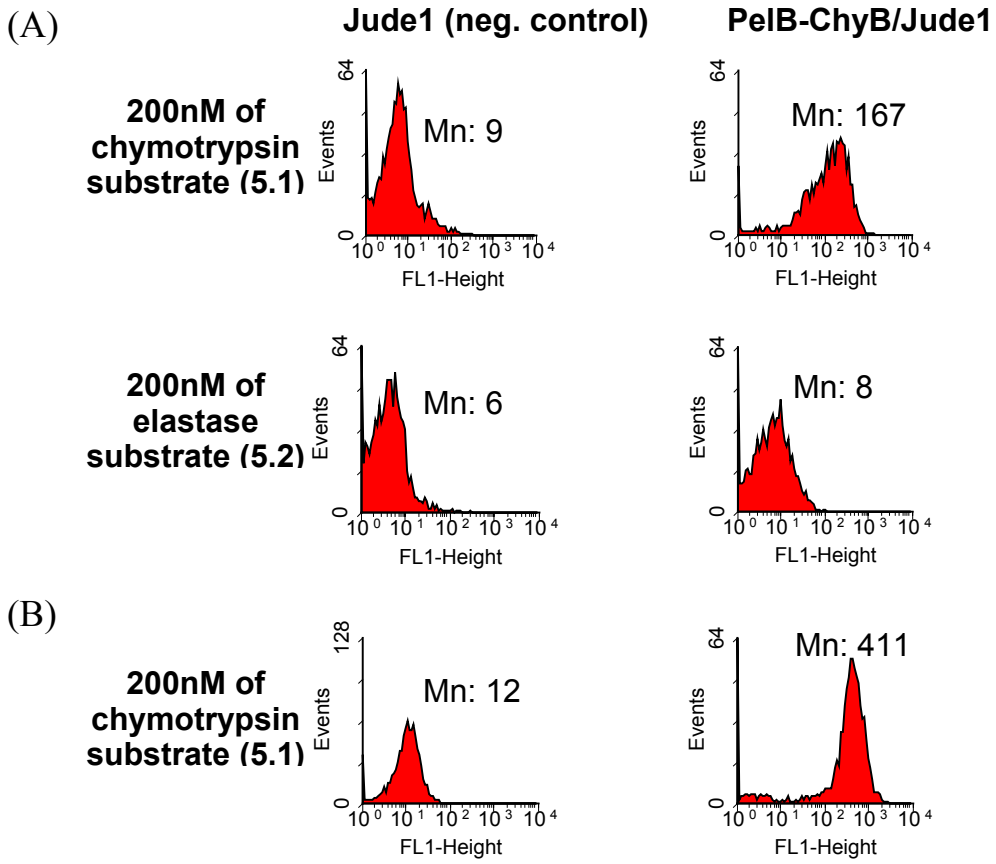

Figure 5.4 Detection of enzymatic activity on FACS. (A) Jude1 and pMoPac12-chyB cells were incubated with chymotrypsin substrate **5.1** (glutaric acid-AAPY•SLRGK(BODIPY)R-NH_2) or elastase substrate **5.2** (glutaric acid-AAPA•SLRGK(BODIPY)R-NH_2) as a negative control. (B) Cells were incubated with 0.5 mM of EDTA.

FACS analysis of mixed cells and activity test of supernatants

In spite of FACS detection of chymotrypsin in cells, when the two cell types (Jude1 and Jude1/pMoPac10-ChyB) were mixed and analyzed on FACS, histogram showed only one positive peak instead of two peaks. (Figure 5.5). The negative control Jude1 cell appeared to have gained higher fluorescence intensity (signal). Changing a host cell (Jude1) to the D21f2 strain did not improve peak resolution on the histogram. There are two reasons why this might have occurred; 1) The peptide product was transferred from the positive cells to the negative cells because of insufficient electrostatic interaction between the peptide product and cell surface. 2) The soluble chymotrypsin expressed in *E. coli* was leaking from the periplasm and exerted the hydrolytic activity to the substrate in the reaction medium. The resulting positively charged peptide product has equal probability of interacting with the surface of the two different types of cells.

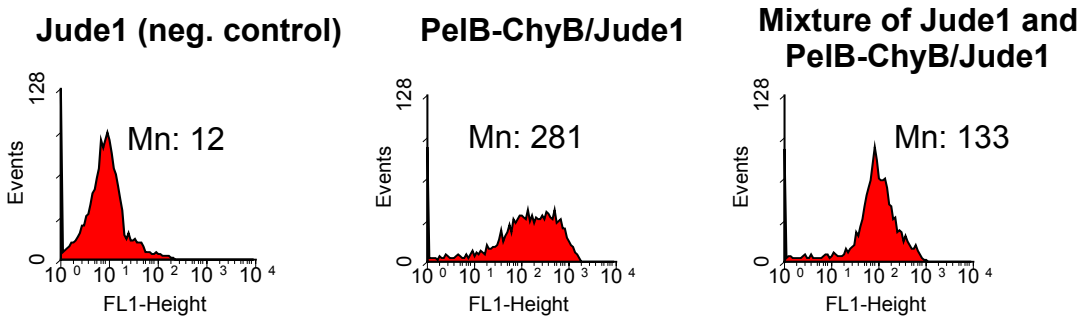

Figure 5.5 FACS analysis of mixed cells of negative (Jude1) and positive (Jude1/pMoPac10-chyB) control with 200nM of the substrate **5.1**.

To check if peptide product can have enough positive charges to stay on the surface of cells, the substrate **5.1** and **5.2** were pre-digested with chymotrypsin (0.1 mg/ml) and elastase (0.2 mg/ml), respectively. Jude1 cells and D21f2 (no chymotrypsin expression) were incubated with the pre-digested substrates. Figure 5.6A showed high signals for Jude1 cells with both pre-digested substrates, which imply that peptide products are captured electrostatically enough to stay on the cells.

The identical results were observed when D21f2 was used. Hence, this demonstrates that the positively charged product will bind to the cell surface.

The Jude1 cells with undigested substrate **5.1** and the Jude1 cells with pre-digested substrate **5.1** by chymotrypsin were pelleted to remove the excess substrate or peptide product in the supernatants. They were resuspended with 1% fresh sucrose solution and then mixed, followed by a 20 min incubation to allow potential transference of the peptide product between the cells. However, the FACS histogram displayed two clear peaks (Figure 5.6B). Different incubation times (1, 5 and 15 min) showed the same pattern of the FACS histogram. These separated peaks imply that the positively charged peptide product is not transferring between the cells, and is not the explanation for our mixed population in the chymotrypsin FACS experiments.

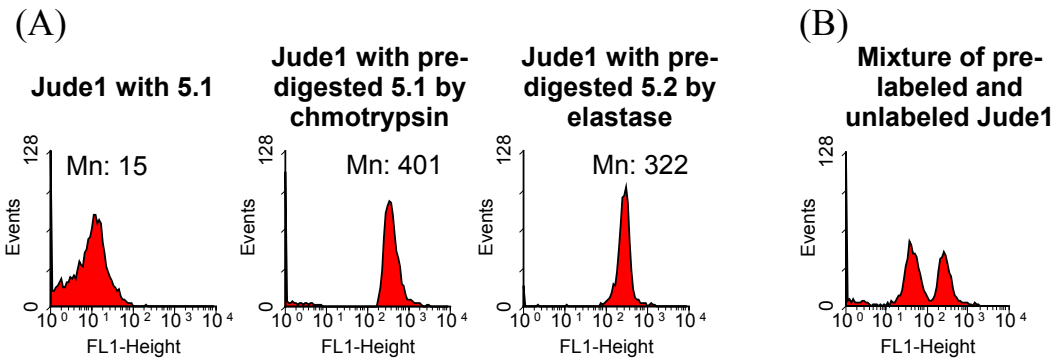

Figure **5.6** (A) FACS analysis of Jude1 (negative control cell) with pre-digested substrates (**5.1** and **5.2**) by their corresponding proteases. (B) FACS analysis of the cell mixture to check potential transference of the product between the cells.

Hence, an enzyme-leaking test was performed on FACS. The cell suspension of Jude1/pMoPac10-ChyB in 1% sucrose was pelleted again and the supernatant (10 µl) was added to Jude1 (no chymotrypsin expression) with substrate **5.1**. Although Jude1 cells do not express chymotrypsin, it gave a high signal on FACS (Figure 5.7).

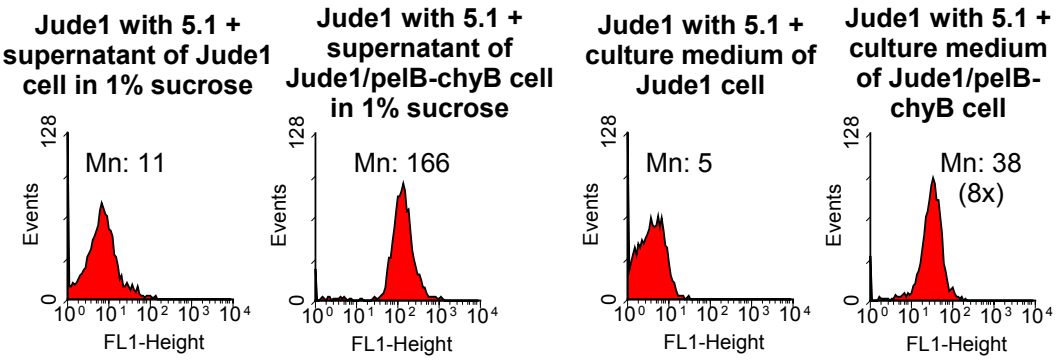

Figure 5.7 FACS analysis of Jude1 (negative control cell) with supernatants (10 μl) or culture media (10 μl) of the negative cell (Jude1) and the positive cell (Jude1/pMoPac10-chyB) with 200 nM of the chymotrypsin substrate **5.1**.

Supernatant of culture media of Jude1/pMoPac10-ChyB also had similar FACS results as in the reaction with supernatant of 1% sucrose. This apparently revealed that the supernatants had chymotrypsin activity as well as the cell pellets. The detected activity of pellets on FACS was thought to be from continuous leaking of periplasmic chymotrypsin from the cells. The periplasmic chymotrypsin may leak out through a weakened outer membrane by digesting periplasmic and/or membrane proteins to rupture the outer membrane. The results were consistent with a microplate assay with chromogenic substrates (Table 5.3). This is also consistent with the EDTA data (Figure 5.4B). EDTA may further weaken the outer membrane allowing the enzyme to pass to the media.

Protease activity	Suc-AAPA-*p*NA	Suc-AAPF-*p*NA
(pelB)-ChyB	–	+++
Supernatant of (pelB)-ChyB	–	+++
Culture medium of (pelB)-ChyB	–	++

Table 5.3 Enzymatic activity of total cell and supernatants with chromogenic substrates.

Anchoring of chymotrypsin on the inner membrane of *E. coli*

To reduce the leakage of active enzymes, NlpA (Yamaguchi *et al*., 1988, Yu *et al*., 1986) and gIIIp anchoring protein in pAPEX1 (Harvey, 2003) and pAP200 (Krebber *et al*., 1997) were introduced by fusing *N*- and *C*-terminal anchoring of chymotrypsin on the periplasmic face of the inner membrane of Jude1 and D21f2 strains. As we expected, cells containing ChyB-gIIIp fusion proteins showed chymotrypsin activity on chromogenic plate assay and FACS analysis while no activity was detected for NlpA-ChyB one as in Lpp-OmpA' and MBP fusion chymotrypsin Table 5.4.

Protease activity	Suc-AAPA-*p*NA	Suc-AAPF-*p*NA
(pelB)-ChyB	–	+++
Supernatant of (pelB)-ChyB	–	+++
NlpA-ChyB	–	–
Supernatant of NlpA-ChyB	–	–
(pelB)-ChyB-gIIIp'	–	+++
Supernatant of (pelB)-ChyB-gIIIp'	–	–

Table 5.4 Enzymatic activity of *N*- and *C*-terminal anchored chymotrypsin with chromogenic substrates.

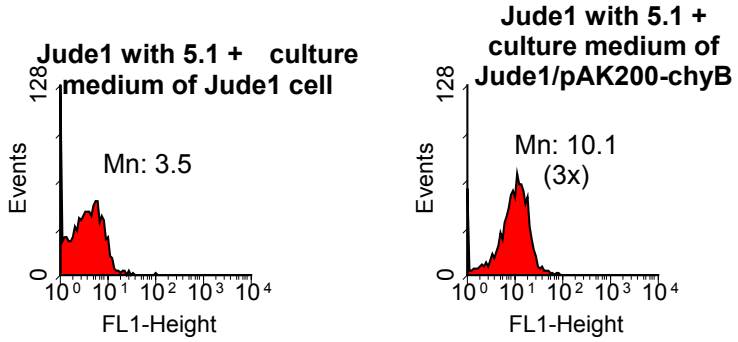

Figure 5.8 FACS analysis of Jude1 (negative control cell) with culture media (10 µl) of the negative cell (Jude1) and the positive cell (Jude1/pAK200-chyB) with 200 nM of the chymotrypsin substrate **5.1**.

Only chymotrypsin that has free *C*-terminus showed activity because the *N*-terminus of chymotrypsin is important for activation (Huber & Bode, 1978). Although the chymotrypsin activity of supernatant of Jude1/pAK200-chyB was too low to be detected in plate assay with chromogenic substrates (Table 5.4) it was detected with FACS. When supernatant (10 μl) of cell culture of Jude1/pAK200-chyB (anchored chymotrypsin) was added (Figure 5.8), Jude1 negative cell showed very weak positive signal (3x fluorescence intensity) compared to high activity (8x fluorescence intensity in Figure 5.7) of cell culture supernatant of Jude1/pMoPac10-chyB. These results demonstrate that a very small amount of chymotrypsin is released from Jude1/pAK200-chyB (anchored chymotrypsin). Furthermore, a mixture of negative cells and gIIIp fused chymotrypsin cell (pAK200-chyB in Jude1 or D21f2) also failed to get separate signals in FACS assay resulting in only one positive signal. Whenever EDTA was added, the fluorescence intensity (positive signal) of ChyB-gIIIp' in Jude1 or D21f2 was increased. This implies that although leakage problem is significantly reduced when chymotrypsin is fused to gIIIp', it still results in a single peak in the FACS histogram. The leakage may be because chymotrypsin cleaves its anchor moiety gIIIp', or some portion of gIIIp fusion protein was not inserted to inner membrane. Optimization of the system is underway to improve the peak resolutions on the histogram.

5.4 CONCLUSION

The work presented in this chapter provides the foundation for high throughput directed enzyme evolution studies of exogenous proteases expressed in *E. coli*. Active chymotrypsin as a model system was chosen for application of the two-colored FACS sorting based on PECS. Only chymotrypsin with the pectate lyase pelB leader sequence in pMoPac-ChyB and pAK200-chyB has been expressed in an active form. The other fusions such as lpp-OmpA, MBP and NlpA did not show any detectable activity. These studies demonstrated that only a *C*-terminal fusion is available for the engineering of chymotrypsin. The activity of total cells

expressing periplasmic chymotrypsin was detected on a plate assay and it turned out to be specific to chymotrypsin using sequence-optimized and unoptimized chromogenic substrates.

Activity of periplasmic chymotrypsin was also detected on FACS analysis using the electrostatic capture substrate. Although positive control cells in the FACS histogram gave a high fluorescence intensity, the signal was believed to emerge from the released chymotrypsin in the reaction medium rather the chymotrypsin in the periplasm. The experiments in this chapter showed that many factors should be considered to set up a high throughput directed evolution of exogenous protease by PECS as follows.

i) Toxicity of exogenous protease. It can originate from proteolytic activity, not from over-expression as in non-protease proteins. It is inevitable because the FACS detection is base on active enzyme. Although chymotrypsin was expressed in periplasmic space, it showed toxic effect to *E. coli*.

ii) Leakage of protease from periplasm. The enzyme is released to the reaction medium due to potential non-specific digestion of the periplasmic and outer membrane proteins of the host *E. coli* cell. In contrast of FACS screening of the active scFv in PECS, only a small amount of released protease in the medium is problematic because as we saw, it can hydrolyze the substrate resulting in high background signal.

iii) Permeability of substrate. The electrostatic capture substrate used in this chapter was thought to be permeable to the outer membrane of D21f2 because molecular weight of the substrate is not very high (1.6 kDa). However, permeability of the substrate should be re-considered because chymotrypsin activities in the periplasm and in the medium may compete each other. If the substrate passed the outer membrane freely, the signal from a small amount of released chymotrypsin in the medium would be relatively low to give resolved peaks on FACS histogram.

iv) Transference of substrate products. For scFv FACS detection, no transference of probe is a problem because compartmentalization between the protein activity (scFv affinity) and the cell is achieved by direct binding of the hapten probe to the antibody strongly with slow dissociation. The enzyme detection system using FACS utilizes the charge-charge interaction of the protein activity (peptide product) and the cell surface, which is a non-specific interaction. Inevitably, loss of signal was observed gradually with time in the SIP tube during FACS screening of OmpT cell using charge-charge interaction as in the FRET substrates and the electrostatic capture substrates (chapter 3). If transferring rate of charged peptide products on positive cells to negative cells is faster than enzymatic hydrolysis during reaction of the mixed cells with the substrate, lower or no resolution of peaks would be obtained in the FACS histogram.

v) Expression levels. In general, the signals from spectrophotometric and FACS assays are proportional to expression. However, high expression level can be detrimental to the cells. For example, FACS analysis displayed several blunt cell populations on SSC and FSC cell density-plot, which is a signature for damaged cells. These damaged cells may be responsible for more enzymes to be released.

vi) Anchoring protein and position for protease display on the membrane. When a protease anchoring strategy is applied to reduce leakage, the anchoring protein should not affect the enzymatic activity. For example, the *N*-terminal fusion of chymotrypsin did not show any activity.

Considering the factors above may provide direction for the successful PECS application of directed protease evolution. Thrombin or caspase are good candidates for an evolution study since they are highly specific. Unlike the chymotrypsin family, which is relatively unspecific, these enzymes should be less toxic and have a better chance to be compartmentalized. As an alternative system of PECS, anchoring protease in spheroplast cell can be used by combining APEx system (Harvey, 2003) that removes outer membrane barrier completely when a anchor domain is applied as robust as OmpT protease.

Bibliography

Alakomi, H.-L., Skytta, E., Saarela, M., Mattila-Sandholm, T., Latva-Kala, K., and Helander, M. I. (2000) Lactic Acid Permeabilizes Gram-Negative Bacteria by Disrupting the Outer Membrane. *Applied and Environmental Microbiology 66*, 2001-2005.

Altamirano, M. M., Blackburn, J. M., Aguayo, C., and Fersh, A. R. (2000) Directed evolution of new catalytic activity using the a/b-barrel scaffold. *Nature 403*, 617-622.

Amro, N. A., Kotra, L. P., Wadu-Mesthrige, K., Bulychev, A., Mobashery, S., and Liu, G.-y. (1999) Structural basis of the Escherichia coli outer-membrane permeability. *Proceedings of SPIE-The International Society for Optical Engineering 3607*, 108-122.

Amro, N. A., Kotra, L. P., Wadu-Mesthrige, K., Bulychev, A., Mobashery, S., and Liu, G.-y. (2000) High-Resolution Atomic Force Microscopy Studies of the Escherichia coli Outer Membrane: Structural Basis for Permeability. *Langmuir 16*, 2789-2796.

Arnold, F. H. (1998) Design by directed evolution. *Accounts of Chemical Research 31*, 125-131.

Arnold, F. H., Peters, M. W., Meinhold, P., Farinas, E. T., Glieder, A., and Bugg, C. W. (2003) Directed evolution of alkane hydroxylation activity in cytochrome P450 BM-3. *Abstracts of Papers, 225th ACS National Meeting, New Orleans, LA, United States, March 23-27, 2003*, BIOT-363.

Azzazy, H. M. E., and Highsmith, W. E., Jr. (2002) Phage display technology: clinical applications and recent innovations. *Clinical Biochemistry 35*, 425-445.

Backes, B. J., Harris, J. L., Leonetti, F., Craik, C. S., and Ellman, J. A. (2000) Synthesis of positional-scanning libraries of fluorogenic peptide substrates to define the extended substrate specificity of plasmin and thrombin. *Nature Biotechnology 18*, 187-193.

Barrett, A. J. (1999) Peptidases: a view of classification and nomenclature in *Proteases : new perspectives.* (Turk, V., Ed.) pp 1-12, Birkhauser Verlag, Basel.

Blackman, M. J., Corrie, J. E. T., Croney, J. C., Kelly, G., Eccleston, J. F., and Jameson, D. M. (2002) Structural and Biochemical Characterization of a Fluorogenic Rhodamine-Labeled Malarial Protease Substrate. *Biochemistry 41*, 12244-12252.

Boder, E. T., and Wittrup, K. D. (1997) Yeast surface display for screening combinatorial polypeptide libraries. *Nature Biotechnology 15*, 553-557.

Boder, E. T., Midelfort, K. S., and Wittrup, K. D. (2000b) Directed evolution of antibody fragments with monovalent femtomolar antigen-binding affinity.

Proceedings of the National Academy of Sciences of the United States of America 97, 10701-10705.

Boman, H., and Monner, D. (1975) Characterization of lipopolysaccharides from Escherichia coli K-12 mutants. *Journal of Bacteriology 121*, 455-64.

Brabetz, W., Muller-Loennies, S., Holst, O., and Brade, H. (1997) Deletion of the heptosyltransferase genes rfaC and rfaF in Escherichia coli K-12 results in an Re-type lipopolysaccharide with a high degree of 2-aminoethanol phosphate substitution. *European Journal of Biochemistry 247*, 716-724.

Brass, J. M. (1986) Calcium-induced permeabilization of the outer membrane: a method for reconstitution of periplasmic binding protein-dependent transport systems in Escherichia coli and Salmonella typhimurium. *Methods in Enzymology 125*, 289-302.

Bukau, B., Brass, J. M., and Boos, W. (1985) Ca2+-induced permeabilization of the Escherichia coli outer membrane: comparison of transformation and reconstitution of binding-protein-dependent transport. *Journal of Bacteriology 163*, 61-8.

Cadwell, R. C., and Joyce, G. F. (1992) Randomization of genes by PCR mutagenesis. *PCR Methods and Applications 2*, 28-33.

Chen, G., Dubrawsky, I., Mendez, P., Georgiou, G., and Iverson, B. L. (1999) In vitro scanning saturation mutagenesis of all the specificity determining residues in an antibody binding site. *Protein Engineering 12*, 349-356.

Chen, G., Hayhurst, A., Thomas, J. G., Harvey, B. R., Iverson, B. L., and Georgiou, G. (2001) Isolation of high-affinity ligand-binding proteins by periplasmic expression with cytometric screening (PECS). *Nature Biotechnology 19*, 537-542.

Cherry, J. R., and Fidantsef, A. L. (2003) Directed evolution of industrial enzymes: an update. *Current Opinion in Biotechnology 14*, 438-443.

Cohen, G. H., Silverton, E. W., and Davies, D. R. (1981) Refined crystal structure of g-chymotrypsin at 1.9 .ANG. resolution. Comparison with other pancreatic serine proteases. *Journal of Molecular Biology 148*, 449-79.

Cristobal, G., Remedios, d., and Pierre, D. J. M. (1995) Fluorescence resonance energy transfer spectroscopy is a reliable "ruler" for measuring structural changes in proteins. Dispelling the problem of the unknown orientation factor. *J Struct Biol 115*, 175-85.

Daugherty, P. S., Chen, G., Olsen, M. J., Iverson, B. L., and Georgiou, G. (1998) Antibody affinity maturation using bacterial surface display. *Protein Engineering 11*, 825-832.

Daugherty, P. S., Chen, G., Iverson, B. L., and Georgiou, G. (2000a) Quantitative analysis of the effect of the mutation frequency on the affinity maturation of single chain Fv antibodies. *Proc. Natl. Acad. Sci. USA 97*, 2029-2034.

Daugherty, P. S., Iverson, B. L., and Georgiou, G. (2000b) Flow cytometric screening of cell-based libraries. *Journal of Immunological Methods 243*, 211-227.

Decad, G. M., and Nikaido, H. (1976) Outer membrane of Gram-negative bacteria. XII. Molecular-sieving function of cell wall. *Journal of Bacteriology 128*, 325-36.

Dekker, N., Cox, R. C., Kramer, R. A., and Egmond, M. R. (2001) Substrate Specificity of the Integral Membrane Protease OmpT Determined by Spatially Addressed Peptide Libraries. *Biochemistry 40*, 1694-1701.

DeLisa, M. P., Samuelson, P., Palmer, T., and Georgiou, G. (2002) Genetic analysis of the twin arginine translocator secretion pathway in bacteria. *Journal of Biological Chemistry 277*, 29825-29831.

DelMar, E. G., Largman, C., Broderick, J. W., and Geokas, M. C. (1979) A sensitive new substrate for chymotrypsin. *Analytical Biochemistry 99*, 316-20.

Demartis, S., Huber, A., Viti, F., Lozzi, L., Giovannoni, L., Neri, P., Winter, G., and Neri, D. (1999) A Strategy for the Isolation of Catalytic Activities from Repertoires of Enzymes Displayed on Phage. *Journal of Molecular Biology 286*, 617-633.

Di Guan, C., Li, P., Riggs, P. D., and Inouye, H. (1988) Vectors that facilitate the expression and purification of foreign peptides in Escherichia coli by fusion to maltose-binding protein. *Gene 67*, 21-30.

Economou, A. (1999) Following the leader: bacterial protein export through the Sec pathway. *Trends in Microbiology 7*, 315-20.

Evnin, L. B., Vasquez, J. R., and Craik, C. S. (1990) Substrate specificity of trypsin investigated by using a genetic selection. *Proceedings of the National Academy of Sciences of the United States of America 87*, 6659-63.

Farinas, E. T., Bulter, T., and Arnold, F. H. (2001) Directed enzyme evolution. *Current Opinion in Biotechnology 12*, 545-551.

Fersht, A. R., Blow, D. M., and Fastrez, J. (1973) Leaving group specificity in the chymotrypsin-catalyzed hydrolysis of peptides. Stereochemical interpretation. *Biochemistry 12*, 2035-41.

Flexner, C. (1998) HIV-protease inhibitors. *New England Journal of Medicine 338*, 1281-1292.

Francisco, J. A., Campbell, R., Iverson, B. L., and Georgiou, G. (1993) Production and fluorescence-activated cell sorting of Escherichia coli expressing a functional antibody fragment on the external surface. *Proceedings of the National Academy of Sciences of the United States of America 90*, 10444-8.

Glieder, A., Farinas, E. T., and Arnold, F. H. (2002) Laboratory evolution of a soluble, self-sufficient, highly active alkane hydroxylase. *Nature Biotechnology 20*, 1135-1139.

Grahn, S., Ullmann, D., and Jakubke, H. D. (1998) Design and synthesis of fluorogenic trypsin peptide substrates based on resonance energy transfer. *Analytical Biochemistry 265*, 225-231.

Griffiths, A. D., and Tawfik, D. S. (2003) Directed evolution of an extremely fast phosphotriesterase by in vitro compartmentalization. *EMBO Journal 22*, 24-35.

Grodberg, J., Lundrigan, M., Toledo, D., Mangel, W., and JJ., D. (1988) Complete nucleotide sequence and deduced amino acid sequence of the ompT gene of Escherichia coli K-12. *Nucleic Acids Res. 16*, 1209.

Guo, L., Lim, K. B., Poduje, C. M., Daniel, M., Gunn, J. S., Hackett, M., and Miller, S. I. (1998) Lipid A acylation and bacterial resistance against vertebrate antimicrobial peptides. *Cell 95*, 189-198.

Hancock, R. E. W., and Wong, P. G. W. (1984) Compounds which increase the permeability of the Pseudomonas aeruginosa outer membrane. *Antimicrobial Agents and Chemotherapy 26*, 48-52.

Harayama, S. (1998) Artificial evolution by DNA shuffling. *Trends in Biotechnology 16*, 76-82.

Harris, J. L., Backes, B. J., Leonetti, F., Mahrus, S., Ellman, J. A., and Craik, C. S. (2000) Rapid and general profiling of protease specificity by using combinatorial fluorogenic substrate libraries. *Proceedings of the National Academy of Sciences of the United States of America 97*, 7754-7759.

Harvey, B. R. (2003) Ph.D. Thesis, Anchored Periplasmic Expression (APEx): A Versatile Technology for the Flow Cytometric Selection of High Affinity Antibodies from Escherichia coli Expressed Libraries. Unversity of Texas at Austin.

Haugland, R. P. (1996) Handbook of fluorescent probes and research chemicals, Sixth ed.

Hayhurst, A., and Harris, W. J. (1999) Escherichia coli Skp Chaperone Coexpression Improves Solubility and Phage Display of Single-Chain Antibody Fragments. *Protein Expression and Purification 15*, 336-343.

Hayhurst, A., Happe, S., Mabry, R., Koch, Z., Iverson, B. L., and Georgiou, G. (2003) Isolation and expression of recombinant antibody fragments to the biological warfare pathogen Brucella melitensis. *Journal of Immunological Methods 276*, 185-196.

Hedstrom, L., Szilagyi, L., and Rutter, W. J. (1992) Converting trypsin to chymotrypsin: the role of surface loops. *Science (Washington, DC, United States) 255*, 1249-53.

Hedstrom, L. (1998) Converting trypsin into chymotrypsin. *Book of Abstracts, 216th ACS National Meeting, Boston, August 23-27*, BTEC-072.

Helander, I., Alakomi, H., Latva-Kala, K., and Koski, P. (1997) Polyethyleneimine is an effective permeabilizer of gram-negative bacteria. *Microbiology 143*, 3193-9.

Helander, I. M., and Mattila-Sandholm, T. (2000) Fluorometric assessment of gram-negative bacterial permeabilization. *Journal of applied microbiology 88*, 213-9.

Higaki, J. N., Evnin, L. B., and Craik, C. S. (1989) Introduction of a cysteine protease active site into trypsin. *Biochemistry 28*, 9256-63.

Hirvas, L., Nurminen, M., Helander, I. M., Vuorio, R., and Vaara, M. (1997) The lipid A biosynthesis deficiency of the Escherichia coli antibiotic-supersensitive

mutant LH530 is suppressed by a novel locus, ORF195. *Microbiology (Reading, United Kingdom) 143*, 73-81.

Holskin, B. P., Bukhtiyarova, M., Dunn, B. M., Baur, P., de Chastonay, J., and Pennington, M. W. (1995) A continuous fluorescence-based assay of human cytomegalovirus protease using a peptide substrate. *Analytical Biochemistry 227*, 148-55.

Hoseki, J., Yano, T., Koyama, Y., Kuramitsu, S., and Kagamiyama, H. (1999) Directed evolution of thermostable kanamycin-resistance gene: A convenient selection marker for Thermus thermophilus. *Journal of Biochemistry (Tokyo) 126*, 951-956.

Huber, R., and Bode, W. (1978) Structural basis of the activation and action of trypsin. *Accounts of Chemical Research 11*, 114-22.

Hung, S.-H., and Hedstrom, L. (1998) Converting trypsin to elastase: substitution of the S1 site and adjacent loops reconstitutes esterase specificity but not amidase activity. *Protein Engineering 11*, 669-673.

Jones, L. J., Upson, R. H., Haugland, R. P., Panchuk-Voloshina, N., Zhou, M., and Haugland, R. P. (1997) Quenched BODIPY dye-labeled casein substrates for the assay of protease activity by direct fluorescence measurement. *Analytical Biochemistry 251*, 144-152.

Joo, H., Arisawa, A., Lin, Z., and Arnold, F. H. (1999a) A high-throughput digital imaging screen for the discovery and directed evolution of oxygenases. *Chemistry and Biology 6*, 699-706.

Joo, H., Lin, Z., and Arnold, F. H. (1999b) Laboratory evolution of peroxide-mediated cytochrome P450 hydroxylation. *Nature 399*, 670-673.

Jung, W., and Winter, H. (1998) Considerations for the use of clostridial collagenase in clinical practice. *Clinical Drug Investigation 15*, 245-252.

Kadrmas, J. L., Allaway, D., Studholme, R. E., Sullivan, J. T., Ronson, C. W., Poole, P. S., and Raetz, C. R. H. (1998) Cloning and overexpression of glycosyltransferases that generate the lipopolysaccharide core of Rhizobium leguminosarum. *Journal of Biological Chemistry 273*, 26432-26440.

Kaiser, E., Colescott, R. L., Bossinger, C. D., and Cook, P. I. (1970) Color test for detection of free terminal amino groups in the solid-phase synthesis of peptides. *Analytical Biochemistry 34*, 595-8.

Kano, H., Taguchi, S., and Momose, H. (1997) Cold adaptation of a mesophilic serine protease, subtilisin, by in vitro random mutagenesis. *Applied Microbiology and Biotechnology 47*, 46-51.

Karolin, J., Johansson, L. B. A., Strandberg, L., and Ny, T. (1994) Fluorescence and Absorption Spectroscopic Properties of Dipyrrometheneboron Difluoride (BODIPY) Derivatives in Liquids, Lipid Membranes, and Proteins. *Journal of the American Chemical Society 116*, 7801-6.

Kasafirek, E., Fric, P., Slaby, J., and Malis, F. (1976) p-Nitroanilides of 3-carboxypropionyl-peptides. Their cleavage by elastase, trypsin, and chymotrypsin. *European Journal of Biochemistry 69*, 1-13.

Khan, S. A., Everest, P., Servos, S., Foxwell, N., Zahringer, U., Brade, H., Rietschel, E. T., Dougan, G., Charles, I. G., and Maskell, D. J. (1998) A lethal role for lipid A in Salmonella infections. *Molecular Microbiology 29*, 571-579.

Kieke, M. C., Cho, B. K., Boder, E. T., Kranz, D. M., and Wittrup, K. D. (1997) Isolation of anti-T cell receptor scFv mutants by yeast surface display. *Protein Engineering 10*, 1303-1310.

Kimura, Y., Matsunaga, H., and Vaara, M. (1992) Polymyxin B octapeptide and polymyxin B heptapeptide are potent outer membrane permeability-increasing agents. *Journal of Antibiotics 45*, 742-9.

Kramer, R., Dekker, N., and MR., E. (2000) Identification of active site serine and histidine residues in Escherichia coli outer membrane protease OmpT. *FEBS Lett. 468*, 220-4.

Kramer, R., Vandeputte-Rutten, L., de Roon, G., Gros, P., Dekker, N., and Egmond, M. (2001a) Identification of essential acidic residues of outer membrane protease OmpT supports a novel active site. *FEBS Lett. 505*, 426-30.

Krebber, A., Bornhauser, S., Burmester, J., Honegger, A., Willuda, J., Bosshard, H. R., and Plueckthun, A. (1997) Reliable cloning of functional antibody variable domains from hybridomas and spleen cell repertoires employing a reengineered phage display system. *Journal of Immunological Methods 201*, 35-55.

Kretzschmar, T., and von Ruden, T. (2002) Antibody discovery: phage display. *Current Opinion in Biotechnology 13*, 598-602.

Kurtzman, A. L., Govindarajan, S., Vahle, K., Jones, J. T., Heinrichs, V., and Patten, P. A. (2001) Advances in directed protein evolution by recursive genetic recombination: applications to therapeutic proteins. *Current Opinion in Biotechnology 12*, 361-370.

Labischinski, H., Barnickel, G., Bradaczek, H., Naumann, D., Rietschel, E. T., and Giesbrecht, P. (1985) High state of order of isolated bacterial lipopolysaccharide and its possible contribution to the permeation barrier property of the outer membrane. *Journal of Bacteriology 162*, 9-20.

Lee, E.-S., Paik, I.-K., and Hahm, Y.-T. (2000) Screening of phytase overproducing strains in Aspergillus spp. by UV mutagenesis. *Mycobiology 28*, 119-122.

Lehrer, R. I., Barton, A., and Ganz, T. (1988) Concurrent assessment of inner and outer membrane permeabilization and bacteriolysis in E. coli by multiple-wavelength spectrophotometry. *Journal of Immunological Methods 108*, 153-8.

Levy, R., Weiss, R., Chen, G., Iverson, B. L., and Georgiou, G. (2001) Production of Correctly Folded Fab Antibody Fragment in the Cytoplasm of Escherichia coli

trxB gor Mutants via the Coexpression of Molecular Chaperones. *Protein Expression and Purification 23*, 338-347.

Leytus, S., Bowles, L., Konisky, J., and Mangel, W. (1981) Activation of plasminogen to plasmin by a protease associated with the outer membrane of Escherichia coli. *Proceedings of the National Academy of Sciences of the United States of America 78*, 1485-9.

Liebeton, K., Zonta, A., Schimossek, K., Nardini, M., Lang, D., Dijkstra, B. W., Reetz, M. T., and Jaeger, K.-E. (2000) Directed evolution of an enantioselective lipase. *Chemistry & Biology 7*, 709-718.

Lojda, Z. (1996) The use of substrates with 7-amino-3-trifluoromethylcoumarin (AFC) leaving group in the localization of protease activities in situ. *Acta Histochemica 98*, 215-228.

Lutz, S., Ostermeier, M., Moore, G. L., Maranas, C. D., and Benkovic, S. J. (2001) Creating multiple-crossover DNA libraries independent of sequence identity. *Proceedings of the National Academy of Sciences of the United States of America 98*, 11248-11253.

Marme, N., Knemeyer, J.-P., Sauer, M., and Wolfrum, J. (2003) Inter- and Intramolecular Fluorescence Quenching of Organic Dyes by Tryptophan. *Bioconjugate Chemistry 14*, 1133-1139.

Masihi, K. N., Ribi, E., Lange, W., and Werner, H. (1988) Effects of nontoxic lipid A and endotoxin on resistance of mice to Toxoplasma gondii. *Journal of Biological Response Modifiers 7*, 535-9.

Matayoshi, E. D., Wang, G. T., Krafft, G. A., and Erickson, J. (1990) Novel fluorogenic substrates for assaying retroviral proteases by resonance energy transfer. *Science (Washington, DC, United States) 247*, 954-8.

McCafferty, J., Griffiths, A. D., Winter, G., and Chiswell, D. J. (1990) Phage antibodies: filamentous phage displaying antibody variable domains. *Nature 348*, 552-4.

McQuade, T., Tomasselli, A., Liu, L., Karacostas, V., Moss, B., Sawyer, T., Heinrikson, R., and Tarpley, W. (1990) A synthetic HIV-1 protease inhibitor with antiviral activity arrests HIV-like particle maturation. *Science 247*, 454.

Melo, R. L., Alves, L. C., Del Nery, E., Juliano, L., and Juliano, M. A. (2001) Synthesis and Hydrolysis by Cysteine and Serine Proteases of Short Internally Quenched Fluorogenic Peptides. *Analytical Biochemistry 293*, 71-77.

Morris, C. M., George, A., Wilson, W. W., and Champlin, F. R. (1995) Effect of polymyxin B nonapeptide on daptomycin permeability and cell surface properties in Pseudomonas aeruginosa, Escherichia coli, and Pasteurella multocida. *Journal of Antibiotics 48*, 67-72.

Nakae, T., and Nikaido, H. (1975) Outer membrane as a diffusion barrier in Salmonella typhimurium. Penetration of oligo- and polysaccharides into isolated

outer membrane vesicles and cells with degraded peptidoglycan layer. *Journal of Biological Chemistry 250*, 7359-65.

Ness, J. E., Welch, M., Giver, L., Bueno, M., Cherry, J. R., Borchert, T. V., Stemmer, W. P. C., and Minshull, J. (1999) DNA shuffling of subgenomic sequences of subtilisin. *Nature Biotechnology 17*, 893-896.

Neuweiler, H., Schulz, A., Boehmer, M., Enderlein, J., and Sauer, M. (2003) Measurement of submicrosecond intramolecular contact formation in peptides at the single-molecule level. *Journal of the American Chemical Society 125*, 5324-5330.

Nikaido, H. (1976) Outer membrane of Salmonella typhimurium. Transmembrane diffusion of some hydrophobic substances. *Biochemica et Biophysica Acta 433*, 118-32.

Nikaido, H., and Vaara, M. (1985) Molecular basis of bacterial outer membrane permeability. *Microbiological Reviews 49*, 1-32.

Nikaido, H. (1996) Outer membrane in *Escherichia coli and Salmonella typhimurium; Cellular and Molecular Biology.* (Neidhardt, F. C., Ed.) pp 29-47, ASM Press, Washington, DC.

Ohno, N., and Morrison, D. C. (1989a) Lipopolysaccharide interaction with lysozyme. Binding of lipopolysaccharide to lysozyme and inhibition of lysozyme enzymatic activity. *Journal of Biological Chemistry 264*, 4434-41.

Ohno, N., and Morrison, D. C. (1989b) Effects of lipopolysaccharide chemotype structure on binding and inactivation of hen egg lysozyme. *European Journal of Biochemistry 186*, 621-7.

Okuno, K., Yabuta, M., Kawanishi, K., Ohsuye, K., Ooi, T., and Kinoshita, S. (2002a) Substrate specificity at the P1' site of Escherichia coli OmpT under denaturing conditions. *Bioscience, Biotechnology, and Biochemistry 66*, 127-134.

Okuno, K., Yabuta, M., Ohsuye, K., Ooi, T., and Kinoshita, S. (2002b) An analysis of target preferences of Escherichia coli outer-membrane endoprotease OmpT for use in therapeutic peptide production: efficient cleavage of substrates with basic amino acids at the P4 and P6 positions. *Biotechnology and Applied Biochemistry 36*, 77-84.

Olsen, M. J., Stephens, D., Griffiths, D., Daugherty, P., Georgiou, G., and Iverson, B. L. (2000) Function-based isolation of novel enzymes from a large library. *Nature Biotechnology 18*, 1071 - 1074.

Olsen, M. J. (2003a) Ph.D. Thesis, High Throughput Directed Enzyme Evolution Using Fluorescence Activated Cell Sorting. The University of Texas at Austin.

Olsen, M. J., Gam, J., Iverson, B. L., and Georgiou, G. (2003b) High-throughput FACS method for directed evolution of substrate specificity. *Methods in Molecular Biology (Totowa, NJ, United States) 230*, 329-342.

Ostermeier, M., Shim, J. H., and Benkovic, S. J. (1999) A combinatorial approach to hybrid enzymes independent of DNA homology. *Nature Biotechnology 17*, 1205-1209.

Packard, B. Z., Toptygin, D. D., Komoriya, A., and Brand, L. (1996) Profluorescent protease substrates: Intramolecular dimers described by the exciton model. *Proceedings of the National Academy of Sciences of the United States of America 93*, 11640-11645.

Parker, C. T., Kloser, A. W., Schnaitman, C. A., Stein, M. A., Gottesman, S., and Gibson, B. W. (1992) Role of the rfaG and rfaP genes in determining the lipopolysaccharide core structure and cell surface properties of Escherichia coli K-12. *Journal of Bacteriology 174*, 2525-38.

Patten, P. A., Howard, R. J., and Stemmer, W. P. (1997) Applications of DNA shuffling to pharmaceuticals and vaccines. *Currrent Opinion in Biotechnology 8*, 724-33.

Plesiat, P., and Nikaido, H. (1992) Outer membranes of Gram-negative bacteria are permeable to steroid probes. *Molecular Microbiology 6*, 1323-33.

Powell, K. A., Ramer, S. W., Del Cardayre, S. B., Stemmer, W. P. C., Tobin, M. B., Longchamp, P. F., and Huisman, G. W. (2001) Directed evolution and biocatalysis. *Angewandte Chemie, International Edition 40*, 3948-3959.

Raetz, C. R. (1996) Bacterial lipopolysaccharides: a remarkable family of bioactive macroamphiphiles in *Escherichia coli and Salmonella typhimurium; Cellular and Molecular Biology.* (Neidhardt, F. C., Ed.) pp 1035-1063, ASM Press, Washington, DC.

Raetz, C. R. H. (1986) Molecular genetics of membrane phospholipid synthesis. *Annual Review of Genetics 20*, 253-95.

Raetz, C. R. H. (1993) Bacterial endotoxins: Extraordinary lipids that activate eukaryotic signal transduction. *Journal of Bacteriology 175*, 5745-53.

Rakonjac, J., Feng, J.-n., and Model, P. (1999) Filamentous phage are released from the bacterial membrane by a two-step mechanism involving a short C-terminal fragment of pIII. *Journal of Molecular Biology 289*, 1253-1265.

Razatos, A., Ong, Y.-L., Sharma, M. M., and Georgiou, G. (1998) Molecular determinants of bacterial adhesion monitored by atomic force microscopy. *Proceedings of the National Academy of Sciences of the United States of America 95*, 11059-11064.

Reid, A. J. (2000) DNA shuffling: modifying the hand that nature dealt. *In Vitro Cellular & Developmental Biology: Plant 36*, 331-337.

Roth, L. A., and Keenan, D. (1971) Acid injury of Escherichia coli. *Canadian Journal of Microbiology 17*, 1005-8.

Rowe, L. A., Geddie, M. L., Alexander, O. B., and Matsumura, I. (2003) A Comparison of Directed Evolution Approaches Using the b-Glucuronidase Model System. *Journal of Molecular Biology 332*, 851-860.

Schellenberger, V., Turck, C. W., and Rutter, W. J. (1994) Role of the S' Subsites in Serine Protease Catalysis. Active-Site Mapping of Rat Chymotrypsin, Rat Trypsin, a-Lytic Protease, and Cercarial Protease from Schistosoma mansoni. *Biochemistry 33*, 4251-7.

Schnaitman, C. A., and Klena, J. D. (1993) Genetics of lipopolysaccharide biosynthesis in enteric bacteria. *Microbiological Reviews 57*, 655-82.

Sedliakova, M., Masek, F., Slezarikova, V., and Pirsel, M. (1997) The effect of the OmpT protease on excision repair in UV-irradiated Escherichia coli. *J. Photochem. Photobiol. B. 41*, 245-8.

Shamrock, J., DFritsch, E. F., and Maniatis, T. (1989) Molecular cloning, 2nd Ed., Cold Spring Harbor Laboratory Press.

Sharma, R. C., and Schimke, R. T. (1996) Preparation of electrocompetent E. coli using salt-free growth medium. *BioTechniques 20*, 42-4.

Sheets, M. D., Amersdorfer, P., Finnern, R., Sargent, P., Lindqvist, E., Schier, R., Hemingsen, G., Wong, C., Gerhart, J. C., and Marks, J. D. (1998) Efficient construction of a large nonimmune phage antibody library: the production of high-affinity human single-chain antibodies to protein antigens. *Proceedings of the National Academy of Sciences of the United States of America 95*, 6157-6162.

Shirasu, Y., Yoshida, H., Mikayama, T., Matsuki, S., Tanaka, J., and Ikenaga, H. (1986) Isolation and expression in Escherichia coli of a cDNA clone encoding porcine pancreatic elastase. *Journal of Biochemistry (Tokyo, Japan) 99*, 1707-12.

Shotton, D. M., and Watson, H. C. (1970) Three-dimensional structure of tosyl-elastase. *Nature 225*, 811-16.

Smit, J., Kamio, Y., and Nikaido, H. (1975) Outer membrane of Salmonella typhimurium. Chemical analysis and freeze-fracture studies with lipopolysaccharide mutants. *Journal of Bacteriology 124*, 942-58.

Sodeinde, O., Subrahmanyam, Y., Stark K, Quan , T., Bao, Y., and Goguen, J. (1992) A surface protease and the invasive character of plague. *Science 258*, 1004-7.

Stambolieva, N., Ivanov, I., and Iomtova, V. (1992) N-Anthraniloyl-Ala-Ala-Phe-4-nitroanilide, a highly sensitive substrate for subtilisins. *Archives of Biochemistry and Biophysics 294*, 703-6.

Stemmer, W. P. C. (1994a) Rapid evolution of a protein in vitro by DNA shuffling. *Nature 370*, 389-91.

Stemmer, W. P. C. (1994b) DNA shuffling by random fragmentation and reassembly: in vitro recombination for molecular evolution. *Proceedings of the National Academy of Sciences of the United States of America 91*, 10747-51.

Stevenson, J. D., and Benkovic, S. J. (2002) Combinatorial approaches to engineering hybrid enzymes. *Journal of the Chemical Society, Perkin Transactions 2*, 1483-1493.

Stryer, L., and Haugland, R. P. (1967) Energy transfer: a spectroscopic ruler. *Proceedings of the National Academy of Sciences of the United States of America 58*, 719-726.

Stumpe, S., Schmid, R., Stephens, D., Georgiou, G., and Bakker, E. (1998) Identification of OmpT as the protease that hydrolyzes the antimicrobial peptide protamine before it enters growing cells of Escherichia coli. *J. Bacteriol. 180*, 4002-6.

Taguchi, S., Ozaki, A., Nonaka, T., Mitsui, Y., and Momose, H. (1999) A cold-adapted protease engineered by experimental evolution system. *Journal of Biochemistry (Tokyo) 126*, 689-693.

Takeuchi, Y., and Nikaido, H. (1981) Persistence of segregated phospholipid domains in phospholipid-lipopolysaccharide mixed bilayers: studies with spin-labeled phospholipids. *Biochemistry 20*, 523-9.

Tao, H., and Cornish, V. W. (2002) Milestones in directed enzyme evolution. *Current Opinion in Chemical Biology 6*, 858-864.

Tawfik, D. S., and Griffiths, A. D. (1998) Man-made cell-like compartments for molecular evolution. *Nature Biotechnology 16*, 652-656.

Taylor, S. V., Kast, P., and Hilvert, D. (2001) Investigating and engineering enzymes by genetic selection. *Angewandte Chemie, International Edition 40*, 3310-3335.

Traeuble, H., and Overath, P. (1973) Structure of Escherichia coli membranes studied by fluorescence measurements of lipid phase transitions. *Biochimica et Biophysica Acta 307*, 491-512.

Tschantz, W. R., and Dalbey, R. E. (1994) Bacterial leader peptidase 1. *Methods in Enzymology 244*, 285-301.

Tsien, R. Y., Heim, R., and Cubitt, A. (1997) Fluorogenic assay substrates for proteinases with cleavage sites flanked by moieties that exhibit fluorescence resonant energy transfer. *PCT Int. Appl.* Wo9728261, 87 pp.

Turner, N. J. (2003) Directed evolution of enzymes for applied biocatalysis. *Trends in Biotechnology 21*, 474-478.

Vaara, M. (1981) Increased outer membrane resistance to ethylenediaminetetraacetate and cations in novel lipid A mutants. *Journal of Bacteriology 148*, 426-34.

Vaara, M., and Vaara, T. (1983a) Sensitization of Gram-negative bacteria to antibiotics and complement by a nontoxic oligopeptide. *Nature 303*, 526-8.

Vaara, M., and Vaara, T. (1983b) Polycations sensitize enteric bacteria to antibiotics. *Antimicrobial Agents and Chemotherapy 24*, 107-13.

Vaara, M., and Vaara, T. (1983c) Polycations as outer membrane-disorganizing agents. *Antimicrobial Agents and Chemotherapy 24*, 114-22.

Vaara, M. (1990) Do salicylates and ascorbate increase the outer membrane permeability to hydrophobic antibiotics in Pseudomonas aeruginosa? *Drugs under Experimental and Clinical Research 16*, 569-74.

Vaara, M. (1992) Agents that increase the permeability of the outer membrane. *Microbiological reviews 56*, 395-411.

Vandeputte-Rutten, L., Kramer, R., Kroon, J., Dekker, N., Egmond, M., and Gros, P. (2001) Crystal structure of the outer membrane protease OmpT from Escherichia coli suggests a novel catalytic site. *EMBO J. 20*, 5033-9.

Vasquez, J. R., Evnin, L. B., Higaki, J. N., and Craik, C. S. (1989) An expression system for trypsin. *Journal of Cellular Biochemistry 39*, 265-76.

Viljanen, P., Matsunaga, H., Kimura, Y., and Vaara, M. (1991) The outer membrane permeability-increasing action of deacylpolymyxins. *Journal of Antibiotics 44*, 517-23.

Wahler, D., and Reymond, J.-L. (2001) Novel methods for biocatalyst screening. *Current Opinion in Chemical Biology 5*, 152-158.

Wang, G. T., Matayoshi, E., Huffaker, H. J., and Krafft, G. A. (1990) Design and synthesis of new fluorogenic HIV protease substrates based on resonance energy transfer. *Tetrahedron Letters 31*, 6493-6.

Warren, G. H., Gray, J., and Yurchenco, J. A. (1957) Effect of polymyxin on the lysis of Neisseria catarrhalis by lysozyme. *Journal of Bacteriology 74*, 788-93.

Watson, H. C., Shotton, D. M., Cox, J. M., and Muirhead, H. (1970) Three-dimensional Fourier synthesis of tosyl-elastase at 3.5 Ang. resolution. *Nature 225*, 806-11.

Weitz, J. I., Stewart, R. J., and Fredenburgh, J. C. (1999) Mechanism of action of plasminogen activators. *Thrombosis and Haemostasis 82*, 974-982.

Wittrup, K. D. (2000) The single cell as a microplate well. *Nature Biotechnology 18*, 1039-1040.

Wright, S. D., Ramos, R. A., Tobias, P. S., Ulevitch, R. J., and Mathison, J. C. (1990) CD14, a receptor for complexes of lipopolysaccharide (LPS) and LPS binding protein. *Science (Washington, DC, United States) 249*, 1431-3.

Xia, G., Chen, L., Sera, T., Fa, M., Schultz, P. G., and Romesberg, F. E. (2002) Directed evolution of novel polymerase activities: mutation of a DNA polymerase into an efficient RNA polymerase. *Proceedings of the National Academy of Sciences of the United States of America 99*, 6597-6602.

Yamaguchi, K., Yu, F., and Inouye, M. (1988) A single amino acid determinant of the membrane localization of lipoproteins in E. coli. *Cell 53*, 423-32.

Yethon, J. A., Heinrichs, D. E., Monteiro, M. A., Perry, M. B., and Whitfield, C. (1998) Involvement of waaY, waaQ, and waaP in the modification of Escherichia coli lipopolysaccharide and their role in the formation of a stable outer membrane. *Journal of Biological Chemistry 273*, 26310-26316.

You, L., and Arnold, F. H. (1996) Directed evolution of subtilisin E in Bacillus subtilis to enhance total activity in aqueous dimethylformamide. *Protein Engineering 9*, 77-83.

Yu, F., Inouye, S., and Inouye, M. (1986) Lipoprotein-28, a cytoplasmic membrane lipoprotein from Escherichia coli. Cloning, DNA sequence, and expression of its gene. *Journal of Biological Chemistry 261*, 2284-8.

Zaccolo, M., and Gherardi, E. (1999) The effect of high-frequency random mutagenesis on in vitro protein evolution: a study on TEM-1 b-lactamase. *Journal of Molecular Biology 285*, 775-783.

Zhao, H., Giver, L., Shao, Z., Affholter, J. A., and Arnold, F. H. (1998) Molecular evolution by staggered extension process (StEP) in vitro recombination. *Nature Biotechnology 16*, 258-261.

Zhao, H., and Arnold, F. H. (1999) Directed evolution converts subtilisin E into a functional equivalent of thermitase. *Protein Engineering 12*, 47-53.

Vita

Jongsik Gam was born in Jinju, Korea on November 5, 1965, the second son of Sang-man Gam and Gab-seon Jeon. After graduation from Gyeongnam High School in Busan, Korea in 1984, he enrolled in the Department of Pharmacy of Seoul National University in Seoul, Korea. He received the degree of Bachelor of Science in Pharmacy in 1988. In March of 1988, he entered the graduate school program in Seoul National University and received the Master of Science in Pharmacy degree after completing his thesis titled "Addition of nucleophiles to isocyanates derived from Hofmann rearrangement" in 1990. He worked for Sunkyoung Industries, Ltd. in Suwon, Korea as a research scientist from 1990 until he entered the graduate school of the University of Texas at Austin in the fall of 1997.

Permanent Address: 117-903 Olympic Apt. Oryun-Dong, Songpa-Gu
Seoul, Korea

This dissertation was typed by the author.